A FIELD INVESTIGATION OF AIR FLOW IMMEDIATELY ABOVE OCEAN SURFACE WAVES

by

JOHN RICHARD SEESHOLTZ

B.S. U.S. Naval Academy

(1956)

SUBMITTED IN PARTIAL FULFILLMENT
OF THE REQUIREMENTS FOR THE
DEGREE OF DOCTOR OF PHILOSOPHY

at the

MASSACHUSETTS INSTITUTE OF TECHNOLOGY

May, 1968

Signature of Author ....
Department of Meteorology, May 9, 1968

Certified by ....
Thesis Supervirsor

Accepted by ....
Chairman, Departmental Committee
on Graduate Students

A FIELD INVESTIGATION OF AIR FLOW IMMEDIATELY ABOVE OCEAN SURFACE WAVES

by

John R. Seesholtz

Submitted to the Department of Meteorology on 9 May 1968 in partial fulfillment of the requirement for the degree of Doctor of Philosophy

ABSTRACT

Simultaneous measurements of wind velocity and water height were made on eleven days at an exposed site off the New England coast. While a wave gauge measured water height, a vertical array of anemometers recorded wind velocities at as many as eight heights up to 12 meters above mean sea level (MSL). The three lowest anemometers were arranged to float 30, 50 and 70 cm above the instantaneous water surface. Continuous atmospheric pressure and temperature measurements were made during several runs.

An analysis of this data indicates that to a good first approximation, the horizontal wind velocity increases as a logarithmic function of height. Cross-correlations made between the horizontal wind velocity and water height reveal the maximum velocity at heights between 30 cm and 4 m occurs somewhere just above the trough of the dominant water wave present under a variety of wind and sea conditions. Cross-correlations of the wind at different heights indicate that disturbances of the wind field usually arrive at upper levels first, probably because of the vertical wind shear. Moreover, this is even true when the wave travels faster than the mean wind. Limited data from cross-correlations of pressure and wave indicate that at a height of 1 to 2 meters above MSL, the maximum pressure occurs near the trough.

The measured energy transfer rate to the waves in a developing sea and the rate predicted by Miles' theory are in reasonable agreement. The averaging of data over long periods or making strong assumptions about the wind profile and its slope seriously degrade calculations based on Miles' theory. Short-term changes in wind velocity and the profile and shear stresses near or at the surface may be very important in the wave generation process.

Thesis Supervisor: Erik Mollo-Christensen
Title: Professor of Meteorology

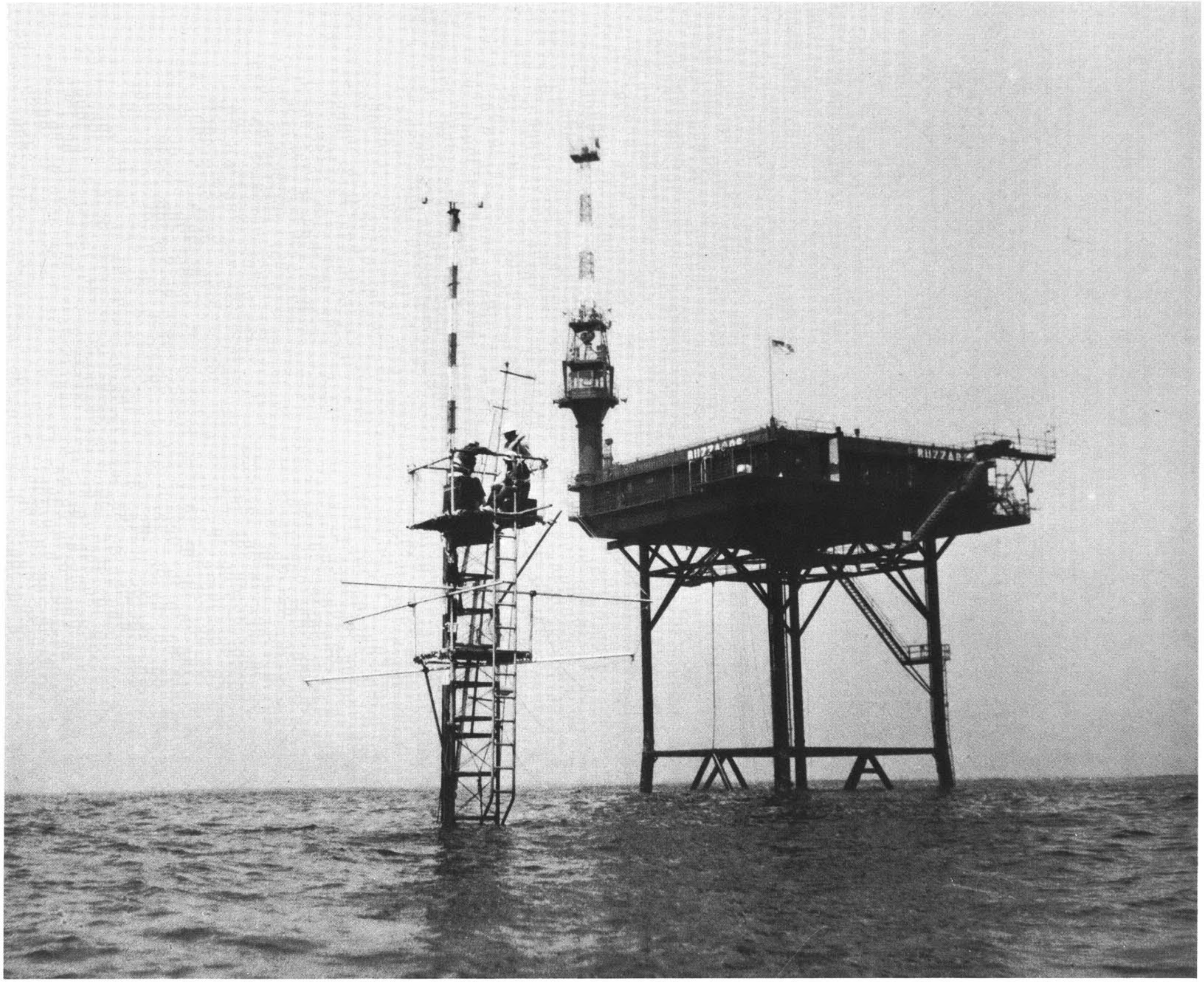

"... Down below I could often tell when there was a big surfing breaker on the way. First there would be a low, quiet roar, and then the wind would increase suddenly by 10-15 knots. Next, the boat would heel sharply to windward, then whip across to the leeward heel, with white water boiling along the lee deck. ..."

Sir Francis Chichester

Gipsy Moth Circles the World

page 152

Coward-McCann, Inc.

New York 1967

Abbreviations

a = amplitude.

B&W = Beckman & Whitley (anemometer).

BBELS = the U. S. Coast Guard's Buzzards Bay Entrance Light Station.

Be = frequency bandwidth.

Br = half-power point bandwidth.

Bs = equivalent statistical bandwidth.

c = phase velocity of a wave.

°C = degrees Celsius.

$C(\tau)$ = auto- or cross-correlation function.

cm = centimeter (s).

cps=cycles per second.

E = energy per unit surface area.

$\mathring{E}$ = rate of energy transfer.

f = frequency.

f(z) = amplitude function which decays with increasing z.

°F = degrees Fahrenheit.

g(z)=amplitude function which decays with increasing z.

H = wave height.

Hg = mercury.

ips = inches per second.

k = radian wave number

k' = wave number = $1/\lambda$.

kcs = kilocycles per second.

kt = knot (s).

L = distance constant.

m = meter (s).

mbs = millibar (s).

MKS = manufacturer of pressure system used.

mm = millimeter.

MSL = mean sea level.

nm = nautical mile (s).

PAR = Princeton Applied Research Corporation.

PI = Precision Instrument Company.

RMS = root mean square.

rms = root mean square.

SD = Spectral Dynamics Corporation.

t = time.

T = sampling time or record length.

°T = degrees, true direction.

u = horizontal wind velocity.

U(z) = mean horizontal wind velocity.

U'(z) = first derivative of U(z) with respect to z.

U"(z) = second derivative of U(z) with respect to z.

U_{12} = mean horizontal wind velocity, 12 m above MSL.

V = tidal current velocity.

w = vertical component of wind velocity.

W = the surface wave induced component of the vertical wind velocity, measured in a reference frame moving with the velocity of the dominant surface wave (Miles' vertical velocity).

x = distance downwind in horizontal plane. Flow is assumed to be two dimensional.

Z, z = height above water surface.

$Z_{\hat{c}}$ = height of critical layer.

α = phase angle between maximum atmospheric pressure and wave trough.

β = angle by which maximum horizontal wind velocity leads the wave trough.

$\beta(z)$ = vertical phase factor of horizontal wind velocity.

γ = phase angle between horizontal wind velocity at various heights.

ε = normalized standard error.

η = wave displacement.

λ = wavelength.

ρ = density.

τ = delay time in the correlations.

ϕ = angular phase lag of anemometer response.

ω = radian frequency.

TABLE OF CONTENTS

FIGURES

TABLES

Review of previous work

A careful search of the literature on oceanography and meteorology reveals a deficiency of quantitative measurements of wind and pressure structure close to the sea's surface. There is only very limited information available below a height of 4 meters. Because of the difficulty in taking adequate measurements in close proximity to the sea surface, many of our current ideas about wind generation of waves result from applying what is known about shear profiles and pressure fluctuations over land or in the laboratory to the situation over water. This technique normally requires extending profiles taken at sea at relatively great heights right down to the surface. The end result usually is an assumption of a logarithmic profile. Much of current theory of wave generation is based on this profile. Wave-induced or other perturbations of the wind and their relationship to the surface are also not well known or understood.

Until about 10 years ago the most significant theory for wave generation was Jeffreys' (1924). Jeffreys predicted a minimum wind for generation of water waves and his sheltering hypothesis provides a mechanism for transfer of energy to the waves by normal stresses but neglects tangential stresses. Using this work and others, Sverdrup and Munk (1947) developed a theory for forecasting waves. Other important works appeared also, but the basic state of the model remained unchanged for 30 years.

More recently Miles (1957) and Phillips (1957) have presented mathematical models for wave generation which have been expanded and altered to a considerable extent by Miles (1959,1960,1962,1967), Brooke Benjamin (1959) and Stewart (1967).

In the Miles' theory, air flow is regarded as quasi-laminar, with atmospheric turbulence neglected except for its effect upon the mean vertical velocity profile. The flow of air is considered over a water surface $\eta = a \cos kx$ about which the actual surface fluctuates randomly due to the presence of other wave components. Motzfeld (1937) observed the flow over a rigid wavy surface and found that flow in a boundary layer where no separation occurs follows to a first approximation the contours of the surface.

The critical layer is defined as the height (Z_c) above the surface where the wind speed is equal to the wave speed. In Miles' theory the transport of momentum downward takes place across the critical layer and is shown to be an important part of the wave generating mechanism. Air moving upward through the layer carries with it negative vorticity, while air moving downward carries a lesser amount of negative vorticity. The shape of the mean vertical profile determines the vorticity at any height and is therefore very important in this theory. The flow as pictured by Phillips (1966) appears in figure 1a. In the coordinate system moving with wave velocity c, the horizontal and vertical velocities take the form:

(1) $u \text{ (horizontal)} = U(z) - c + f(z) \cos (kx + \beta(z))$,

(2) $w \text{ (vertical)} = g(z) \sin (kx + \beta(z))$,

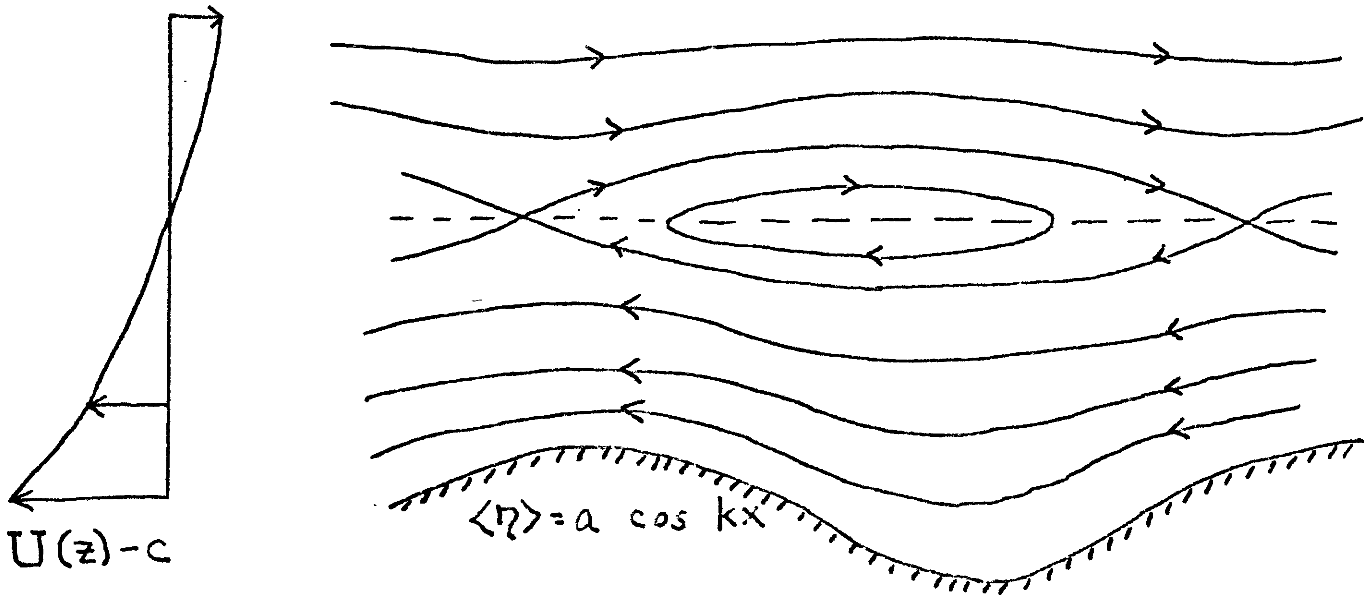

Fig. 1a. Main streamlines in turbulent flow above waves as seen in a reference system moving with the wave profile. Lighthill (1962) shows the closed streamlines centered directly over the trough, and still others show them elsewhere. The critical height is shown as the dotted line (from Phillips, 1966).

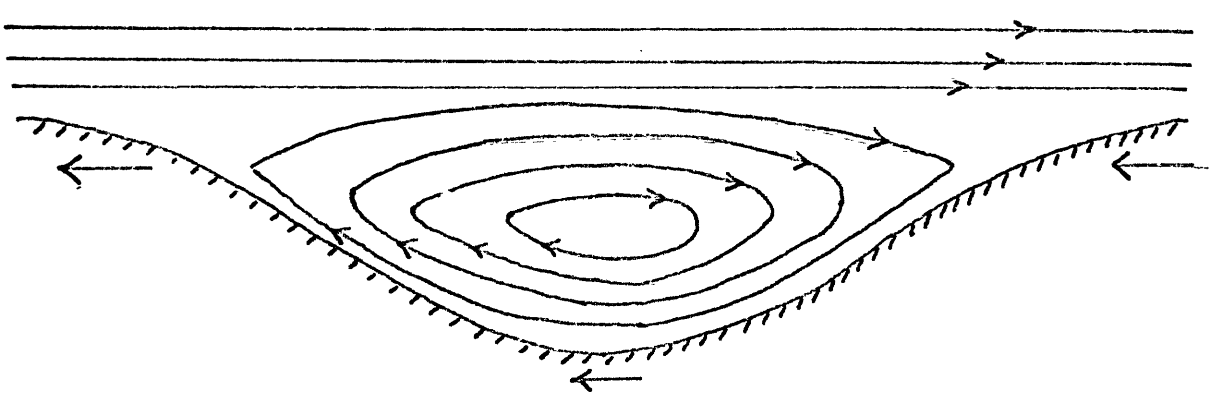

Fig. 1b. Possible configuration of streamlines, with the coordinate system as in Fig. 1a, which would account for Stewart's observation that only a short distance above the waves the airflow does not seem to be wave-like. The rightward acceleration at the left side of the figure would be produced by a shear stress gradient, the leftward acceleration on the right side by a horizontal pressure gradient (from Stewart, 1967).

respectively, where U(z) is the mean vertical profile of horizontal velocity and the cosine terms are the components of the wave induced perturbations. Here $\beta(z)$ is a vertical phase factor for which Bryant (Kinsman (1965) p 571) argues convincingly. The presence of the $\beta(z)$ factor results in a shift of the pressure distribution with respect to the surface. The out-of-phase component of pressure determines the magnitude of energy flux to the wave. Shemdin and Hsu (1966) in wind tunnel tank studies observed in the velocity perturbations in flow over waves, lags increasing with height and finally a complete phase reversal.

Wiegel and Cross (1966) found in wind tunnel tank experiments a phase difference between pressure variations in air and wave height indicating a coupled normal pressure mechanism such as that of Miles or Jeffreys. Longuet-Higgins et al (1963) measured pressure near the surface from a drifting buoy and concluded only that the results were not inconsistent with Miles' theory. It appears that in-the-field determinations of velocity and pressure variations in relation to the surface are necessary in order to corroborate the laboratory experiments and to expand on the findings of Longuet-Higgins et al.

Miles (1957) also estimated the energy transfer rate to be:

(3) $$\overset{\circ}{E} = \frac{\pi \rho c}{k} \cdot \frac{- U''(Z_c)\ \overline{W^2}}{U'(Z_c)} ,$$ where

$U(Z)$ = the mean horizontal wind velocity,

W = amplitude of vertical velocity variations at the critical layer induced by the wave,

k = radian wave number,

c = velocity of the wave,

ρ = density.

The primes denote differentiation with respect to z. This energy transfer is due to the loss of air momentum at the critical layer at a rate E/c. We see that Miles' theory requires $U''(Z_c)$ be negative. The logarithmic profile assumed in the development of the theory satisfies this criterion.

Recent field measurements by Snyder and Cox (1966) indicate the energy transfer to gravity waves with a 17 meter wavelength is about an order of magnitude larger than that calculated using Miles' theory. Other field data support this conclusion. Based on such experimental evidence Miles (1967) suggested that the theoretical laminar flow model may be adequate in the laboratory, but it is not on an oceanographic scale. He generalized the laminar flow model so that momentum transfer to a particular frequency component considers not only profile curvature, vertical velocity, and vorticity but the perturbation in the mean turbulent shear stress at the air-sea interface.

Stewart (1961) questioned the logarithmic profile and noted that over land there is no energy sink such as waves. Over the sea we expect energy to be drained from the lowest part of the profile. Thus, if the profile is logarithmic to begin with, as it is over land, it is soon altered. Stewart suggested that below the critical layer defined by the fastest component of the sea the profile is not logarithmic. Kinsman (1965) in measurements made at a small cove on the Severn River in 1960 found mean wind profiles not compatible with the logarithmic profile. Hidy and Plate (1966) in wind tunnel tests observed a non-logarithmic profile, especially near the surface of the water. Shemdin and Hsu (1966) also reported non-logarithmic profiles near the surface and a marked variation of the profile over trough and crest. However, Miles (1966) has pointed out that the energy loss from the air should not appreciably alter the logarithmic profile. Roll (1965) in a review of various field investigations noted that most of them reported a mean logarithmic profile under adiabatic conditions. These profiles were averages over a number of wave lengths. In cases where thermal stratification existed, the vertical profiles observed departed markedly from the logarithmic, some even contained kinks.

Stewart (1961) indicated it was possible most of the momentum transfer from air to water was effected by wave drag. Recently, Stewart (1967), using energy density spectra of the horizontal and vertical wind and the quadrature spectrum between the two, which spectra were obtained in the University of British Columbia program, calculated that the available energies as measured at or near the predominant surface wave frequency were not comparable to those based on Miles' theory. Furthermore, the low level of the quadrature spectrum indicated that the air flow may not be wave-like. Also, as generating waves tend to be peaked rather than rounded at the crest, the smooth streamlines of Miles are not possible there. Instead Stewart proposed that the streamlines of flow look somewhat as they are shown in figure 1b. Here the boundary flows rapidly to the left, and in this coordinate system, the maximum speed occurs in the trough and the minimum at the crest.

Stewart (1967) states that probably the shear distribution is at least as important as the pressure distribution in determining the flow. He explains the flow, "The thin layer of air which follows the water surface must be accelerated downwards over the crest and upwards over the troughs. Therefore, a low-pressure region must remain over the crest and a high-pressure region over the troughs, although the magnitudes of the deviations of these pressures from the average will be significantly less than with the Miles' assumption. Thus, air moving to the left from the trough to the crest is moving down a pressure gradient. With the suggested streamline pattern the pressure gradient is not great and so the demands on the stress gradient are not excessive. It is not improbable that the surface stress in the trough is small." (Stewart, 1967, p. S53) The shear then is concentrated near the crest. Stewart demonstrates too that the acceleration produced by the pressure gradient is not dominant when compared to the acceleration due to the shearing stress gradient. Furthermore, he points out that the process is in a way reversible; i.e., if the wind blows against the waves, the existing waves would tend to be reduced, if the shear stress is concentrated at the crest.

Super (1964) in studies on Lake Mendota found that air when it first moves over water undergoes rather marked velocity changes for at least the first two miles. Kraus _et al_ (1966) also noted similar changes. Thus, it seemed desirable to take measurements further off shore where the profile would be more stationary and the waves longer and faster. Therefore, hopefully the critical layer would be higher, which is of advantage in experiments, since then it is possible to measure wind velocities both above and below the critical layer and to determine if Miles' and/or Stewart's hypothesis is plausible. (I, in fact, had no knowledge of Miles' or Stewart's 1967 papers when this work was begun.)

Description of the experiment

Field site

The site selected for the air-sea interface field studies conducted by the Meteorology Department of M.I.T. was Buzzards Bay, Massachusetts. The Buzzards Bay Entrance Light Station (BBELS) is a Texas Tower type structure maintained by the U. S. Coast Guard as a navigational aid marking a 37-foot shoal at the entrance to Buzzards Bay. BBELS is located at 41°23.8'N, 71°02.0'W, 4 miles west southwest of Cuttyhunk, Massachusetts.

The location is exposed to a prevailing southwesterly afternoon sea breeze in the summer. Block Island, 26 nautical miles (nm) to the southwest, is the nearest upwind observation. Water depth at the site is 60 feet (19 meters) and is 70 feet (22 meters) or more for at least 20 nm to the west and southwest. The site is therefore suitable for studying wind generated waves of about 40 meters wavelength or less. The open Atlantic Ocean lies to the south, but from the southeast through east and north to the northwest the location is protected from Northeasters with their high winds and seas by the islands and mainland which enclose Buzzards Bay. Nevertheless a good Northeaster can generate high seas at the site. Also an occasional ocean swell from the sector 150° to 220° is a problem at the site.

BBELS was and is used in numerous oceanographic studies conducted by various groups. Shonting (1966) did extensive work from the tower and his work provides valuable information on wind, waves, currents, temperature, weather and tides at the site.

The buoy

Originally plans were made to use the BBELS tower itself as the platform for the sensors. However, wind tunnel tests indicated the interference of the large BBELS tower was too great for the studies planned (Mollo-Christensen and Seesholtz, 1967). Therefore a smaller sensor platform was necessary.

The platform used in this study was a special buoy with a semi-taut mooring. The same buoy had previously been used in a different configuration in studies conducted by the Woods Hole Oceanographic Institution. Wind tunnel tests of sections of a meteorological mast, similar to the structure of this buoy, indicated that for the sensor positions used in these studies, the interference of the buoy on the observed wind field is negligible (Gill, et al, 1966). Fortunately the buoy required no modification to the basic structure for our purposes. It did, however, require substantially different rigging and mooring capabilities than in its previous work.

The buoy was moored about 140 meters southeast of BBELS in 19 meters of water. This location was selected because the buoy was relatively small, and a support vessel or platform on which support equipment could be located was required. It was decided BBELS would provide the best support platform available. Four water-proofed cables of seven conductors each connected a terminal box, referred to as "the buoy box", on the buoy with the oceanographic support room (6' ×6') on BBELS. This arrangement permitted all power supplies, the tape recorder, amplifiers, monitoring and control devices and other major equipment to remain on the BBELS tower where it was not exposed to the elements and ship board motions. Only the sensors, the wave gauges, anemometers, thermistors, wind vane, current meters and vanes were exposed to the elements. This ideal set-up was departed from in the last week at the site during a special run to measure pressure variations over the waves.

One technician could operate the equipment on BBELS. Two men normally were required on the buoy to rig sensors and handle the lines necessary to control the booms and carriages. Communications between the buoy, BBELS, and a support boat were by citizen's band radio.

With a good swell running, buoy motion was a problem. When first set the buoy also vibrated, apparently from the shedding of Karman vortices in the tidal current. These vibrations were eliminated by wrapping a length of 2 1/2 inch rubber suction hose around the completely submerged cylindrical buoyancy tanks. Swell with a period of six seconds or greater caused the buoy to roll (or pitch). The roll amplitude was highly dependent upon the swell period and amplitude. A swell period of 7 to 8 seconds caused the greatest roll, and once with a swell more than a meter in height running the roll had a peak amplitude of 9°. Usually the roll was less than 2° and with a tide of 0.1 to 0.5 knots running was frequently unnoticeable

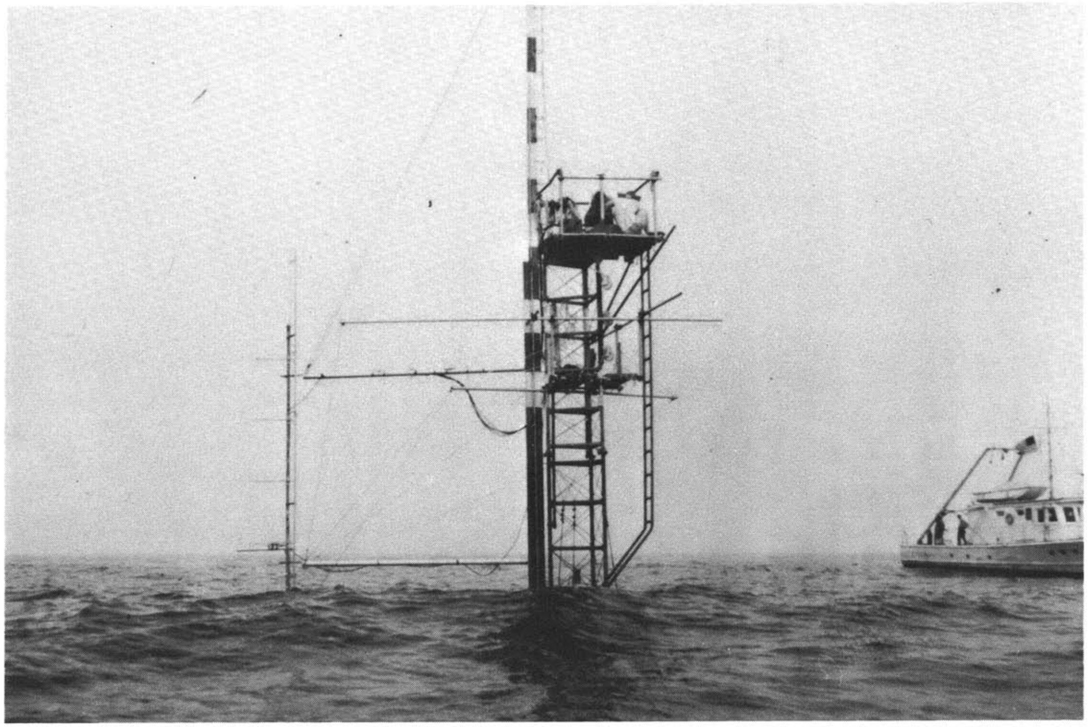

Figure 2. The buoy rigged for an observation run. The two horizontal booms are fastened by pivots to the vertical instrumentation mast. The smaller booms on the buoy were used for fair leading steadying guys to the main rig.

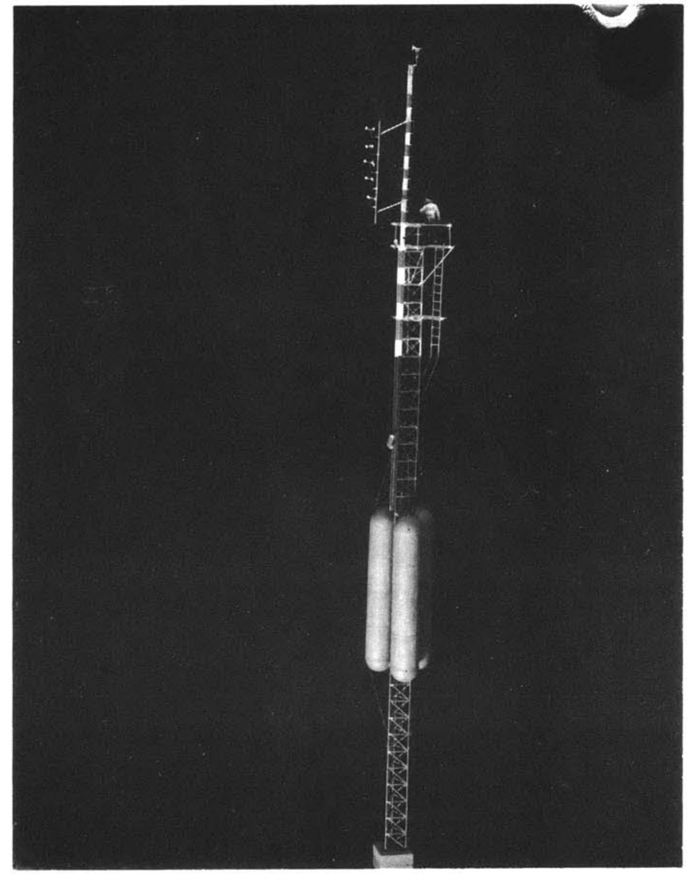

Figure 3. A model of the buoy showing the location of the floatation tanks and main structural members.

as the slight strain of the tide served to steady the buoy with a list of 1° to 3° from the vertical. During a strong spring tidal current, greater than 1 knot, the buoy vibrated and listed dangerously, as much as 15° (with $V_{tide} \approx$ 1.5 knots), and was not occupied at such times. There was no observable buoy motion with a period less than 5 seconds. Buoy yaw was about 1° in a swell and usually had a period of 7 seconds.

Figures 2 and 3 show the buoy as it appeared at the site. Appendix A contains additional information about the buoy.

Instruments

Wind velocities were measured using Thornthwaite, 3-cup, fast response anemometers (system model 106). The anemometers have a distance constant of 1 meter and are rugged enough to withstand limited exposure to a marine atmosphere.

A Beckman and Whitley (B and W), series 50, 6-cup anemometer and wind vane were mounted at the top of the buoy 12 meters above mean sea level (MSL).

Capacitance type wave gauges, built in the fluid dynamics laboratory of the Meteorology Department at M.I.T., were used to continually measure water height. Each gauge had a sensing cable two meters long. On at least three days waves of greater height were occasionally encountered while taking data.

A commercially available MKS Baratron Electronic Pressure System, type 77, was fitted to a static pressure probe and used in atmospheric pressure measurements. The system has eight full-scale ranges from ±.001 mm Hg (±.00133 mbs) to ± 3mm Hg (± 4 mbs) in steps of 1:3:10; it performed well. This was the only equipment system where the control console, signal modifiers, and power supply were located on the buoy. The system was available in the field only during the last few days of data collection in late September.

An air temperature probe consisting of a ventilated but radiation shielded thermistor controlling the output frequency of an oscillator was available for air temperature measurements on several days.

All instrument outputs were in pulse rate or frequency format or in the case of pressure measurements the output was converted to a frequency at the buoy before transmission to BBELS. This format eliminated the need to correct for line loss between the buoy and the recorder on BBELS.

Current measurements were made by the drift block and stop watch technique.

Instrumentation is discussed more fully in Appendix B.

Techniques

Eight channels of information were normally recorded on a Precision Instrument (PI), model 6208, 3-speed tape recorder located on BBELS. The Thornthwaite cup anemometers could also drive a modular print-out unit which provided 6 channels of wind velocity averages over a specific period. One minute averaging was usually used. In addition the technician on BBELS could monitor and record the masthead anemometer output to provide an extra channel of wind velocity data. During runs when a tape recorder channel was available, the masthead anemometer output was recorded on tape.

In August 1967 typical runs were concerned with wind velocity determination. Vertical velocity profiles were made using 3 or 4 fixed Thornthwaite anemometers spaced one meter apart, the lowest about 1 meter above MSL. Usually three Thornthwaite anemometers were also mounted to float 30, 50 and 70 cm above the surface. The floating arrangement was the end result of several attempts to design a suitable flotation system and worked well under all conditions encountered. The two lowest anemometers did take a few dunkings on two very rough days. One or two wave gauges were also used with the anemometers. All sensors except the B and W (masthead) anemometer and the temperature probe were mounted on an instrumentation mast held vertically by controllable booms which could extend the mast 4 meters out from the buoy. The fixed anemometers and the wave gauge were arranged to form a single vertical axis. The floating anemometers formed another much shorter vertical axis located 30 cm cross-wind from the longer axis. Figures 4 and 5 show how the instruments were arranged. The second wave gauge when used was located 1 meter down sea from the first. The air temperature probe was used during mid-August and was located on a continuous pulley arrangement on the opposite side of the buoy from the main mast. The probe could manually be positioned from a height of 70 cm to 11 m above MSL.

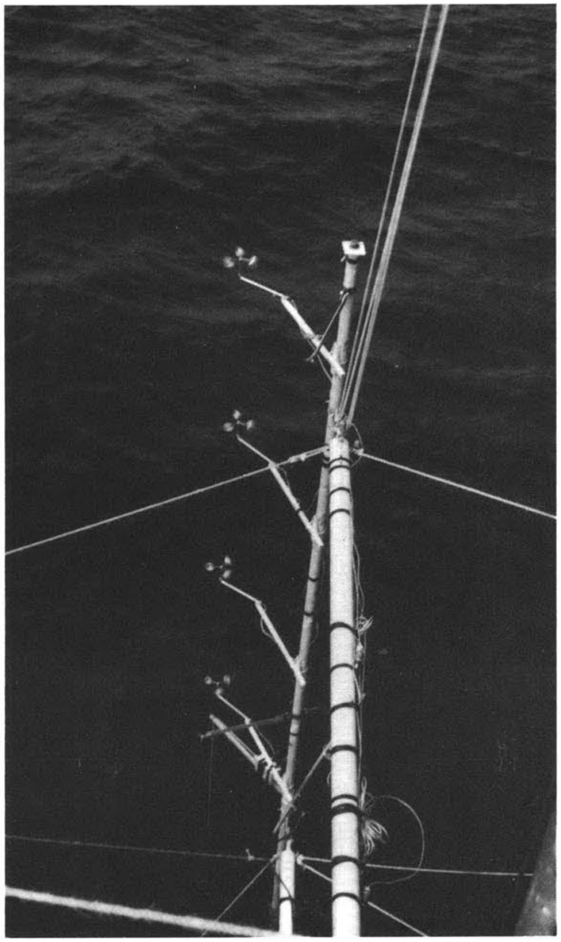

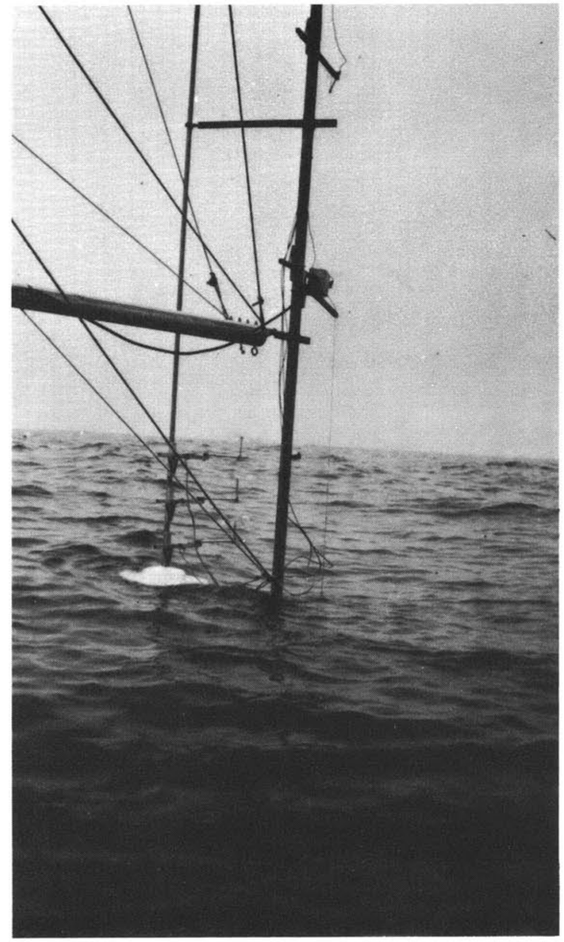

Fig. 4. A view of the fixed Thornthwaite anemometers in position at the buoy, looking from the upper buoy platform. The wave gauge cable can be seen below the lowest anemometer. The floating anemometers are not in use here.

Fig. 5. A sea-level view of the instrumentation rig. The floating anemometers are on the vertical mast at the left which is free to move up and down with the float at the surface.

During measurements of atmospheric pressure variations in late September, the pressure probe was mounted at the upper end of the wave gauge cable, 30 cm below the lowest fixed anemometer.

The instrument location and mounting is discussed fully in Appendix B along with the instruments.

On six days in August 6 or 7 Thornthwaite anemometers and 1 or 2 wave gauge outputs were recorded. On three additional days the four fixed anemometers and a wave gauge plus a various mixture of data (temperature vs height; mast head velocity) were recorded continuously. In September pressure data were taken on two days, while wind and wave measurements were also recorded. Most data collection runs were 65 minutes long but varied from 25 minutes to 3 hours depending upon equipment performance and the meteorological conditions prevailing at the time.

Data processing

The wind velocity profiles were plotted by hand from modular print out information, monitor readings, and tape recorder averages. The MSL reference was established from the tape recorded wave gauge data by averaging over many wave periods. The remaining data was processed mostly by analog means described below.

Using two similar PI tape recorders the data taken in the field were rerecorded, demodulated, and speeded up by a factor of 1000. Real time events with frequencies of .02 to 0.5 cycles per second then appeared as frequencies of 20 to 500 cps. These higher frequencies can be handled efficiently by many analog electrical devices. Each PI recorder has 2 record and 2 playback heads, the spacings of which are critical. Any difference in spacing between pairs of heads results in the introduction of an apparent phase shift in the data. With the rerecording and speeding up of the data this became a serious problem which required considerable time and effort for successful resolution.

An attempt was made to modify and use primarily equipment already available to the Meteorology Department at M.I.T. for processing the data. We were finally successful in setting up a satisfactory means of performing spectral analysis. Our signal from a tape loop containing about 21 minutes of real time information was fed to a narrow band wave analyzer (or filter) whose center frequency was slowly increased. The output of the wave analyzer was integrated and plotted against frequency. By squaring the wave analyzer output before integrating, this system produced satisfactory energy density spectra. Tape loops with 50 minutes of information were also analyzed and agreed well with the summation (averages) of shorter records covering the same period.

A great deal of effort was spent trying to modify an available 2 channel tape recorder, which had two separate pairs of record and playback heads, to do correlations. While successful, this effort produced only fair quality correlations.

The use of a Princeton Applied Research (PAR) Corporation correlator model 100 was obtained and proved very satisfactory for the correlation work. The PAR correlator calculates a correlation's value at 100 evenly spaced points between 0 and a variable maximum delay time. The maximum delay is adjustable from 100 microseconds to 10 seconds in steps of 1, 2, 5 and 10.

The analog data processing is covered in detail in Appendix C.

Results

Measurements were made from the Buzzards Bay buoy on 11 days in August and September 1967 under a variety of meteorological conditions ranging from fog and misty rain to bright, clear, and cool weather on a typical New England early autumn day. Conditions in the lowest layer of the atmosphere were usually neutral or near neutral as air-sea temperatures differed by 1°C or less. On 15 and 18 August the lapse rate was negative, and conditions were stable, being more so on the 15th than on the 18th. The 26th of September was the only day on which the atmospheric boundary layer was unstable. It was also one of the two days on which pressure measurements were obtained. Active generation of waves at the site occurred on 4 and 18 August and 21 and 26 September. There was minor generation also on 7 and 9 August, but swell predominated on those days. Conditions on the five remaining days were a light wind blowing over old swell.

Velocity profiles

The profiles of vertical velocity as observed were, to a first approximation, logarithmic. This was true even for anemometers floating 30, 50 and 70 cm above the surface in waves of 1 meter in height. Figure 6 shows profiles from the various days.

The very lowest part of the profile has a noticeably positive curvature on all the non-generating days and also on 4 August.

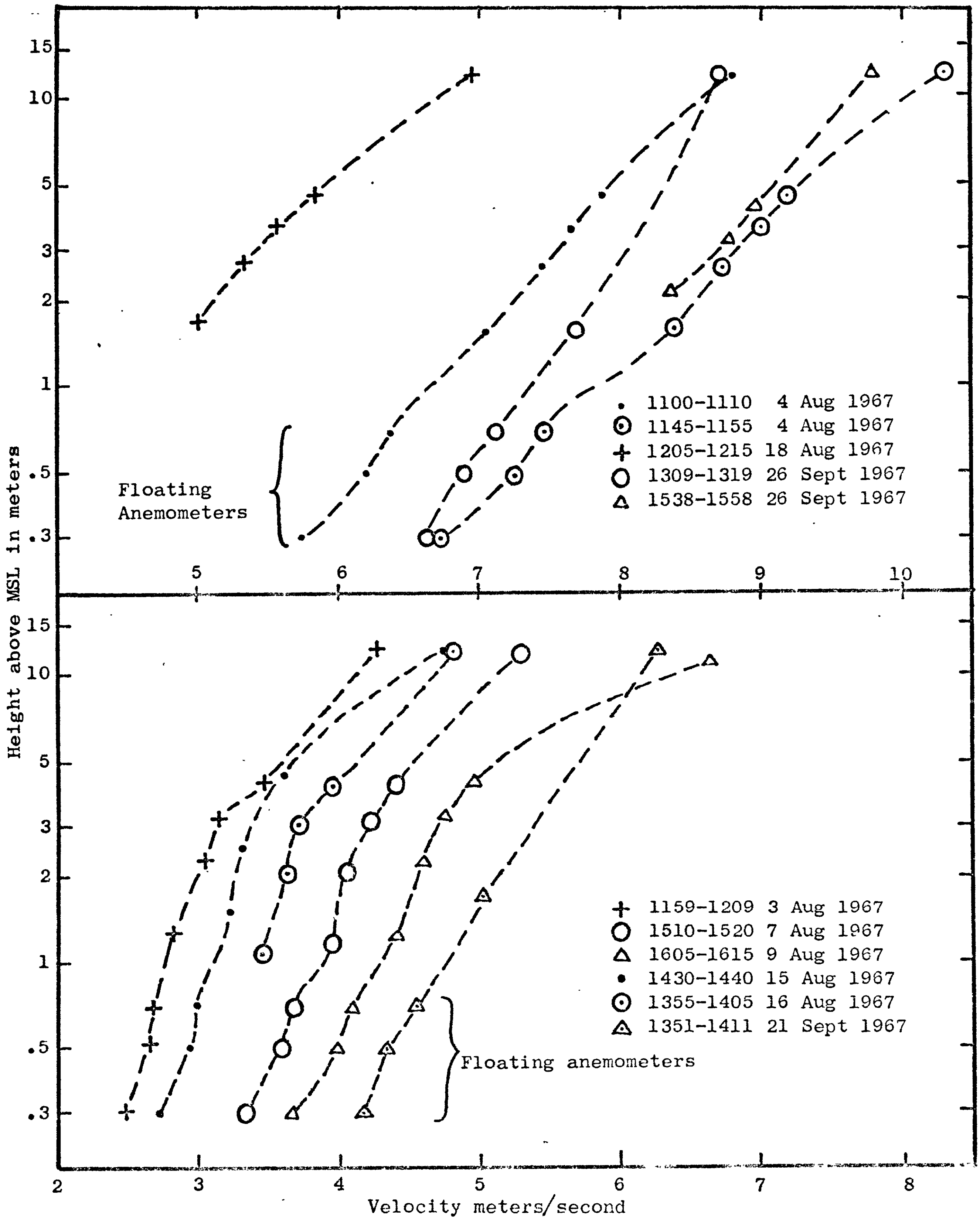

Figure 6. Examples of vertical profiles of horizontal wind velocity from Buzzards Bay Project. Atmospheric conditions were stable on 15 and 18 August, unstable on 26 September, and neutral or nearly so on all other days.

The curvature near the surface on 21 and 26 September is slightly positive. No observations from floating anemometers were made on 16, 17, or 18 August or during the last runs on 26 September. On seven days a negative curvature of the profile occurs above a height of about 1 meter and is particularly marked on 9 and 15 August. A kink at 2 or 3 meters above MSL was present on 3, 16 and 17 August. During the first 20 minutes of data recording on 15 August a kink so strong was observed that the recorded velocity at a height of 1.2 meters was greater than that at 2.2 meters. The kink disappeared and was not observed again that day. Generally the profiles are logarithmic, but with a tendence for the velocity to increase faster than log Z with increasing height, particularly under neutral and stable conditions.

Numerous one-minute averages of wind velocity profiles were plotted and indicated that in the great majority of cases changes in the wind modified the shape or slope of the profile only a little. In several cases, however, marked but brief (about one minute) distortions of the profile were observed, sometimes for no apparent reason. Examples of such distortion appear in figure 7. The anemometer performance was excellent, and the possibility that these distortions were due to sticking anemometers can be disregarded.

The rms value of wind velocity variations generally decreased with height on the generating days which were the only days for which this was determined. There was a noticeable minimum at a height of 1 to 2 meters above MSL on 4 August.

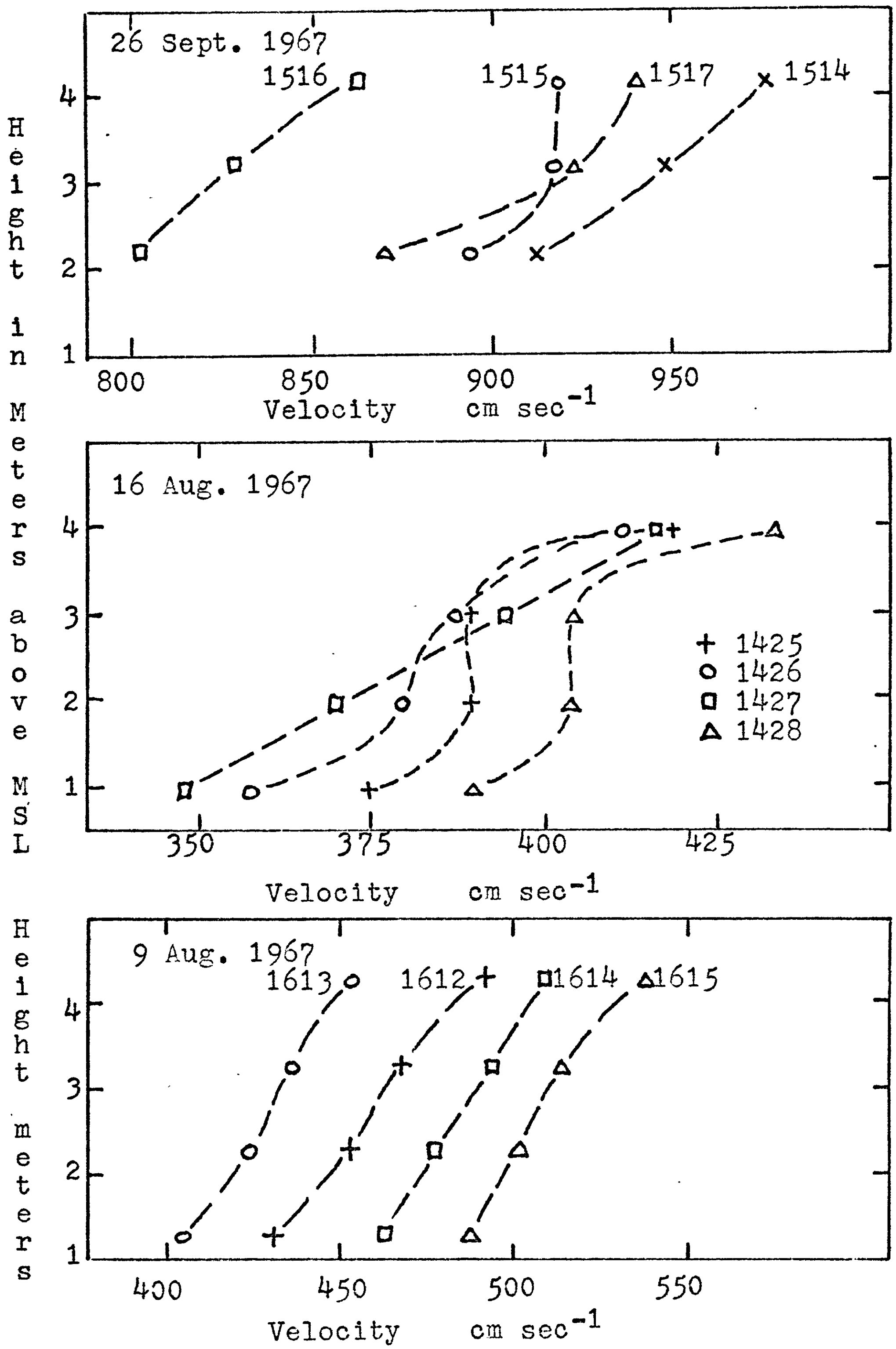

Figure 7. One minute averages of the vertical profile of horizontal wind velocity illustrating the change in the profile over brief periods of time. Note that the vertical scale is linear. In the lowest figure the slope is modified very little; however, in the following five minutes the slope increased noticeably as the velocity increased.

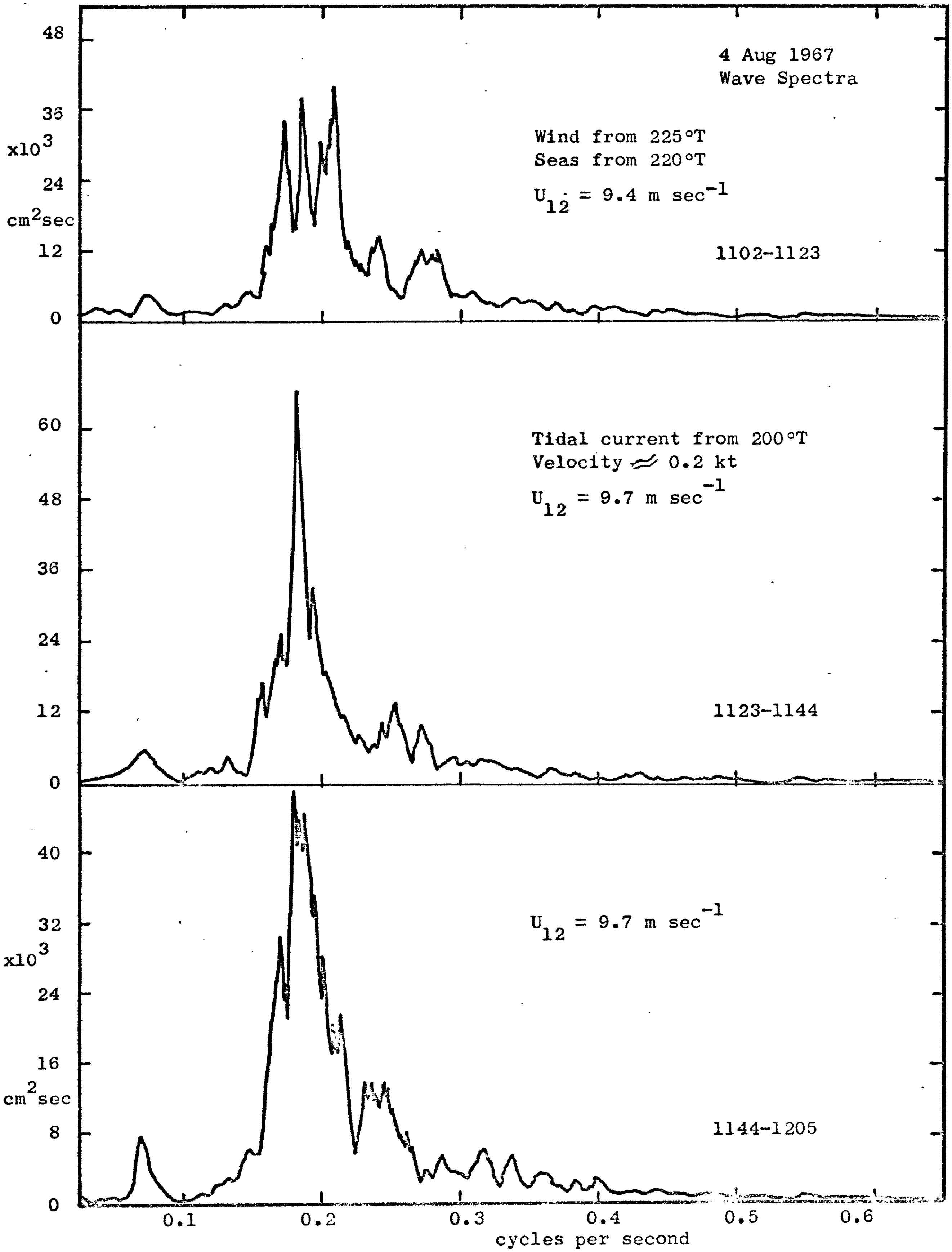

Figure 8. Wave energy spectra taken on Buzzards Bay. The 21 minute time period covered by the spectrum is listed to the right of each trace. From 1110 to 1150 the total wave energy increased by about seven percent.

A complete set of profiles and some wind variation data appear in Appendix D.

Spectra

One-dimensional wave spectra taken under active generating conditions appear in figures 8 through 12. Energy in the spectra below a frequency of about 0.15 cps represents swell not generated locally. If the part of a spectrum due to swell is disregarded a smoothed envelope of the spectrum fits well the accepted shape of wind generated wave spectra. In the longer series of records, 21 and 26 September, it appears the generation of wind waves reduces the energy of the swell, but note also that the vertical scale differs from figure to figure.

The spectra for 4 August, figure 8, were obtained about 6 hours after the wind had increased to 15 knots. Prior to that the wind had been 10 to 12 knots since the previous afternoon. The energy of the waves increased 6.5 percent in the period from 1110 to 1150 as determined from the rms level of the demodulated wave gauge signal. These are the only spectra which can be considered to be those of a nearly fully developed sea.

The waves with a frequency greater than 0.24 cps in the spectra for 18 August, figure 9, were generated by wind blowing 60° to the direction of the swell. This day began with heavy fog until 0800 local time, when it began to burn off. At 0900 the visibility was 1 to 2 nm and a 5 knot breeze was blowing from 240°T. When the run began at 1155, the wind was 15 knots and visibility 2 to 3 nm

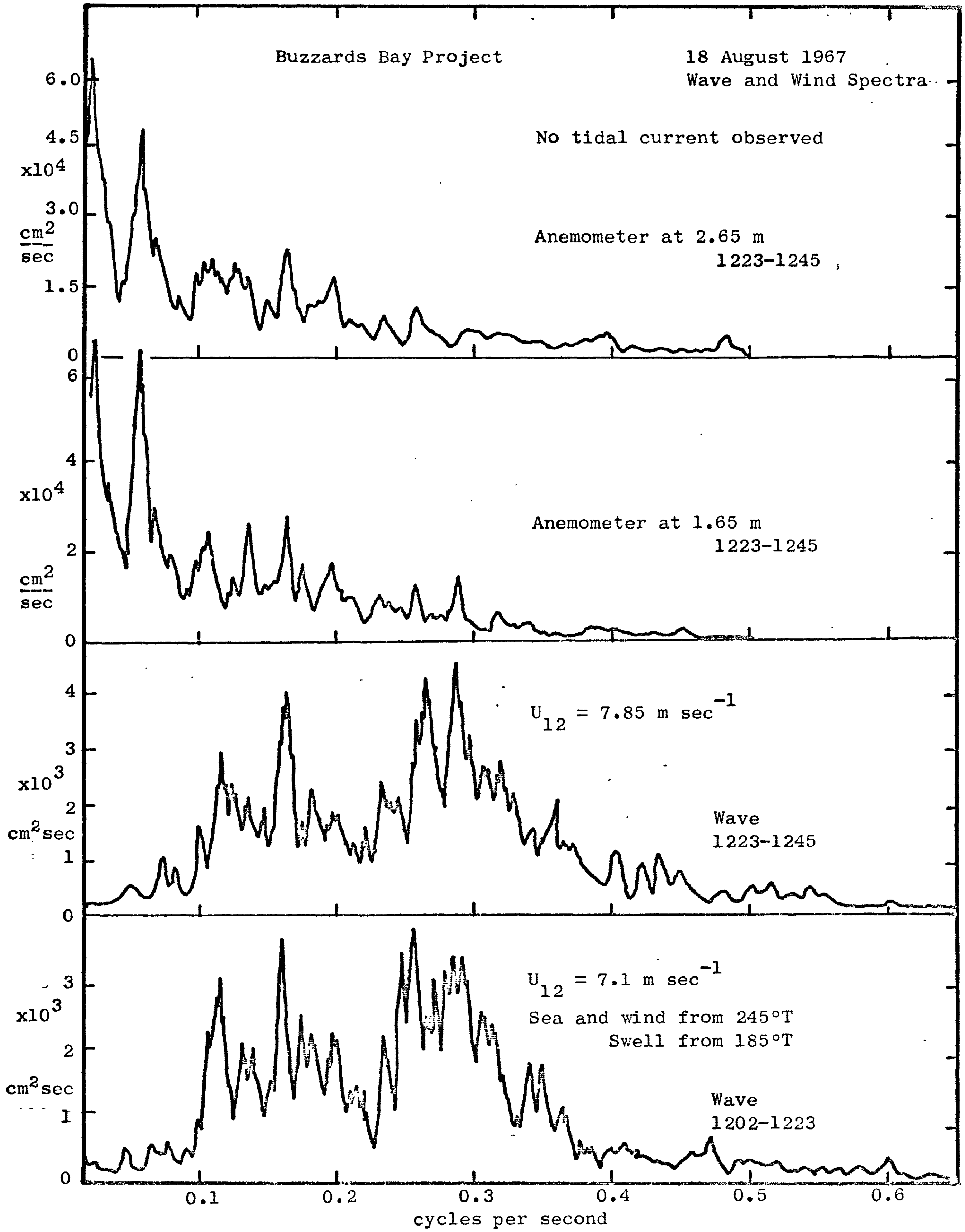

Figure 9. Wind and wave energy spectra. Anemometer height given is average height above MSL for period of record. U_{12} is average wind velocity 12 meters above MSL.

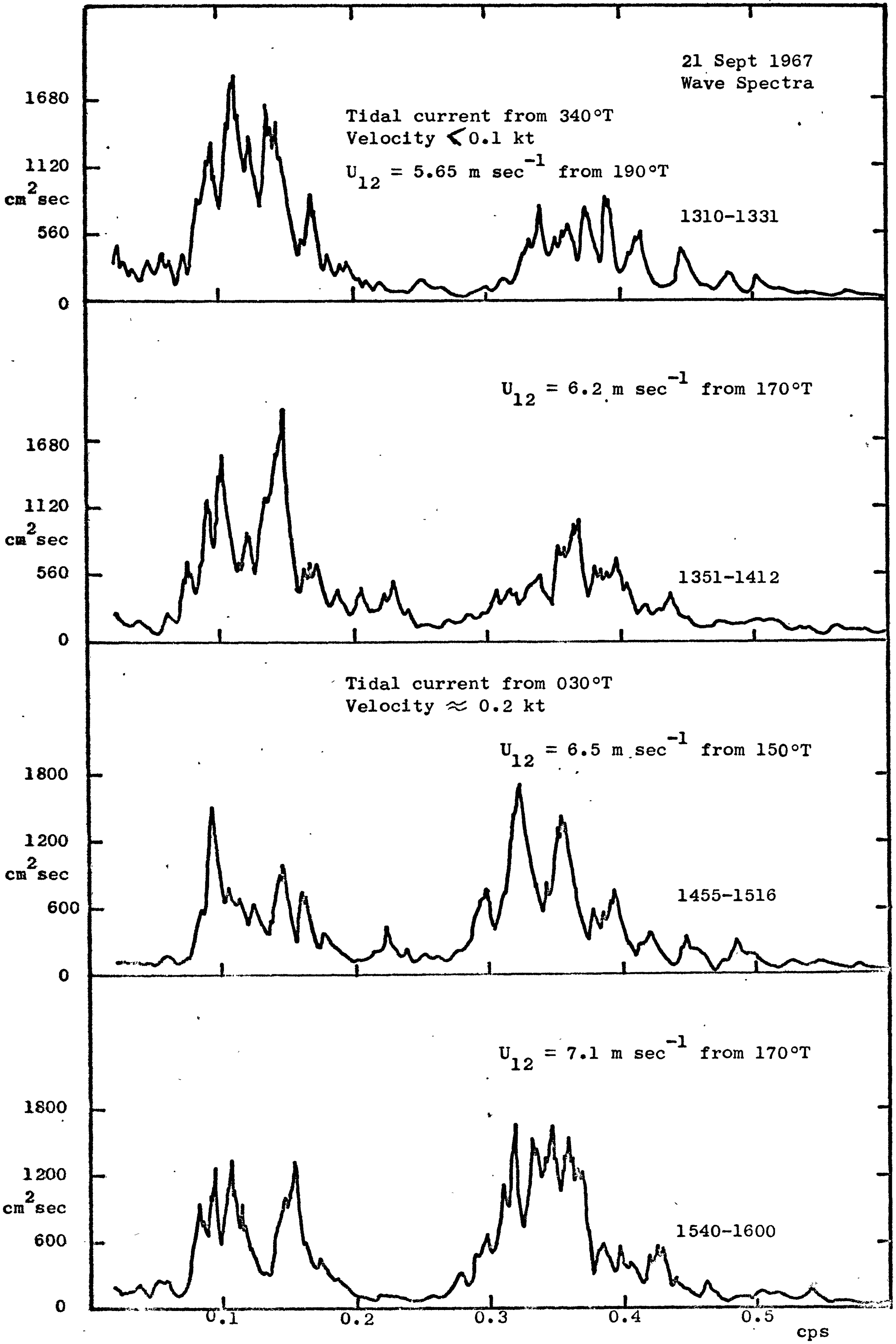

Figure 10. Wave energy spectra.

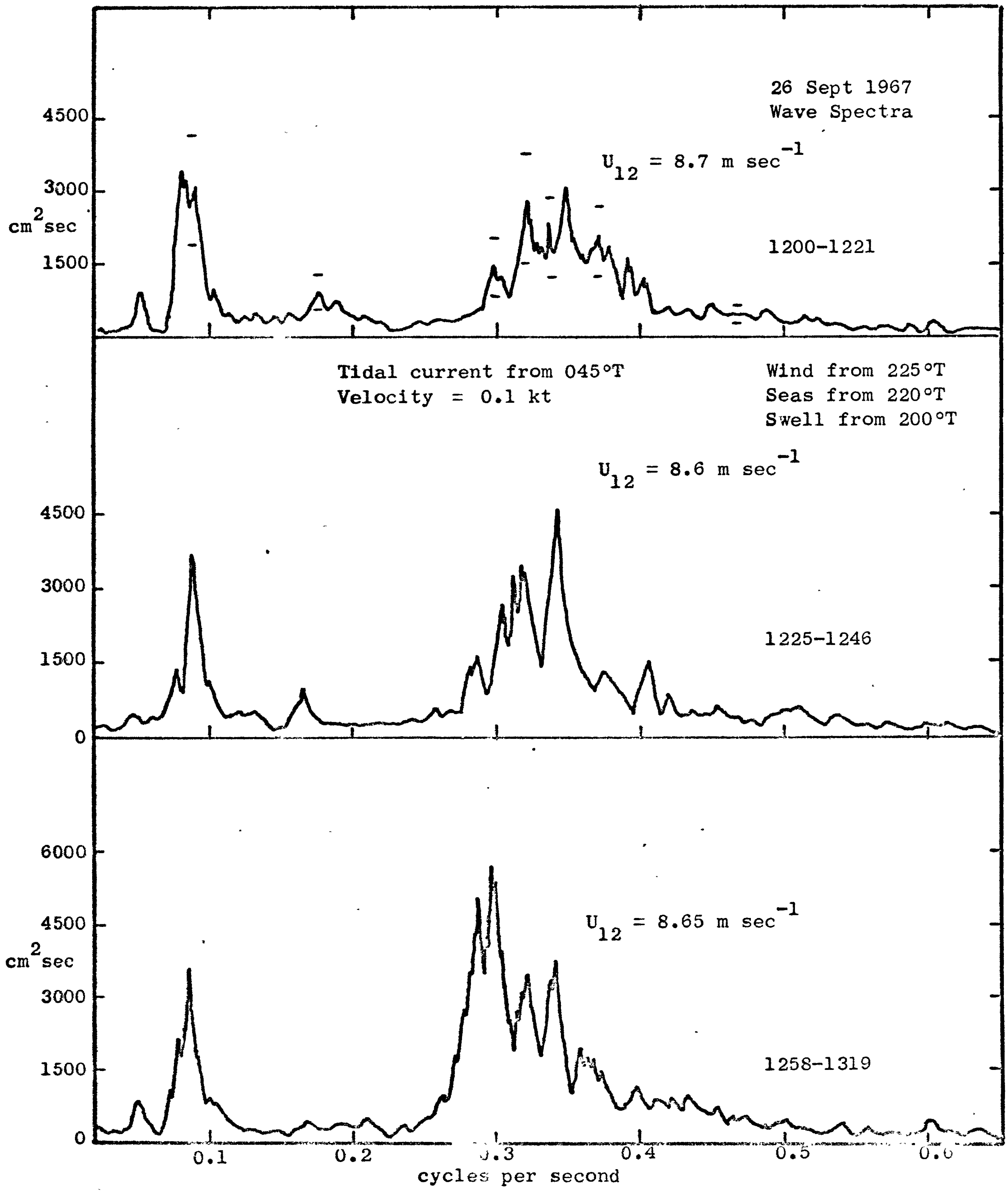

Figure 11. Wave energy spectra. The 95 percent confidence limits are shown at several points on the spectrum for 1200-1221. These limits are applicable to all energy spectra which cover a similar period of time.

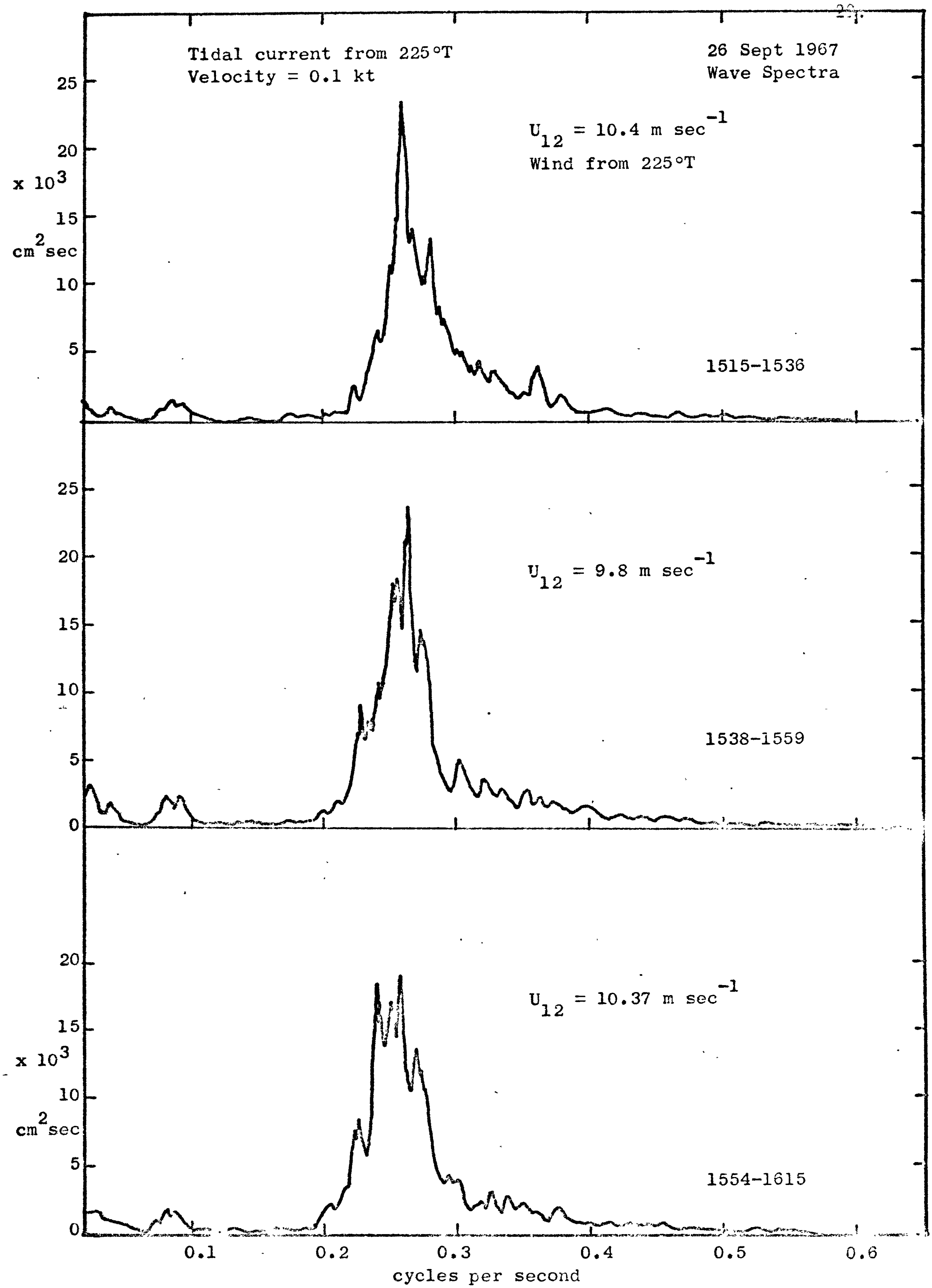

Figure 12. Wave energy spectra for 26 September 1967 from Buzzards Bay Project. The total energy in the 1554-1615 run is 240% of the energy in the 1200-1221 run (Figure 11). (RMS of wave amplitude = 31 cm.)

on a hazy, but sunny day.

On 21 September, a clear, sunny day, the wind was light and variable until about 1200 when it blew from 220°T at 5 knots. The wind then backed and increased steadily as indicated in figure 10. During the 3 hours covered by the observations, the increase in energy near a frequency of 0.32 cps was very noticeable. The total energy as determined from the rms level of the signal increased by 30 percent. Notice the decrease in the energy of the swell.

The last day of observations, 26 September, began clear and cool with almost no wind and a very slight swell from the south southwest. At about 1000, there was a 5 knot breeze from 240°T which increased rather steadily through the day. At 1700 the wind was blowing at 25 knots. Figures 11 and 12 show how the wave spectrum developed during the period from 1200 to 1615. Again a decrease in the energy of the swell portion of the spectrum was recorded.

Energy density plots were obtained from data collected by the Thornthwaite anemometers, primarily to see if a peak in the spectra of the horizontal wind velocity corresponding to the predominant wave period was present. For a sinusoidal disturbance in air of the same wave length as the dominant surface wave, the energy as measured by the Thornthwaite cup anemometer should be 96% of the true energy for a disturbance with a period of five seconds. The percent of response decreases with a decrease in the period, so that for a period of 2.5 seconds the instrument measures but 68%

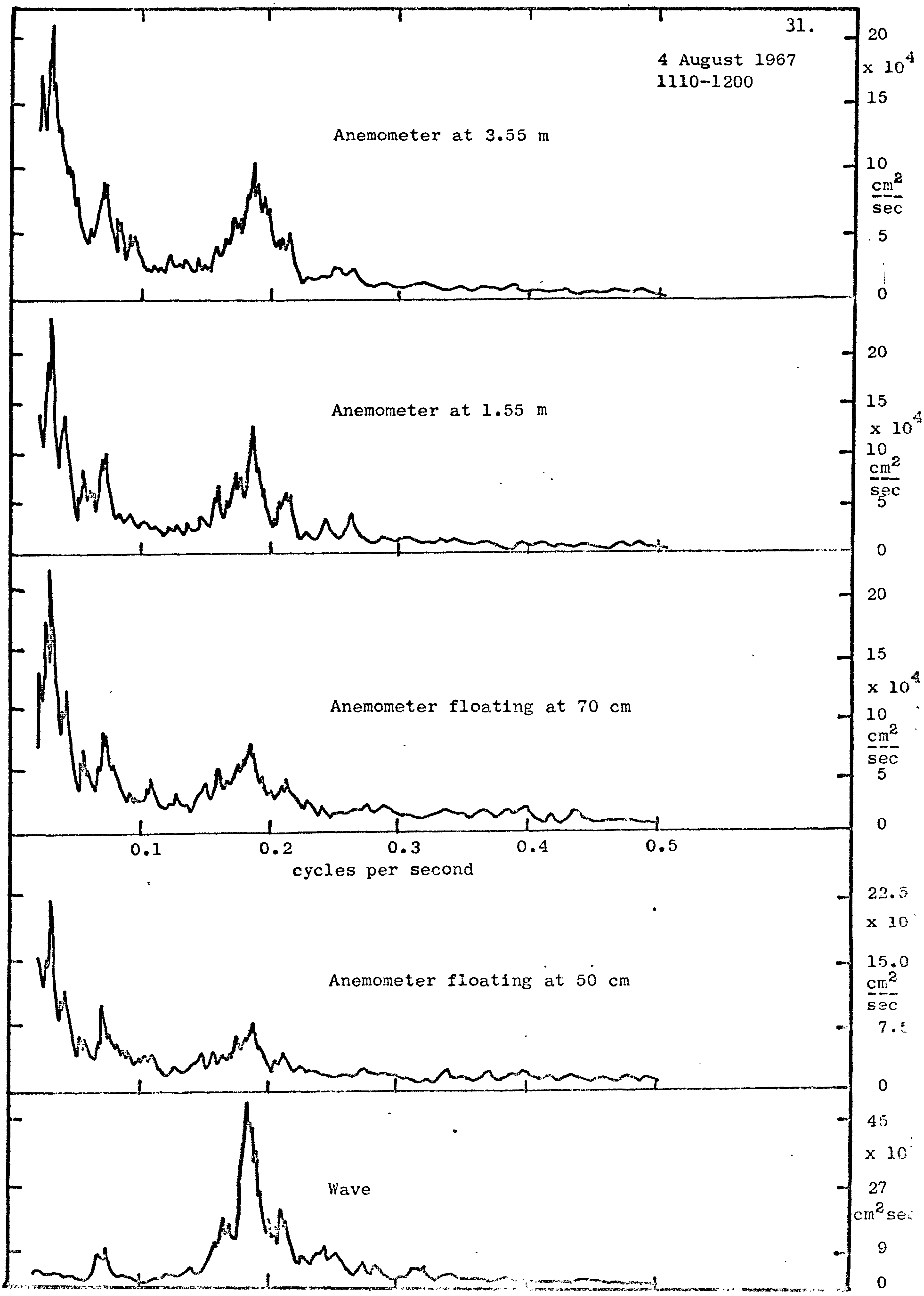

Figure 13. Wave and wind energy spectra taken on Buzzards Bay.

of the energy of the actual variation. This response should be good enough to locate peaks in the spectra of the horizontal velocity for the frequencies of interest here.

On 4 August, figure 13, there was a definite peak in the spectra of the velocity which corresponded to the peak in the wind generated wave spectrum. Peaks in the spectra of the wind on other generating days are not pronounced at the wave frequency and are missing in some instances. See figures 9, 14 and 15. An examination of generating and non-generating days indicates a peak in the spectra of the wind from floating and fixed anemometers corresponding to the period of the swell in each instance.

Pressure spectra from 21 and 26 September have no definite peaks corresponding to the wind generated wave frequency. See figures 14 and 15. There are peaks corresponding to the swell period. (The pressure measurements on 21 September were taken using a battery-powered, voltage controlled oscillator which had inadvertently been left on overnight and may be suspect for the modulated signal level was low. However, the demodulated signal looked good, and the spectra for the 21st do not differ significantly from those obtained on the 26th.)

Appendix D contains more wave, wind and pressure spectra.

Correlations

Correlations made between unfiltered variables or those filtered with a band-pass filter having a center frequency near the frequency of the predominant surface wave generally provided distinct

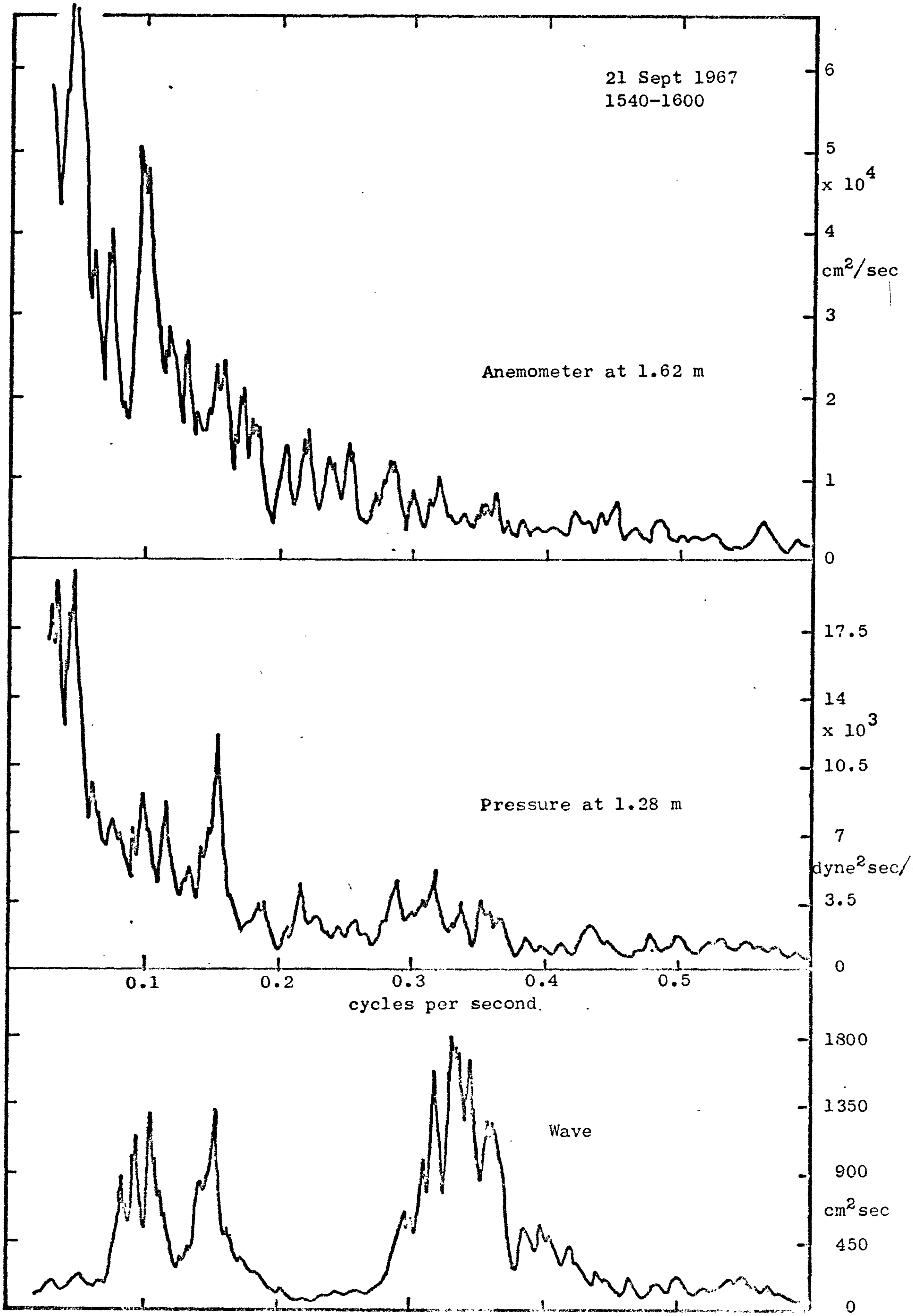

Figure 14. Wave, wind and pressure energy spectra

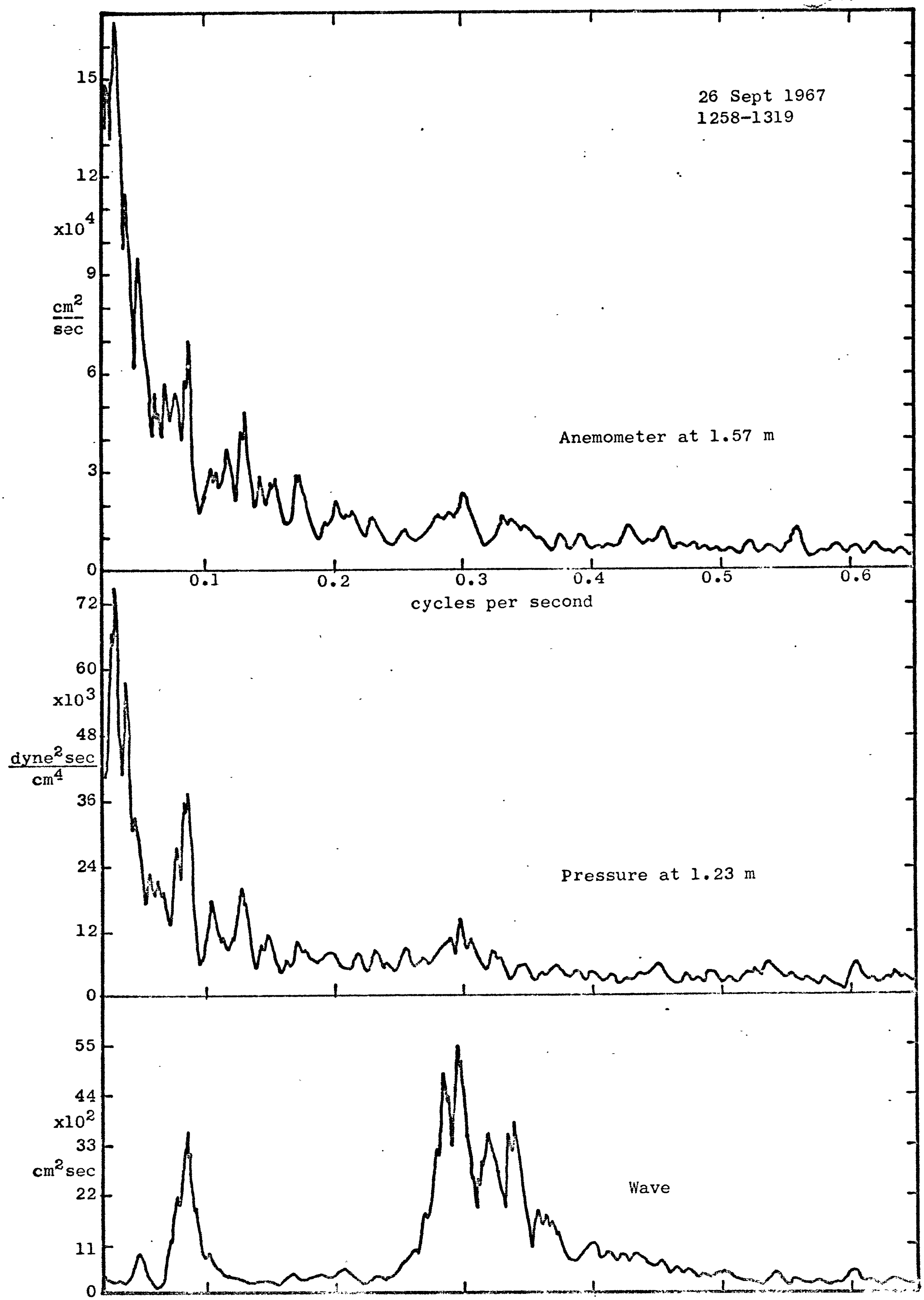

Figure 15. Wave, wind and pressure energy spectra

maxima. When filters were used in an attempt to do correlations of frequency components with smaller amplitudes the results were sometimes erratic. The investigation was, therefore, confined mainly to the predominant frequencies present. On the basis of many repeated runs and variations in technique the phase angles given are probably correct to within ±5° in most instances.

The results of correlating the water surface variations with the wind velocity at the lowest fixed anemometer, height usually about 1 meter above MSL, appear in table 1. The angle β is the phase angle by which the maximum wind velocity at the anemometer leads the trough of the waves. In all cases the maximum wind velocity occurs at nearly the same time as minimum water level, i.e., above the trough! The velocity recorded by the anemometer is of course the magnitude of horizontal velocity, and the velocity above the trough may have a strong lateral component. Although on 16 to 18 August and 21 September there is no satisfactory data from floating anemometers available because of either instrumentation failures or time limitations, cross-correlations of the wave with the wind at all heights on all days indicate the maximum velocity occurs somewhere above the trough. Visual observation of the floating anemometers on two days with a light breeze blowing over old swell confirm this finding. There is one exception. On 26 September during the run from 1200 to 1320 filtered cross-correlations of wave with the floating anemometers at 50 and 70 cm indicate the maximum velocity occurred 90° to 145° before the trough at those heights; however, these correlations were of a low level. Moreover,

TABLE 1

Phase Relationship of Wind and Wave - Buzzards Bay Project - 1967

Date	Time	Filter[1] cps	τ_m[2] sec.	β_r[3]	Anemo. corr.	Period sec.(T)	Height meters	β[4]
Non-generating Conditions								
8/2		none	+.57	+30°	+5°	6.7	1.2	+35°
		150	+.54	+29°	+5°	6.7	1.2	+34°
8/3		none	-.12	-6°	+5°	6.7	1.22	-1°
8/7	1441-1502	none	+.21	+11°	+5°	6.9	1.18	+16°
	1602-1622	none	+.55	+29°	+5°	6.9	0.92	+34°
	1624-1645	none	+.38	+20°	+5°	6.9	0.80	+25°
8/9		none	+.45	+30°	+8°	5.4	1.2	+38°
8/16		none	+.13	+6°	+4°	7.1	1.0	+10°
Generating Conditions								
8/4	1102-1123	none	-.3	-20°	+8°	5.4	1.5	-12°
	1102-1123	185	-.26	-17°	+8°	5.4	1.5	-9°
	1123-1144	none	-.1	-7°	+8°	5.4	1.65	+1°
	1143-1204	185	-.25	-17°	+8°	5.4	1.55	-9°
	1143-1204	none	-.3	-20°	+8°	5.4	1.55	-12°
	1110-1200	185	-.18	-12°	+8°	5.4	1.55	-4°
8/18	1201-1223	none	-.1	-9°	+15°	4.0	1.65	+6°
	1201-1223	275	+.43	+39°	+15°	4.0	1.65	+54°
	1223-1244	none	-.3	-27°	+15°	4.0	1.61	-12°
	1223-1244	275	+.31	+28°	+15°	4.0	1.61	+43°
	1223-1244	260	-.12	-11°	+15°	4.0	1.61	+4°
9/21	1540-1600	330	+.21	+24°	+24°	3.1	1.62	+48°
9/26	1202-1223	300	-.02	-2°	+24°	3.1	1.62	+22°
	1202-1223	300	+.01	+1°	+24°	3.1	1.62	+25°
	1225-1246	300	+.32	+36°	+22°	3.2	1.59	+58°
	1256-1317	none	-.04	-4°	+19°	3.4	1.57	+15°
	1258-1319	300	+.13	+14°	+19°	3.4	1.57	+33°
9/26	1538-1558[5]	250	-.6	-54°	+15°	4.0	4.16	-39°

Notes:

1. Filter - The center frequency of the band-pass used in filtering. (Data is speeded up by a factor of 1000.)
2. τ_m - Delay time for maximum peak of correlation between wave (trough) with wind velocity (maximum) delayed in real world time.
3. $\beta_r = \frac{\tau_m}{T}(360°)$. $\beta = \beta_r +$ anemo. corr.
4. β = phase angle by which the wind velocity maximum leads the trough, using the predominant wave period as a reference.

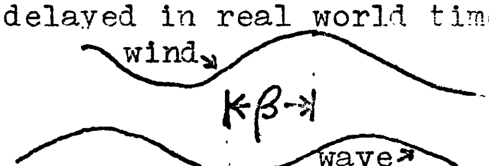

5. This correlation was of a low level; i.e., the amplitude of the peak was small.

checks against the fixed anemometer at 1.6 meters above MSL indicated a maximum velocity near the trough. Unfortunately this one inconsistency was never satisfactorily resolved.

Cross-correlating the horizontal wind velocities at various heights against one another, permits the determination of a time and phase relationship between the wind at various heights. Table 2 gives the results of such correlations. The data from 4 August was analyzed extensively as it was the one day on which waves were actively being generated and on which a complete set of anemometer data was obtained. The results indicate that for periodic disturbances in the air close to the surface, the maximum correlation usually occurs if the signal from the higher anemometer is delayed in time with respect to the signal from the lower. On 4 August the critical layer had a height of 2 to 8 meters depending upon the time period considered. As compared to other days there was no marked difference in the phase relationship of the wind variations near these heights except that they seemed to be a little larger than for non-generating conditions. On 18 August the critical layer was at a height between 2 to 3 meters. On this date the phase of wind velocity variations appears to have shifted first upwind, then downwind, and finally upwind with increasing height. On 21 September the critical layer varied between 120 and 40 cm in height. Only two sets of cross-correlations between floating anemometers and the fixed anemometer were run. The correlations were of a low level and not at all symmetrical. The phase as determined from the correlation peak was similar to 4 August. These were the only days

TABLE 2 - Phase Relationship of Wind at Various Heights - Part I

Date	8/2	8/3	8/7	8/7	8/9	8/16	8/4	8/4
Time			1441-1502	1602-1622			1110-1200	1102-1123
Filters[1]	150	HP	HP	HP	185	140	185	None
Quantity[2]	τ_m γ	τ_m γ	τ_m γ	τ_m γ	τ_m γ	τ_m γ	τ_m γ	τ_m γ
Anemo. 4	+0.1 +5°	+0.15 +7°	+0.15 +8°	+0.3 +15°		+.15 +7°	+.19 +12°	+.15 +10°
3	+0.1 +5°				+.15 +10°	+.15 +7°	+.2 +13°	
2	+.07 +3°	+.11 +5°	+0.1 +5°	+0.2 +10°		+.1 +5°	+.14 +9°	+.2 +13°
Height 1[3]	1.2 m	1.22 m	1.18 m	0.92 m	1.2 m	1.0 m	1.55 m	1.50 m
70 cm[4]	-.12 -6°	-.1 -5°	-.09 -5°	-.05 -3°	-.14 -9°		-.06 -4°	-.3 -20°
50 cm	-.06 -3°	-.15 -7°	-.15 -8°	-.2 -10°	-.2 -13°		-.05 -3°	-.4 -26°
30 cm	-.04 -2°	-.25 -12°	-.4 -20°	-.19 -10°	-.19 -12°			
Date	8/4	8/4	8/4	8/4	8/4	8/4	8/4	8/4
Time	1102-1123	1123-1144	1123-1144	1123-1144	1143-1204	1143-1204	1143-1204	1143-1204
Filters[1]	HP	185	None	285	185	185	HP	285
Quantity[2]	τ_m γ	τ_m γ	τ_m γ	τ_m γ	τ_m γ	τ_m γ	τ_m γ	τ_m γ
Anemo. 4	+0.2 +13°	+0.3 +20°	+.42 +28°		+.35 +23°	+.35 +23°	+.24 +16°	+.25 +26°
3	+.15 +10°	+.25 +17°						
2	0 0°	+0.2 +13°	+.2 +13°	+.25 +26°	+.2 +13°	+.12 +8°	+.1 +6°	
Height 1[3]	1.50 m	1.65 m	1.65 m	1.65 m	1.55 m	1.55 m	1.55 m	1.55 m
70 cm[4]	-.28 -18°	-.03 -2°	0 0°	+.06 +6°	0 0°	-.05 -3°	-.16 -10°	+.05 +5°
50 cm	-.15 -10°	-.03 -2°	-.03 -2°	-.04 -4°	0 0°	-.05 -3°	-.2 -13°	-.04 -4°
30 cm		-.04 -3°	-.13 -8°	+.05 +5°	-.03 -2°	-.1 -6°	-.28 -18°	+.05 +5°

Notes: An explanation of filters, quantity, anemo., and height is included in Part II.

TABLE 2 - Phase Relationship of Wind at Various Heights - Part II

Date	8/18		8/18		8/18		8/18		8/18		9/26		9/26	
Time	1202-1223		1202-1223		1202-1223		1223-1244		1223-1244		1538-1558		1538-1558	
Filters[1]	275		265-285		None		275		None		250		None	
Quantity[2]	τ_m	γ	τ_m	γ	τ_m	γ	τ_m	γ	τ_m	γ	τ_m	γ	τ_m	γ
Anemo. 4	+.1	+9°	-.1	-9°	+.05	+4°	+.2	+18°	+.15	+14°				
3	+.2	+18°	+.1	+9°	+.05	+4°	+.24	+22°	+.2	+18°	+.5	+47°	+.1	+9°
2	-.1	-9°	-.2	-18°	-.05	-4°	-.04	-4°	-.05	-4°	+.15	+17°	+.4	+27°
Height 1[3]	1.65 m		1.65 m		1.65 m		1.61 m		1.61 m		2.16 m		2.16 m	

Date	9/26		9/26		9/26	
Time	1202-1222		1225-1246		1256-1317	
Filters[1]	300		300		300	
Quantity[2]	τ_m	γ	τ_m	γ	τ_m	γ
Anemo. at Height 1	1.62 m		1.59 m		1.57 m	
70 cm[4]	-.1	-12°	-.2	-23°	-.2	-21°
50 cm	-.28	-34°	-.15	-18°	-.16	-17

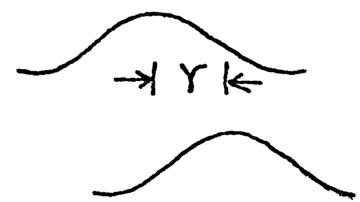

Notes: 1. Filters: The center frequency of the band pass used in filtering. Data was speeded up by a factor of 1000, so 150 represents a frequency of 0.150 cps in real time. HP indicates a high pass filter with a 3 db cutoff near 0.150 cps in real world time was used.

2. Quantity: τ_m = time delay of maximum correlation peak between velocity at anemometer 1 with velocity at indicated anemometer delayed. $\gamma = \tau_m(360°)/\text{period}$ where γ is the phase angle by which the velocity at a height leads or lags the velocity at anemometer 1. The period is the period of the predominant wave present.

3. Height 1 is the height of reference anemometer above MSL. This is the reference point for the data in the table. Anemometers 2, 3 and 4 were 1, 2 and 3 meters above 1, respectively.

4. The floating anemometers floated at the height indicated in centimeters above the water surface.

on which the critical layer was within the height range of the anemometer arrangement in use. On 26 September when the inconsistency previously mentioned was observed the critical height was below the level of the lowest floating anemometer.

Atmospheric pressure measurements made on 21 and 26 September were correlated against the waves. The results appear in table 3. The delay time was determined both from the time delay of the maximum correlation peak and the zero crossings of the correlations, for these correlations were not as symmetrical about the maximum correlation peak as most of the other correlations encountered in this study. On 26 September the maximum pressure occurred above or after the trough. On 21 September the maximum pressure, 1.28 m above MSL, was observed to occur before the trough. As previously mentioned the data on 26 September was obtained under more suitable conditions than on 21 September. Also on 21 September the pressure probe was 15° from pointing into the wind during part of the run because of a slow yaw of the buoy. This should not, however, have degraded the data, as the probe was not very sensitive to small variations in wind direction.

TABLE 3

Phase Relationship of Pressure and Wave

Time	Period sec.	τ_m[1] from max. peak of correl.	α[2]	Filtered	τ_{om} from zero crossings	α[2]	Height of probe above MSL in meters
26 Sept. 1201-1222	3.0	0	0°	no	-.07	-7°	1.28
1225-1246	3.1	-.05	-6°	no	-.09	-10°	1.25
1225-1246	3.1	-.06	-7°	yes	-.10	-11°	1.25
1256-1317	3.4	+.07	+7°	no	+.06	+6°	1.23
1256-1317	3.4	+.01	+1°	yes	+.08	+8°	1.23
1258-1319	3.4	+.05	+5°	no	-.01	-1°	1.23
1258-1319	3.4	0	0°	yes	+.01	+1°	1.23
1516-1615	4.0	-.38 to -.6	-35° to -55°	yes			1.82
1518-1540	4.0			yes	-.55	-51°	1.82
1522-1543	4.0	-.3	-28°	yes	-.28	-26°	1.82
1522-1543	4.0	-.4	-37°	no	-.15	-14°	1.82
1538-1558	4.0	-.47	-43°	no			1.82
21 Sept. 1540-1600	3.1	+.5	+58°	no	+.1	+12°	1.28
1540-1600	3.1	+.25	+29°	yes	+.25	+29°	1.28

Notes:

1. τ_m = delay time for maximum correlation between wave (trough) with pressure(maximum) delayed.
2. α = phase difference between wave and pressure.

$$\alpha = \frac{\tau_m}{\text{period}}(360°)$$

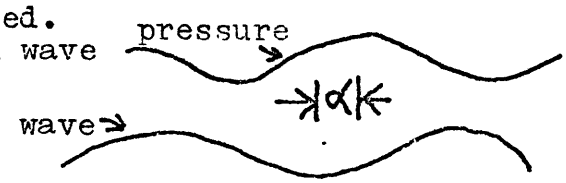

The 1201-1319 runs of 26 Sept. were made under the most suitable conditions of wind, sea, and instrument location. Conditions for other runs on 26 Sept. were also quite good.

Pressure measurements on 21 Sept. were made using a battery-powered voltage controlled oscillator whose batteries had been on for a considerable time just prior to this run. Although the modulated signal recorded had a low level, the demodulated signal appeared normal when compared to the measurements of 26 September.

Discussion

The wind velocity profiles are similar to those reported by numerous other investigators and are not much different from those observed over open fields. Except for the slight positive curvature from the floating anemometers under non-generating conditions, the profiles are similar to those from Project Windy Acres (1967) where data were taken at a site on a nearly flat plain in Kansas. Under generating conditions it appears the logarithmic profile is a good first approximation to the actual profile. The slight negative curvature near the surface on 21 and 26 September is puzzling when contrasted to the other profiles which have positive curvature at that height. Perhaps the profiles are substantially modified because of the use of floating anemometers. Roll (1965) comments on this, suggesting that floating cup anemometers because of their characteristics will reflect more the flow conditions above the crest than those above the trough. However, he assumed the velocity above the crest was greater than above the trough (Motzfeld, 1937); nevertheless, he found the mean wind speed from a floating anemometer should be about 5 percent less than from a fixed anemometer at the same average height (due largely to the effect of a logarithmic profile). In checking this I found that the U vs log Z profile should acquire negative rather than positive curvature. In this investigation the profile continuity between the unadjusted outputs of the floating and fixed anemometers matches well on some days, and not too well on others. The continuity does appear to be better on the generating days than on the non-generating days where the floating anemometers may be giving low values.

At higher levels, 1 to 4 meters and above, the U vs log Z profile curvature is negative on most non-generating days and only slightly negative or even positive on generating days. On 18 August, a generating day with a negative lapse rate (stable conditions), the curvature is not nearly so negative as might be expected when compared to other profiles. This tendency to a more positive curvature at upper levels under generating conditions may be an indication of the increased transfer of kinetic energy to lower levels from above.

The gustiness of the wind is important in profile modification and might be significant in the generation process. Any small change in the profile can result in large changes of the second derivative of the velocity with respect to height, and therefore substantially change the calculated momentum (Miles' theory) transfer to the surface. A gusty wind with a certain average velocity contains more energy than a steady wind with the same velocity. On the basis of numerous one-minute profiles obtained in this study, this increase in energy only rarely approaches 10 percent. The same conclusion is true when rms variations of wind velocity obtained from the taped signal are considered.

Drag coefficients were computed using the profiles and compare favorably with those obtained by other observers. For a height of 2 meters the values lie mostly between 0.0007 and 0.0036 depending upon the particular day and period. The drag coefficient was not a constant and the friction velocity seemed to have at best a weak dependence upon the horizontal velocity at 2 meters above the surface. A table of friction velocities and drag coefficients appears in Appendix D.

The most surprising result is that the maximum wind velocity occurs above the trough. I must confess that when this observation was first made visually it was temporarily dismissed as being the result of some unknown and unusual air-sea boundary condition. Even when the analysis of the processed data later led to this same result, two weeks were spent in attempting to locate some error to account for the inconsistency between this and wind tunnel observations, but without success.

How does this difference arise? Apparently the air flow over ocean surface waves is different from that in a wind tunnel. Consider wind tunnel flow in the reference system moving with the primary wave component as shown in figure 16. Here the mean air speed is greater than the wave velocity and because of the presence of an upper boundary the streamlines of the air flow are squeezed together above the crest; thus, the maximum velocity occurs near the crest, and the maximum pressure above the trough. The boundary effect may largely determine the relationship of air velocity and pressure with respect to the wave within the tunnel. If the maximum air velocity does occur above the trough, then Stewart's possible streamline configuration, figure 1b, with some modification of the vertical scale may be correct, but there still would be a region of minimum velocity in the very bottom of the trough which was not observed. The lowest anemometer

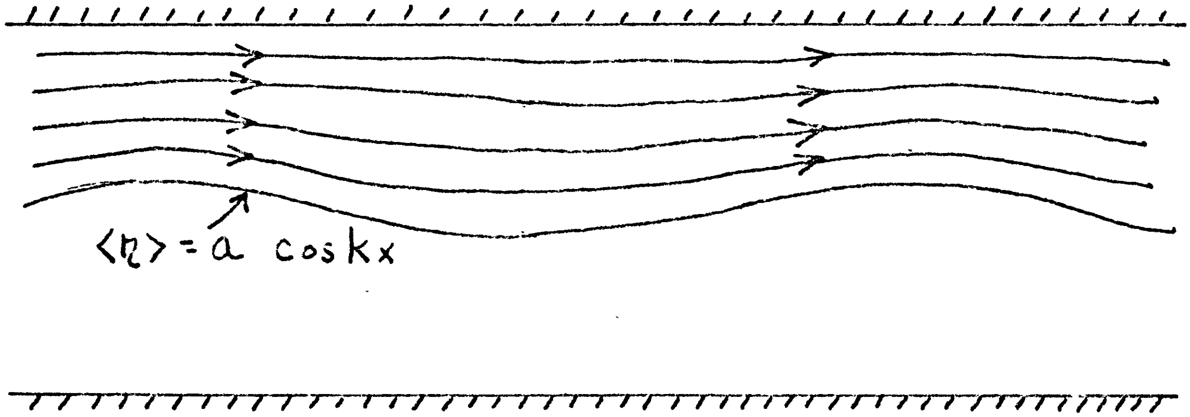

Figure 16. Air flow over water in a wind tunnel with wind velocity greater than wave velocity, showing how the presence of an upper boundary probably dominates the distribution of air velocity. The reference system moves with the wave profile. The maximum pressure in this laminar flow occurs above the trough, and the maximum velocity above the crest.

floated at a height of 30 cm and may not have been low enough to record such a minimum. Another likely explanation might be that the air flow must be considered in 3 dimensions. Smoke floats were used on several days with inconclusive results, but the smoke on occasion did appear to be deflected slightly one way at the crest and then back the other way near the trough; however, the smoke did not follow the surface closely enough to make valid qualitative estimates of any 3-dimensional flow.

The concentration of shear right at the surface below our anemometer level may be involved in the explanation. Perhaps the observation of 26 September that the maximum velocity at the floating anemometers occurred on the back of the wave is a result of concentration of shear; however, no other observations substantiate this. Measurements even closer to the sea surface are needed.

The few pressure observations indicate the pressure maximum does occur above the trough at the height of the pressure probe, although the results cannot be considered conclusive. The asymmetry of the cross correlations between wind and wave about the maximum correlation peak suggests a nonsinusoidal variation of the pressure, such as in flow where separation occurs at the surface. This gives additional support to Stewart's flow field.

The pressure distribution closer to the surface than at the probe height is of course unknown. On 26 September during the 1200-1320 run, the maximum pressure occurred above the trough at the probe height of 1.25 m above MSL. During the 1515-1615 run, the maximum pressure at 1.82 m was observed to lag the trough. If on this day, the change in the maximum pressure point's location with height approximated a linear relationship all the way to the surface, the maximum pressure at the surface would have occurred about 90° before the trough. While these two runs are not very good for comparison, they are all that is available. Actual pressure measurements from floating sensors at the surface are needed to resolve this question.

The relationship of wind velocity disturbances with height is similar to that observed by Favre _et al_ (1958) over a solid boundary in a wind tunnel. Also Taylor (1958) had observed a maximum correlation of temperature over land at various heights if the output of the upper sensor was delayed.

No dependence upon wind velocity of the time delay necessary to produce maximum correlation was found. As the band-pass of the filters used was not sufficiently narrow, it is impossible to make a statement about the behavior of any discrete frequency component. However, the major periodic disturbance to the flow field appears to originate at or near the surface and is propagated fast enough, upward and downwind, so it reaches an upper level before lower levels experience the disturbance. (The different lags on 18 August are puzzling and might be the result of generation during stable stratification, or perhaps reflect a transition stage where a mechanism like that of Miles is being supplanted or aided by another. Also recall that the generating wind was blowing at an angle of 60° to the swell.) Because of the vertical wind shear, it is not surprising that disturbances originating at the surface are propagated more rapidly downwind at higher levels, but why they do this where the swell or sea travels faster than the wind is not at all clear.

As a check on Miles' theory some computations based on equation (3) were made. As an example, on 4 August the critical height varied between 2 and 8 meters in height during the period from 1110 to 1150. The average profile for this period put the critical height at 4.2 meters. Using this height and the average profile one finds,

$$U''(Zc) = 0.337 \times 10^{-3} \text{ cm}^{-1} \text{ sec}^{-1}$$

$$U'(Zc) = 0.184 \text{ sec}^{-1}.$$

For the dominant wave component the velocity is 880 cm sec^{-1} and the wavelength 49 meters; thus, $k = 1.3 \times 10^{-3} \text{ cm}^{-1}$.

The wave Energy can be obtained from

$$E = \rho g a^2, \tag{4}$$

where ρ = density of sea water,

a = the rms value of wave amplitude,

g = 980 cm sec^{-2}, the acceleration of gravity.

Using a = 50 cm we find E = 2.5 × 10^6 ergs cm^{-2}. The energy changed 6.5 percent during the 40 minute period in question; therefore,

$$\overline{dE}/dt = \frac{2.5 \times 10^6 (.065)}{2.4 \times 10^3} = 67.5 \text{ ergs} \cdot \text{cm}^{-2} \text{ sec}^{-1}.$$

Using these values in (3) one can solve for $|\bar{W}|$ = 4.10 cm sec^{-1}. This is the mean absolute value of the vertical velocity, in the reference frame moving with the wave, necessary to sustain the energy transfer rate according to Miles' theory.

Miles and Lighthill both give a first order approximation for W which Stewart (1967) presents in the form,

$$\overline{W^2} = \frac{1}{2}\left[\frac{4\pi^3 H}{\frac{dU}{dz}(z_c)\ \lambda^3} \int_{z_c}^{\infty} (U-c)^2 e^{-kz}\, dz\right]^2, \tag{5}$$

where H = wave height. The integral in (5) was solved numerically using the actual profile to find 5.56 × 10^6 cm^3 sec^{-2}. Solving (5) with H = 140 cm, one finds $|\bar{W}|$ = 3.16 cm sec^{-1}. This is in surprisingly good agreement with the value obtained from the real energy transfer.

Using the measured energy change in 0.1 cps bands, centered at the dominant wind wave frequency, and the observed wind profiles a series

Similar computations were made using the data for 21 and 26 September. The results are presented in Table 4. On 4 August and 21 September, Miles' theory provides a good estimate of the energy transfer rate. The predicted increase is low in each case. On 26 September the energy computations are not as good, and predict <u>too much</u> energy. For the 1210-1600 run on 26 September, the profile used was a mean of the profiles for the beginning and end of the period. No measurements were made from 1320 ~~until~~ to 1515 while rearranging instruments. The profile changed markedly during this period, and the results are poor. In this case using averaged data over a long time period is apparently not a valid procedure. Some of the energy deficiency may also be traced to the wave gauge. The original reference wave gauge's bracket broke after the first run, and another gauge was used during the second run. Calibration of records against the original reference gauge gave wave heights ten percent less than for the reference gauge. No correction was made for this difference, as all gauges were originally matched, and a later check revealed only a minor difference between the gauges. At best this correction would reduce the energy ratio to five.

In the five other cases the predicted and observed energy changes differ by a factor of four or less. Potential errors in the energy measurements could reduce this by 50 percent. These days were the only ones where energy data was available for computations. The data record from 18 August was not long enough to produce a measurable energy change.

TABLE 4

Comparison of Measured Energy Transfer and Miles' Theory

Date	4 August	21 September	21 September
Time	1110-1150	1310-1505	1505-1555
ΔE ergs cm^{-2}	1.62×10^5	$.39 \times 10^5$ ($.256 \times 10^5$)	$.191 \times 10^5$
$\overline{dE/dt}$ ergs $cm^{-2}sec^{-1}$	67.5	5.7 (3.75)	7.1
$\dot{E}m$ ergs $cm^{-2}sec^{-1}$	40.5	1.85	6.1
$\lvert\overline{W}\rvert$ energy cm sec^{-1}	4.10	1.43 (1.16)	1.31
$\lvert\overline{W}\rvert$ profile cm sec^{-1}	3.16	0.82	1.22
Z critical cm	420	102	63.5
Ratio of $\lvert\overline{W}\rvert$	.77	.57 (.71)	.93
Ratio of energies	.60	.33 (.49)	.86
H (cm)	140	23	27
λ (cm)	5000	1320	1500
U'(Zc) sec^{-1}	.184	.489	.69
U"(Zc) $cm^{-1}sec^{-1}$	$.337 \times 10^{-3}$	$.425 \times 10^{-2}$	$.76 \times 10^{-2}$
U(Zc) cm sec^{-1}	880	475	500
Integral cm^3sec^{-2}	5.56×10^6	$.454 \times 10^6$	1.194×10^6

Notes: $\overline{dE/dt}$=The rate of energy change determined from the energies measured in the spectra divided by the time between the spectra.

$\dot{E}m$=Rate of energy transfer from Miles' theory.

Ratios are $\frac{\text{calculated value}}{\text{measured value}}$.

H = Wave height.

Zc = Critical height.

(continued on next page)

TABLE 4 (continued)

Comparison of Measured Energy Transfer and Miles' Theory

Date	26 Sept.	26 Sept.	26 Sept.
Time	1210-1300	1525-1605	1210-1600
ΔE ergs cm^{-2}	1.0×10^5	1.61×10^5	7.25×10^5 (5.63×10^5)
$\overline{dE/dt}$ ergs $cm^{-2} sec^{-1}$	33.3	67	52.5 (41)
$\mathring{E}m$ ergs $cm^{-2} sec^{-1}$	116	249	342
$\lvert\overline{W}\rvert$ energy cm sec^{-1}	0.53	1.60	0.83 (0.74)
$\lvert\overline{W}\rvert$ profile cm sec^{-1}	0.99	3.08	2.12
Z critical cm	3.55	28.3	11.7
Ratio of $\lvert\overline{W}\rvert$	1.87	1.92	2.56 (2.86)
Ratio of energies	3.48	3.72	6.50 (8.3)
H (cm)	57	81	73
λ (cm)	1500	2450	1950
U'(Zc) sec^{-1}	20.9	3.7	7.46
U"(Zc) $cm^{-1} sec^{-1}$	6.6	.127	1.03
U(Zc) cm sec^{-1}	500	625	565
Integral $cm^3 sec^{-2}$	14.1×10^6	23.4×10^6	18.9×10^6

Notes: (continued) U(Z) = Horizontal wind velocity.

Quantities in parenthesises were based on total energy changes rather than on a spectral band. The lower value for total energy results from the reduction of swell as the wind driven part of the spectrum grew.

Integral for the period is the value as determined from the wind profile of the integral

$$\int_{z_c}^{\infty} (U-c)^2 e^{-kz} dz,$$

where c = U(Zc), the phase velocity of the dominant wind driven wave.

Thus, using actual profile data indicates Miles' theory may account for most of the energy transfer under the conditions encountered here. The ratio of wind speed at a height of 10 meters to the speed of the dominant wave was always in the range 1.0 to 1.7. For higher ratios, as one might find near shore in limited fetch conditions, this may not be true.

The slope and curvature of the profile effect U"(Zc) and U'(Zc) considerably. When extending anemometer observations to the surface a small change in the slope may raise or lower Zc substantially and in turn alter the derivatives even more so. On 26 September the critical layer was always well below the lowest velocity observation height. On the other 2 days the critical height was bracketed by anemometers. This cannot account for all the difference in the computations, but it may account for some.

I am unable to explain why the spectra of horizontal wind velocities contain a distinct peak at the dominant wave frequency on one generating day and not on others. The sea was nearly fully developed only on 4 August, the day with the distinct peak, and this may have significance. Also, a check of wind spectra from two very weakly generating days, 3 and 7 August, revealed peaks in the wind corresponding only to the frequency of the swell. All waves being actively generated were deep water waves, and therefore underwent little if any velocity change because of shoaling. Therefore, wave velocity and amplitude changes due to shoaling cannot here be considered as possible factors in the coupling or uncoupling of the wind and wave.

While Miles' theory may be important under many circumstances the shear right at the surface and the three dimensional aspects of the flow have yet to be investigated and may provide insight into the processes taking place near the surface. Had I observed a maximum wind velocity above the crest where expected and distinct peaks in the horizontal wind velocity spectra, I would feel Miles' theory may explain the energy transfer process satisfactorily, however, I feel other processes not now understood are also important.

Summary

Using cup anemometers, wave gauges and a pressure probe mounted on a stabilized buoy it has been possible to obtain and analyze simultaneous records of wave height, wind at several levels just above the surface and pressure at a single height. Information was gathered under different conditions of wind, sea and weather. The results are:

(1) The horizontal wind velocity to a good first approximation increases as a logarithmic function of height.

(2) A small distance above the surface, about 1 meter, the maximum wind velocity occurs above the trough, whether the critical layer is above or below that level.

(3) At a height of 1 to 2 meters the maximum pressure, on the two days when pressure measurements were made, occurred above the trough. This suggests that 3 dimensional flow and turbulence are important in view of (2).

(4) Under developing conditions the peak of the wave energy spectrum moves to a lower frequency. An earlier maximum spectral component reaches a final state with 50 to 80 percent of its maximum energy value.

(5) In two cases the generating part of the wave spectrum appeared to take energy from the swell.

(6) Wind disturbances at a location are observed first at upper levels, even when the swell travels faster than the wind.

(7) Peaks in the horizontal wind velocity spectra at the frequency of the generating waves are present at times during generation,

but they are often very weak or missing.

(8) Using the actual wind profile data, Miles' theory provides reasonable estimates of the rate of energy transfer to the waves.

(9) Short term changes (10 minutes to about 1 hour) in the vertical profile of the horizontal wind velocity are significant in energy transfer to the sea. Small velocity changes can result in considerable changes in the critical height, and therefore changes in $U''(Zc)$ and $U'(Zc)$ and more especially the ratio $U''(Zc)/U'(Zc)$. Where the vertical profile of the wind is well known, and the generating conditions well defined, the rate of energy transfer according to Miles' theory gives reasonable agreement with observations. However, by averaging over large time periods where conditions are not stationary, and by making strong assumptions about the profile and its slope, the data becomes virtually useless. Very short term changes (less than 10 minutes) of the wind are probably significant too. Also, shear stresses near and at the surface may be very important in wave generation.

Recommendations

More and better simultaneous observations of water level, pressure, temperature, and wind at and just above the surface are required. These measurements require a vertical and horizontal scope to provide a more complete description of the processes at work. This can be achieved within the present program.

Fast response anemometers, preferably hot film probes, should measure the air flow in three dimensions. Horizontal wind velocity measurements at four or more levels with cup anemometers are required for reference and calibration purposes. At least one anemometer should be used between 4 and 12 meters, where there was none in this study. Using a float or other surface following device, pressure, temperature and wind measurements at several points, at least one of which is closer than 30 centimeters to the surface should be made under various sea conditions. Modifications of the temperature thermistors and the pressure system as used in this work are probably suitable for use close to the surface. The wave gauges are already satisfactory.

In the horizontal field one set of instruments, aligned with the wind and wave direction, ought to be spaced at less than one half the expected predominant surface wave length. For Buzzards Bay a good wave length is 25 meters. Cross wind placement of wind and temperature sensors is also needed.

Specific data processing recommendations are included at the end of Appendix C.

Improvements planned in the Meteorology Department's data processing system will permit far better and faster analysis of the data than was possible in this work. With the use of narrow band filters, cross spectra can provide more accurate information on phase and amplitude relationships. Variation in the behavior of disturbances at close but separate frequencies may be more clearly determined. The need for correlating the different velocity components and temperatures from horizontally as well as vertically separated locations is obvious.

I believe that the basic approach attempted here is the proper one. With refinement and the use of new ideas and equipment in both data collection and processing, a great deal more useful information will be obtained by continuing measurements at the present site.

Acknowledgements

Professor Erik L. Mollo-Christensen has provided me for three years with excellent advice and encouragement. His suggestion to investigate the wind flow around a model of the BBELS tower eventually lead me to this study. I am also thankful for his continuing confidence in me and my work.

Professor D. P. Keily who provided me with a place to work during my stay at M.I.T. offered advice and encouragement on numerous occasions for which I am grateful. Dr. Seelye Martin provided help and encouragement in the field and in attempting to interpert the results of the analysis. Professor T. F. Webster also provided me with assistance and advice.

Mr. Ortwin Von Zweck who has worked closely with me in this project has been a most helpful colleague as well as a good friend. He has been instrumental in the success of the study at each step since its inception.

I am also indebted to Messrs. James Peers and Ken Morey for their excellent electronic and technical support both at M.I.T. and on Buzzards Bay. Their attention to detail and willingness to work long hours under unpleasant conditions contributed greatly to the success of this project. Mr. David Berrian also assisted ably in the field work.

Professor Patrick Leehey of the Department of Naval Architecture and Marine Engineering provided the use of certain data processing equipment and the space to use it which were vital to this work. Mr. Edward Bean in his machine shop fabricated much of the hardware to use on the buoy and also supported me in some of my earlier attempts to take measurements.

Many others deserve credit for contributing to this work. They include; Mrs. J. McNabb and Miss L. Harris who typed the manuscript; Lt. Cdr. K. W. Ruggles who suggested the quotation from Sir Francis Chichester and other references and who also provided assistance in the field; Mr. Tony Cella who assisted me at Lewis Wharf; and my wife, Marylee, and children, Amy and Daniel, who provided love and understanding whether things were going right or wrong.

The U.S. Coast Guard was very cooperative in making available the facilities at BBELS. Their support was very much appreciated by all associated with the project.

I am very thankful that the U.S. Navy has permitted me to pursue a full time program of graduate study while on active duty. This work was financed by the Navy under ONR contract Nonr-1841(74), by the U.S. Naval Underwater Weapons Research and Engineering Station under Grant N 140-(122) 2762B, and the National Science Foundation under grant NSF GP4321.

Appendix A

The Buoy

The buoy was constructed of three, 3 foot diameter, steel, cylindrical tanks each 20 feet long. The tanks provided the flotation and were arranged in a cluster. A triangular, truss type superstructure 27 inches on a side extended 30 feet above and below the tanks. A 4 inch by 6 inch steel mast extended from the top of the tanks to 18 feet beyond the upper superstructure.

At the site the buoy was moored with the tanks completely submerged. During installation the tanks were partly flooded to reduce its reserve buoyancy. The lower end of the buoy was secured by a short cable or bridle to a seven ton concrete block in 60 feet of water. The weight of the mooring exceeded the buoy's reserve buoyancy by about 6,000 pounds. Sixteen feet of the upper superstructure extended above MSL. Underwater the buoy was guyed to two 1,000 pound anchors. The guys were connected to the buoy at the top of the tanks. Originally three guys were to be used, but one of the guys parted under heavy strain during installation and was never replaced. Also a 20 foot long, 8 inch channel yardarm at the bottom of the buoy originally guyed to two anchors for steadying in azimuth was removed as the strain on the channel was excessive. Instead the upper part of the bridle was pulled sideways with a wire to a 3,000 pound anchor. This reduced considerably the original motions of the buoy which had acted as a double pendulum.

The buoy was not affected much by wind driven waves of 5 seconds period or less, but it did respond to swell and had a small amplitude ($\leq 2°$) roll or pitch with a period of 6 to 9 seconds with a 2 foot swell of the same period running. Also at the time of spring tides during maximum flood or ebb tide (>1.0 Knot) the buoy would list with the current, usually about 8° to 10° depending upon the direction of the current and location of the guys. Once it was observed to list 15° at a maximum flood tide of 1.5 knots. Initially in a tidal current the buoy vibrated at 3 cps, probably from the shedding of vortices by the cylindrical tanks. This also contributed to other buoy motions. At the suggestion of Professor E. Mollo-Christensen this problem was eleminated by wrapping a 2 1/2 inch rubber hose around the tanks. The yaw (angular twist) of the buoy was less than 2° during August.

Fortunately information was normally collected under moderate conditions of swell and current, and buoy motion was a minor problem. Late in August one guy parted, and both guys were replaced as a diver's inspection showed that the other guy was chafing. The stability of the buoy surprisingly improved with one exception. As the tide changed the buoy would now suddenly yaw about 100°, this change taking place in about one minute. Apparently both guys were not taut. One guy would hold the buoy against the tide, when the tide reached a critical phase (there is a rotary tide at the site) the buoy would swing as the strain on the first guy was relieved and continue swinging until the other guy took a strain. This occurred about once on a working day and would require interruption of any data run being made. It also scared anyone on the buoy, especially during the first few occasions on which it was observed.

A platform six feet square was built atop the buoy superstructure using staging clamps, 2 inch pipe, and planks. A somewhat similar platform was built around the superstructure 6 feet below the other platform. Space on the lower platform was very limited because of superstructure strength members and work there was very hampered; however, this platform was very useful.

The main mast had mounted on it a stainless steel track on which goose necks rode and provided support for the inboard ends of two equal length booms. The two booms were connected through pivots at their outer ends to a vertical pipe which served as an instrumentation mast. The spacing between the 2 booms was the same at the inboard (main mast) and outboard (instrumentation mast) ends. Each end of the upper boom was connected by a double purchase to the top of the main mast. The hauling part of the double purchases was led to the upper platform from where they could be worked by personnel manning the buoy. The boom and mast formed a parallelogram whose position and shape could be controlled in a vertical plane by working the double purchases. This arrangement kept the seven meter long instrumentation mast nearly parallel to the main mast. With the outer end of the booms in the fully up position the instrumentation mast came to within a meter of the buoy's main mast and the instruments mounted on the mast could readily be serviced in this position. Guys were rigged to position and steady this rig in azimuth. Figure 2 shows the booms and mast as they appeared during a run.

During August the rig could be trained 150° in azimuth from 260° to 050° true because of the orientation of the moored buoy. With the wind from the southwest, 225°T, training the rig toward 305°T gave the instruments excellent exposure to the wind and sea. The rig had enough play in it to permit keeping the instrumentation mast vertical using the steadying guys even though the buoy might list 3°. After the underwater guys were replaced and the buoy yawed with the tide, some modification to the rigging was often necessary. This delayed the taking of data on at least three occasions and prevented taking data once.

Appendix B

Instruments and Mountings

Equipment used in the collection of data was:

1. C.W. Thornthwaite Associates wind profile register system model 106.

The basic system consists of six 3-cup type anemometers, a control console with power supply, and a print-out unit. Modifications were made to permit seven anemometers to operate at one time. The cups are conical plastic cups reinforced by aluminum rings. The three cups are connected to an aluminum hub by stainless steel tubing. The entire assembly weighs less than seven grams. The stainless steel anemometer shafton which the cups are mounted has a shutter which interrupts a light beam activatinga photo-cell. The photo-cell output could be used to trigger an output to a tape recorder and/or the print-out unit. All wind data observed fell within the range 1.2 to 10 cps. The print-out unit can print out time averages for six anemometers. All seven anemometers could be tape recorded if desired. All the equipment except the anemometers was located on BBELS.

The anemometers were calibrated before and after the summer's work in a wind tunnel at M.I.T. Only three anemometers worked in the field at summer's end. The others had electrical shorts caused by exposure to the marine atmosphere. The manufacturer claimed a distance constant of one meter or less. Our calibration indicated a better value to be 90 cm., well within the manufacturer's specification. The cups and anemometers were very closely matched, the error for all instruments being 1.5% or less. The anemometer bodies were well matched, and the errors could be attributed almost completely to the cups.

In turbulent flow as one finds over ocean surface waves a cup anemometer reads the mean horizontal wind $(u^2+v^2)^{1/2}$, where u and v are horizontal wind components. This is different from u which is oriented in the mean downwind direction (Bernstein, 1967). Mac Cready (1966) at a height of four meters over hot sand at White Sands observed that a cup anemometer read a maximum of 11% too high. He attributed 7% to a u,v, and w induced error and an additional 4% to changes in the wind direction. Usually the errors he observed were considerably less. The total error during this work, although not checked, was probably less than 5%. The wind direction was very steady and the underlying surface was always within 4°C of the air temperature, and usually within 1°C.

The Thornthwaite anemometer can be regarded as a first order response system. The system response depends only on the input and first derivative of the output. For a step input the response increases monotonically toward the new equilibrium value, and the system is completely defined by a single constant, T, or a distance constant, L. (Mac Cready, 1964)

The response of such a system can be represented by

$$\frac{dy}{dt} + \frac{1}{T}\,y = f(t) \qquad \text{(B.1)}$$

where y is the instrument's indication (cup rotation rate) and f(t) is the disturbance we wish to measure. If the disturbance is sinusoidal, $f(t) = B \sin \omega t$, then the solution of (B.1) is

$$y = B(1 + \omega^2T^2)^{-1/2} \sin(\omega t + \phi) \tag{B.2}$$

where $\phi = \tan^{-1} \omega T$ = the angle of the phase lag of the response in radians. The term $(1 + \omega^2T^2)^{-1/2}$ is the amplitude of response compared to the input amplitude (Etkin, 1959 p 264). Mac Cready (1964) has put (B.2) in terms of distance by substituting $\frac{X}{U}$ for t and L/U for T. A plot of ϕ and $(1 +\omega^2T^2)^{-1/2}$ versus fT or k'L are given in figure B.1. The k' is the wave number defined by 1/wave length. If we assume a water induced or coupled disturbance with a period of three seconds, then its wave length should be about 13 meters. Using 1 meter as the distance constant, $k'L = \frac{1}{\lambda} L = 0.077$, and from figure B.1, $\phi = 25°$ and the amplitude ratio = 0.91. As energy spectral density measurements are based on the square of the velocity, the cup anemometer would respond to only 82% of the energy present at that wave length. A comparison of spectra from a Thornthwaite anemometer and a hot film probe appears in figure B.2.

Near the end of the 1967 summer program five anemometer bodies were left mounted but capped with a rubber tip on the buoy over a weekend. After this exposure to a marine atmosphere during which heavy fog occurred, four anemometers developed short circuits in their photo-electric cells and could not be restored to working order in the field. Earlier two of these same anemometers had been dunked while being used as floating anemometers. Another anemometer failed a few days later. Anemometers appear in figures 4,5, and B.3.

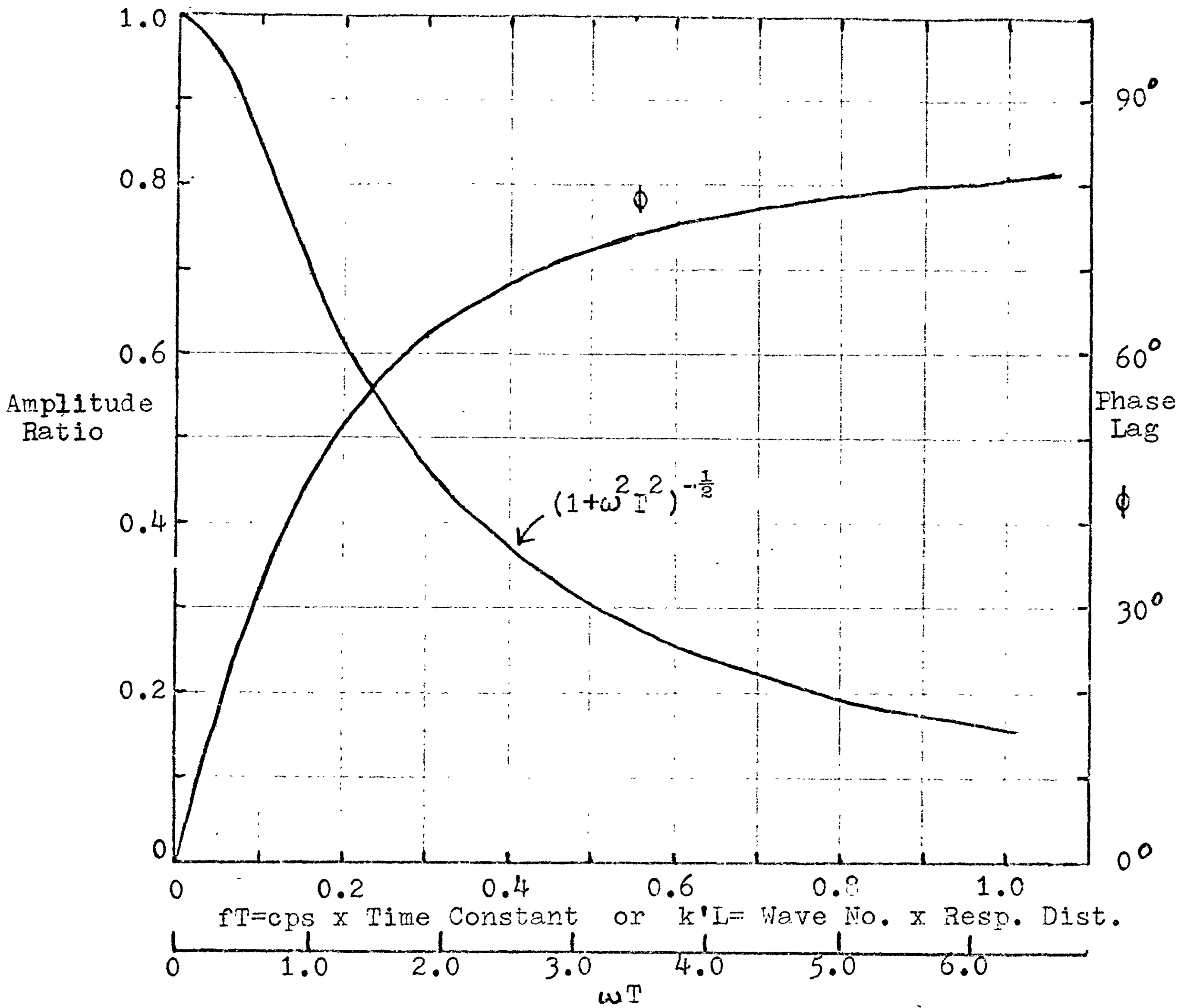

Figure B.1 First order system response to a sinusoidal input (adapted from Etkin, 1959 and MacCready, 1964).

2. Wave gauges.

The wave gauges were a capacitance type designed and built in the fluid dynamics laboratory at M.I.T. A piece of plastic coated steel wire (small craft steering cable) served as the sensing element. The dielectric plastic coating insulated the steel wire from the sea water. The wire was one plate of a capacitor. The other plate was sea water using the steel frame of the buoy as the conductor for the sea water plate and also as ground for the system.

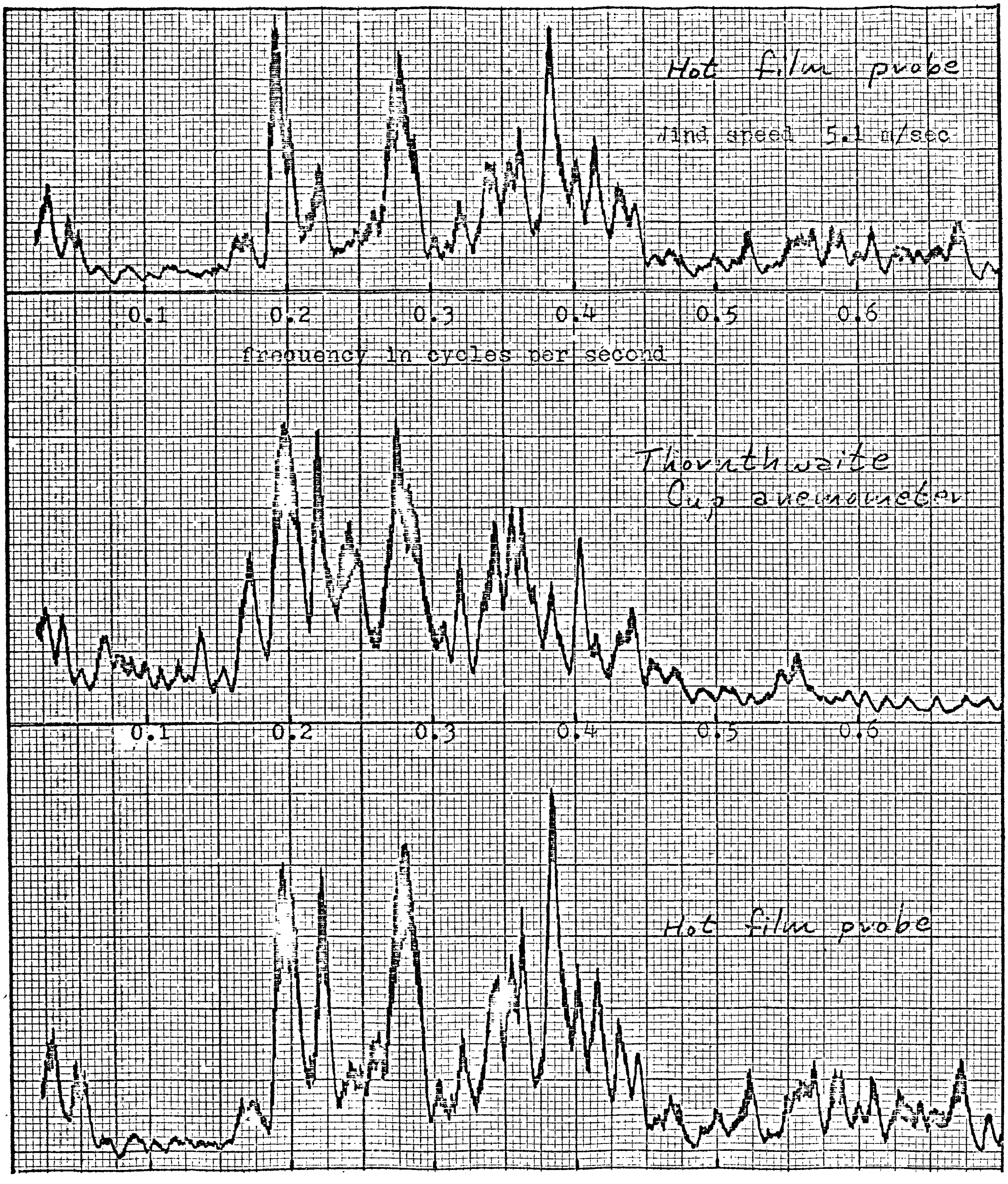

Figure B.2 A comparison of wind velocity power spectral density measurements obtained in a 1'x 1' low turbulence wind tunnel using a DISA hot film probe and Thornthwaite cup anemometer. The wind velocity was varied by partial blocking of the tunnel with a board. The output level of the film probe was very low and required considerable amplification which may account for the difference in the upper and lower spectra which were made from the same record but amplified by different techniques. The cups of the anemometer were 4" above the film probe and 1' from the blocked end of the tunnel during the test. The blocking technique was crude and produced nonuniform flow fields which probably account for the difference between the cup anemometer and hot film spectra. Vertical scale is energy.

As sea water rose and fell about the wire the capacitance changed. This change altered the frequency of an oscillator to which the wire was directly connected, and water height was recorded as the frequency output from this oscillator. The wave gauge center frequency was near 500 cps and decreased 2.7 cps for each cm of immersion in sea water.

On 4 August waves were occasionally encountered which exceeded the measuring range of the gauges. An attempt to modify two gauges for use in high seas was begun, but the changes to the oscillator circuitry required were so extensive that this in-the-field modification was abandoned. Also all wave gauges (6) would have eventually required similar modifications as all were required to be matched for use in another experiment. On two other days waves exceeding the range of the gauge were observed but only at infrequent intervals.

A wave gauge is shown in figure B.3.

3. MKS Baratron Type 77 Electronic Pressure System

This system consists of a type 77H-3 pressure (measuring) head, connecting cable, and a control and pressure indicator console. The pressure head contains a capacitance sensor, a bridge circuit, a cathode follower and heaters for maintaining the 120°F. operating temperature. There are two inlet ports leading to pressure chambers in the head. The head measures the differences in chamber pressures. In the first pressure run two static pressure probes were connected to the chambers by about a meter of 1/4 inch Tygon plastic tubing. This arrangement was used to directly measure the atmospheric horizon-

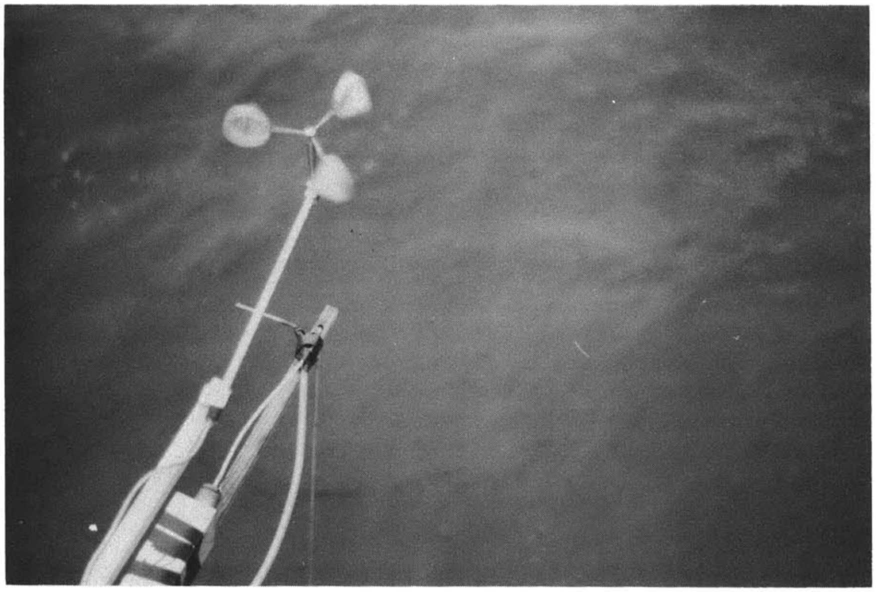

Fig. B.3. A Thornthwaite anemometer, wave gauge, and pressure probe in use at the buoy. The wave gauge oscillator circuit is in the box at the bottom of the picture. The probe is connected to 1/4" Tygon plastic tubing.

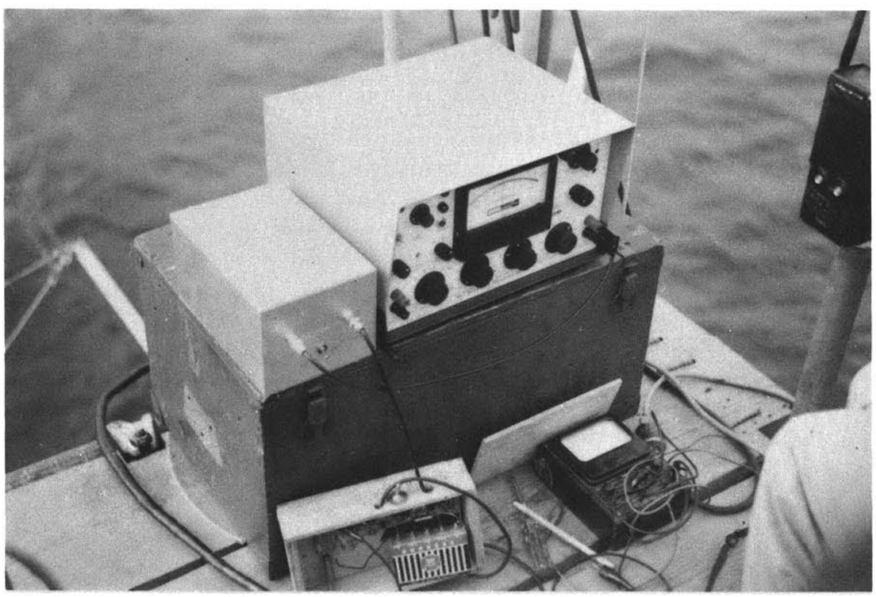

Fig. B.4. The MKS pressure system's control and indicator console in use on the buoy. The smaller box at the left is the amplifier whose output drove the voltage controlled oscillator seen with a battery connected to it at the bottom of the figure.

tal pressure gradient above the waves. One probe was mounted 108 cm downwind from the other. Unfortuantely because of difficulties with the data processing system the information on pressure gradients could not be properly analyzed. During absolute pressure runs a probe was connected to one chamber in the pressure head, while the other chamber was used as a reference connected to the atmosphere through an accumulator and capillary opening. This resulted in recording short period (less than 60 seconds) pressure variations in the "absolute" pressure.

The control and pressure indicator console contains a power supply, phase-sensitive detector, and a precision decade voltage divider to provide the bridge balancing voltage. Output connections for AC or DC voltages are located on the front panel of the console. For our use the DC output was fed to an amplifier whose output drove a voltage controlled oscillator. This oscillator's frequency range was 3 to 7 kcs. The oscillator output was transmitted to BBELS where it was recorded. All the above equipment was located on the buoy and was completely assembled and disassembled on each day it was used. A Sears Robuck 110-120 volt alternator was used as a power supply for the MKS system. The pressure head and console in position at the buoy are shown in figures B.4 and B.5.

The MKS system used had eight full scale pressure ranges of 3; 1; 0.3; 0.1; 0.01; 0.03; 0.003; and 0.001 mm Hg. The full scales 0.1 and 0.03 mm Hg (0.135 and 0.404 mbs) were used in the study. These scales provided a sufficient range to observe all but the most extreme excursions.

The response of the system with the pressure probe attached was very good. If the probe, the tubing, and chamber in the pressure head

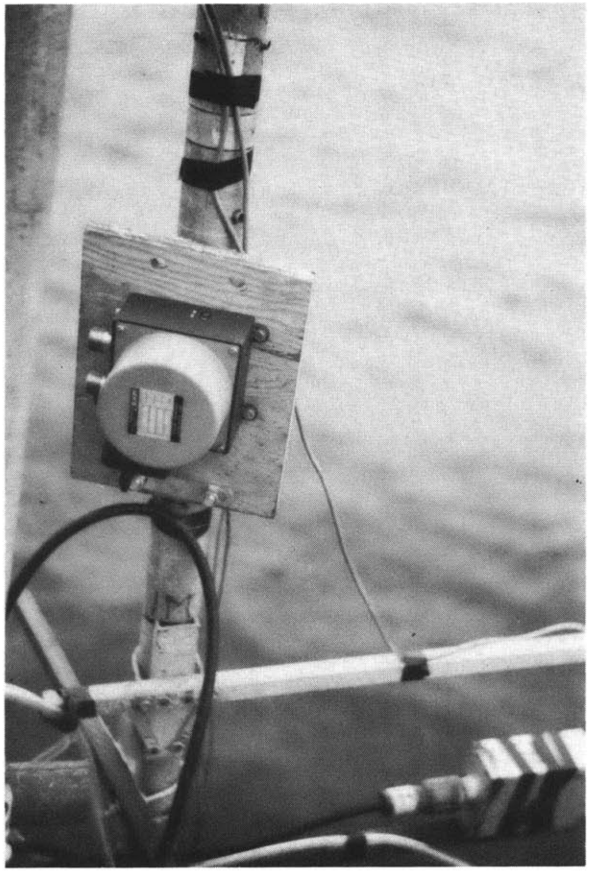

Fig. B.5. The MKS pressure head mounted on the instrumentation mast. The head was not connected to the pressure probe or reference chamber when the picture was taken.

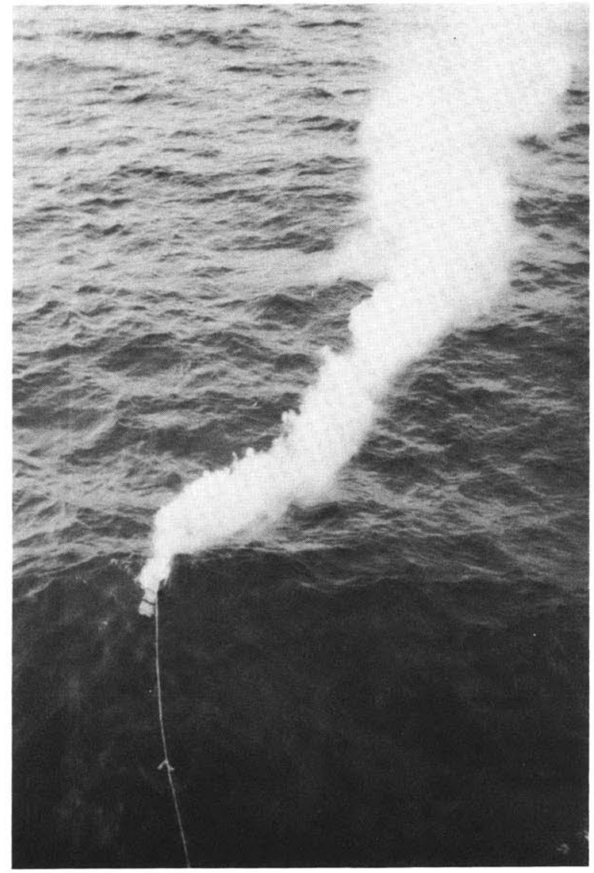

Fig. B.6. A U.S. Navy smoke float in use at the site. Note the change in smoke direction at the crest and again in the trough just downwind of the float.

are regarded as a Helmholtz resonator, which it closely resembles, the resonance frequency of the system is determined to a close approximation from

$$f_o = \frac{C_1}{2\pi}\sqrt{\frac{S}{\ell' V}}$$

where C_1 is the velocity of sound in air, ℓ' is the effective length of the opening (or lead in tube in this case), S is the cross-sectional area of the opening, and V is the volume of the system (Kinsler and Frey 1950 p 194). For the system as used good values for these quantities are $C_1 = 331 \times 10^2$ cm sec $^{-1}$; $S = 0.317$ cm^2 ; $\ell' = 150$ cm and $V = 127$ cm^3. Thus f_o=20 cps and the system should respond very well to the frequencies of interest to us, being at least an order of magnitude lower than the resonance frequency of the measuring system. A wind-tunnel check of the system revealed no detectable delay in response for frequencies of 0.5 cps or less; however, delays in response less than 0.05 seconds would not have been detected during the test.

4. Air Temperature Probe

A thermistor mounted in a sun shield was part of an oscillator circuit. The frequency output of the oscillator (3 to 6.5 kcs) was dependent upon thermistor resistance which varied with temperature.

The sun shield containing the thermistor was connected to a pulley arrangement permitting the thermistor to be moved in the vertical from 70 cm to 11 m above MSL. As the air temperature probe required considerable effort to rig on its separate mast it was used on only two days when profiles were taken.

A mercury in glass thermometer was used for air temperature measurements on other days.

5. Z-winch

The line controlling the height of the sun-shield for the thermistor was reeved across a special winch. This Z-winch had a shaft of one of its pulleys connected to the shaft of a variable resistor. The resistor was again part of an oscillator circuit whose frequency varied from 3.5 to 6.5kcs as the line moving around the pulley turned the resistor's shaft. The frequency output of the oscillator circuit was a measure of height above MSL. By using the Z-winch and air temperature outputs it was possible to record a vertical temperature profile (temp. vs. z). This combination was in use with the Thornthwaite anemometers only on 17 and 18 August.

6. Beckman and Whitley anemometer.

Components of a Beckman and Whitley series 50 wind measuring system were utilized. These included wind speed and direction transmitters (a six cup anemometer and wind vane), a power supply, and translation units. The sensors (transmitters) were mounted on top of the buoy's mast, 12 meters above MSL. The purposes of this system were to determine the wind at "mast head" height for comparison to data from other oceanographic expeditions and also to extend the vertical wind profiles above the height of the main instrumentation rig. Wind velocity only was recorded on the tape recorder. To record wind direction would have required two tape recorder channels and was not done, instead wind direction was recorded manually on the buoy using the wind vane as a guide.

7. Mounts for instruments.

a. The mounting and controlling of the main instrumentation mast is described with the buoy in Appendix A.

b. Thornthwaite anemometers were mounted in two types of positions.

(i) Four were normally fixed to the instrumentation mast by standard support brackets provided with the anemometers. The anemometers were spaced one meter apart in a vertical line about one meter from the instrumentation mast. The lowest anemometer was positioned about one meter above MSL by controlling the main rig in elevation.

(ii) Three "floating" anemometers measured the wind 30, 50 and 70 cm above the surface. These were mounted on special brackets attached to a one inch aluminum tube. The tube was led through circular pipe supports at three points, two above and one well below the surface. The supports had a one and 1/8 inch inside diameter and were lined with teflon tape, so the one inch aluminum tube was free to slide up and down through the supports. Each support was mounted on a bracket one meter long which was fastened to the main instrumentation mast. There was flotation attached to the tube at the water surface in the form of a twelve inch styrofoam life ring and a styrofoam lobster pot float. The support and flotation were positioned so the anemometer could move three meters in the vertical and was restrained from rotating. The vertical axis of the "floating" anemometers was 30 cm (in the horizontal plane) from the vertical axis of the fixed anemometers and the wave gauge. The entire rig was adjusted for each run so all the anemometers were in a plane perpendicular to the direction of the wind. Thus, all the anemometers were above the crest or trough of a wave simultaneously. When the instrumentation mast was raised for storage or servicing of instruments, the flotation came to rest on the lowest (underwater) support, and the entire floating rig then rose with the main instrumentation mast.

The arrangement of "floating" and fixed anemometers had been arrived at after much experimentation with different types of rigs. The "floating" anemometers worked well in wind driven seas up to 1.5 meters in height. These were the highest seas encountered during data runs. At times during runs in rough seas the two lowest anemometers would be dunked by breaking waves.

c. Wave gauges were mounted on horizontal one inch by one inch redwood support brackets attached to the instrumentation mast. The brackets extended out one meter from the mast. The enclosed oscillator circuit was fastened near the mast, and the wave gauge cable was lead out to and through a hole near the end of the bracket. The cable's lower end was fastened to the end of a similar redwood bracket two meters below the first bracket. This arrangement provided a two meter long wave gauge. The rig was lowered so the upper bracket stayed dry while the lower bracket remained submerged. The wave gauge was positioned so it was below, but coincided with the extended vertical axis of the fixed anemometers. When a second wave gauge was used it was mounted in a similar manner but its sensing wire was located one meter down wind from the first. The two wave gauges were to be used to calculate sea surface slope but calibration and data processing problems prevented the success of this effort. Redwood brackets were used as a metallic support affected the capacitive characteristics of the wave gauges.

d. Pressure probes when used were mounted on the outer end of the upper wave gauge bracket directly below the lowest fixed anemometer.

The pressure head itself was mounted to the instrumentation mast.

A pressure probe at the buoy appears in figure B.3.

8. Smoke floats.

Ten standard U.S. Navy white smoke floats were obtained from Woods Hole Oceanographic Institution. When activated they produce a dense white smoke for 45 minutes. The floats were to be used in photographic sequencss of wind flow near the surface; however, these pictures were not very satisfactory. The smoke dispersion pattern did, nevertheless, demonstrate that the direction of the wind was usually very constant and varied no more than 5° in direction in any fifteen minute period when the wind was 10 knots or more. The smoke seems to vary in direction; although only very slightly, as it passes from crest to trough to crest indicating the need for a three dimensional study of wind and wave.

9. Buoy box.

This box located on the buoy was a terminal box for the four, seven conductor cables leading to BBELS. The box was fitted with weather proof jack connections to which leads from the various sensors could be connected providing them with power and an output circuit to BBELS.

10. Auxiliary equipment.

Auxiliary equipment includes power supplies, pulse formers to shape tape recorder inputs, amplifiers, and various test equipment, mostly located on BBELS. This equipment while important in the data gathering was not especially unique. The tape recorders are described fully in Appendix C.

The power supply used for the MKS system was a Sears-Roebuck, 1250 watt alternator driven by a gasoline engine. The alternator was tied down on the lower buoy platform when in use. Originally some electrical interference on the performance of other equipment (pressure and anemometer systems) was observed, when the alternator was running. Locating the alternator so the steel frame of the buoy was between the alternator and affected equipment eliminated the interference.

Appendix C

Analog Data Processing

By far the most demanding and frustrating part of the entire investigation was in the processing of the data. Prior to this project there existed no suitable capability to properly process this type data in analog form in the Meteorology Department at M.I.T. Mr. Ortwin von Zweck and I each spent about 500 hours working on organizing and testing the system and learning the art of analog data processing. Two technicians gave us considerable assistance in this task. We were primarily concerned with determining energy frequency spectra (power spectral density measurements) and auto- and cross-correlation functions.

The following advantages of the anlog data processing system used, as least as experienced by us, are evident:

1. Analog processing makes use of the continuous record of instrument output.

2. Storage and handling of information on tape is relatively simple.

3. Analog processing is very good for quick look analysis.

4. The expense, problems, and labor of digitizing data are avoided.

5. The system can be transported with relative ease. This requires for us two strong men and a one ton truck, but at least it can go into the field or to sea if necessary and desirable.

6. Compared to a complete digital system, an analog system is relatively inexpensive to purchase (or build) and maintain.

7. The experimenter is personally in control and is involved with all phases of the analysis and gets a good "feel" for the data. In fact he can become almost emotionally involved with it, if he is not careful.

Some disadvantages of this type analog data processing are;

1. The system is inflexible. If one wishes to change the data handling it is necessary to physically modify the system. The components necessary to perform one series of operations are frequently of no use in other operations.

2. Your or an aide's constant personal attention is required.

3. Equipment gain (amplification) is important in each stage. Too much gain can amplify noise to an undesirable extent or clip large signals and distort seriously the output. Too little gain can leave valuable information undetected as many electrical analog devices have threshold levels. Some prior knowledge of what you are looking for is of tremendous value here, but one must be careful not to play with the gain to eliminate "noise" or distortion" which may be real data. When cross- or auto-correlating data which has been rerecorded a number of times the magnitude of the correlation obtained are mearly a good approximation to the real values. This is because it is impossible to match exactly the gain of all channels during all processing steps. Fortunately the delay time of maximum correlation is not altered by the slight difference in gains.

4. In certain operations signal polarities and phase relationships are very critical and must be watched closely. We found that the considerable electronic and physical handling of data in preparing and using tape loops can be extremely vulnerable to the introduction of errors.

5. Processing large volumes of statistically similar data is very time consuming.

6. Improving the statistical accuracy of a given computation may require an inordinate amount of additional time and money as compared to the increased time and money needed to achieve a similar improvement

with digital data processing techniques.

The primary instruments used in recording and processing data were the Precision Instrument (PI) models 6108 and 6208 tape recorders. These recorders can simultaneously record or reproduce 8 channels of information of various characteristics depending upon the tape speed and recording mode (FM or Direct) selected. Each recorder has three speeds, 0.375; 3.75; and 37.5 ips. For recording data in the field the 0.375 and 3.75 ips speeds were used exclusively. Each recorder has two record and two playback heads. Each head handles four channels of information designated 1, 3, 5, and 7 for one pair of record and playback heads and 2,4, 6, and 8 for the other pair. One recorder is shown in figure C.1.

The recorders use 1/4 inch wide magnetic tape. Initially 2400 foot reels of 1/2 mil tape were tried, but the tape proved too thin and tended to fold while passing over the capstan resulting in erratic performance. Using thicker tape as recommended by the maufacturer for the model 6208 corrected this problem.

For analysis in the laboratory the original information was speeded up by a factor of 1,000. This could be accomplished by playing the original tape back 10 times faster than it had been recorded. This signal, after demodulation, was recorded on tape loops using the other PI at 0.375 ips. For analysis the loop was run at 37.5 ips, resulting in a total speed up of the original data by 1,000 times. The speeded up frequencies of interest were 20 to 500 cps. The tape loops used averaged 47 inches in length and contained about 21 minutes of real time information.

While the characteristics of the PI 6108 and 6208 recorders are

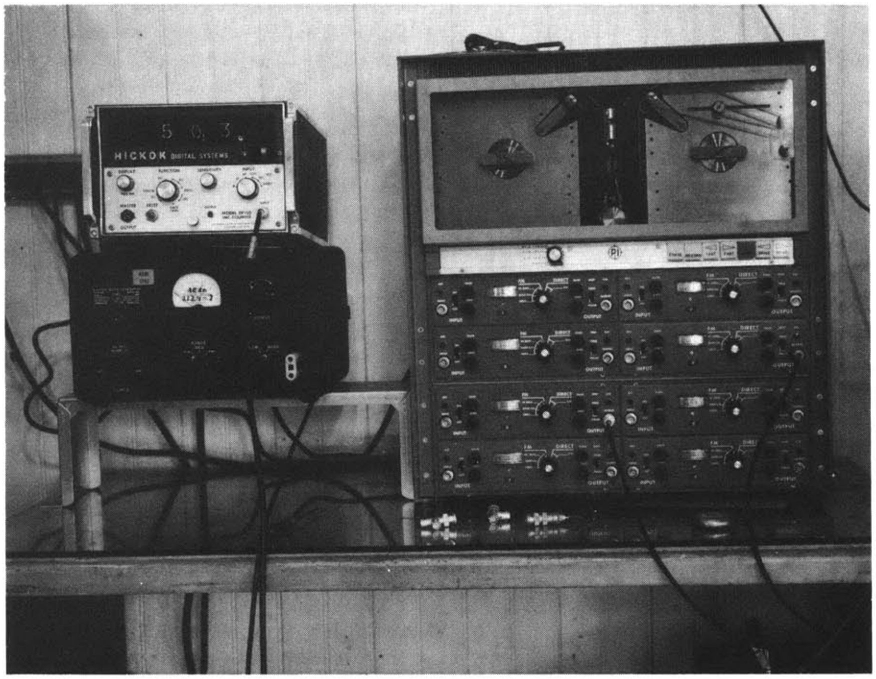

<u>Fig. C. 1a</u>. The Precision Instrument, model 6208 recorder with tape loop adapters installed. A frequency counter and noise generator are at the left.

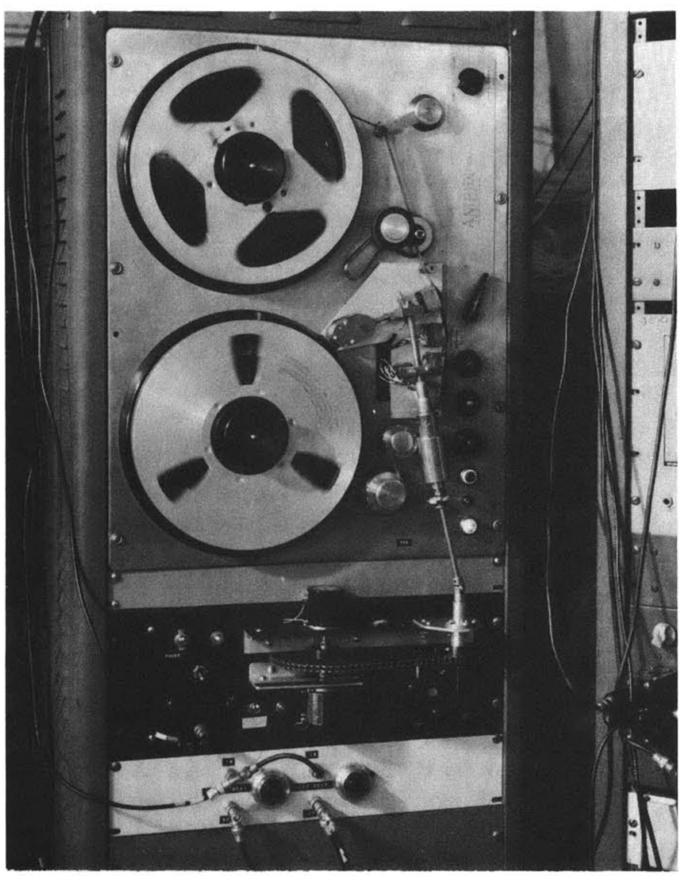

<u>Fig. C. 1b</u>. The Ampex recorder modified to perform correlations. The chain in the lower part of the picture, connected to rotate the shaft at the right, was part of the mechanism for inducing the delay in the signal by moving the uppermost head.

excellent when working properly, a number of problems arose in the field and laboratory. Several of these problems are extremely difficult to correct or describe as they appear only intermittently. The modules (channels) were often difficult and sometimes impossible to tune prior to recording and too frequently required going inside the equipment to make adjustments. Several complete failures of modules and preamplifiers occurred. The model 6108 quit completely and was returned to the vendor who discovered the power supply would intermittently short to the case. After being returned to us problems developed in this recorder's logic circuitry and it refused to run at times or in certain modes. The 6108 is also equipped with a ventilation fan which rubs the casing and is extremely annoying to the operator.

The model 6208 is an improved version of the 6108, but it still requires considerable maintenance. It was determined that the spacings of the two pairs of heads on the model 6208 were different by about 0.002 inch which is just within the manufacturer's specifications. This resulted in the introduction of a minute delay between signals recorded and reproduced by the different heads. However, this did prove to be a major problem. In rerecording data speeded up by a factor of 1,000 the phase shift introduced by the spacing of the heads was 1,000 times larger than at real world frequencies since the physical difference in distances between the heads remained unchanged. Also the error was reintroduced every time the data was rerecorded and played back, compounding the problem. The largest this error, which appeared in correlations, was observed to be after preparing tape loops was a change of 0.3 seconds in real world time. The error was corrected for by keeping track of the recording procedures used. A more suitable method was to simply avoid cross-correlations between data on odd and even recorder channels; however, this unfortunately reduced the flexibility of the system, but had to accepted.

Random noise was observed on the output of several channels in various modes. On several occasions this noise was observed to distort the recorded signal. Use of these channels was kept to a minimum.

When handling wave and anemometer data the different sensor characteristics required separate steps for demodulation. The result was the information on a finished tape loop had been recorded at least three times and in some cases more.

Some additional problems and their solutions associated with the use of tape loops on the PI and other recorders are:

1. The separate erase head feature of the PI cannot be used for recording a loop as it leaves a blank space on the tape. Simply using the record mode without erase sufficiently erases any prior signal on the tape in most instances.

2. When the recording on a loop is ended by pressing the stop button (the only way to do this) an unwanted transient signal is frequently left on the tape by the record head. This signal does not necessarily appear on all channels but seems to be random in nature. If the amplitudes of the data signals recorded on the loop are great enough, the energy level of this transient is then so relatively low that it does not discernably alter the statistics of the data. This requires the amplificaion of all signals to about the same RMS level no matter what their original level. This problem and problem 1 can sometimes be avoided

by cutting up pre-recorded tape to make tape loops.

3. The tape splice is a noise source. If the splice is not fitted properly the signal may be seriously distorted at the splice. If the splice is trimmed too closely, parts of channel 1 and 8 may be cut away.

4. At high speed the tape edge folds on the capstan. Using a heavy grade (1.5 mil) tape normally eliminates this problem.

5. If the DC level of the signal changes during the period covered on the tape loop a large voltage step occcurs where the information on the loop ends and begins again. This is frequently a problem with wind information.

Power Spectral Density and Amplitude Frequency Measurements.

Basically the analog signal of wave, wind, or pressure speeded up by the factor of 1000 was analyzed for frequency components by a wave analyzer whose output was integrated. The integrator output was plotted against frequency to produce the rms amplitude frequency spectrum.

In one arrangement the PI tape loop output (data) was fed to a Hewlett Packard model 302A wave analyzer. This wave analyzer is a tunable voltmeter filter of high selectivity (bandwidth 7 cps) and sensitivity covering the frequency range 20 cps to 50kcs. It can be operated as an oscillator- tuned voltmeter combination, where an oscillator and the tuned voltmeter track together over the frequency range desired. The oscillator-tuned voltmeter was slowly driven by a specially designed, externally attached drive from 20 to 700 cps. The tuned voltmeter output provided the signal amplitude at the frequency to which tuned and was fed to an integrator. The oscillator output was demodulated so the voltage output increased linearlywith the frequency. The integrator (amplitude) and demodulator (frequency) output were plotted against one another on an x-y plotter. By squaring the output of the wave analyzer before integrating, power spectral density measurements can be obtained. A block diagram of this power spectral density analyzer appears in figure C.2.

Many spectra were also produced on equipment made available to us by the Department of Marine Engineering and Naval Architecture at M.I.T. The basis of this system is the Spectral Dynamics (SD) Corporation's dynamic analyzer model SD101A and sweep oscillator model SD-104-5. The dynamic analyzer is a frequency-tuned bandpass filter, the center-frequency of which is continuously and precisely tuned to track a frequency supplied by an external source. The unit provides an output in several forms; a meter, a DC analog voltage, a filtered signal output, and a 100 kcs filtered output. The dynamic analyzer used had two filters available with half-power point bandwidthes of 5.2 and 50 cps. The frequency source for the dynamic analyzer is the sweep oscillator. The sweep oscillator provides a frequency output which can increase or decrease linearly or logarithmically with time. The linear sweep rates can be adjusted over a continuous range from 0.001 to 2000 cps/sec. The logarithmic rates available from the sweep oscillator are 0.04 to 6.0 decades per minute. DC outputs which vary linearly and logarithmically with frequency are also available.

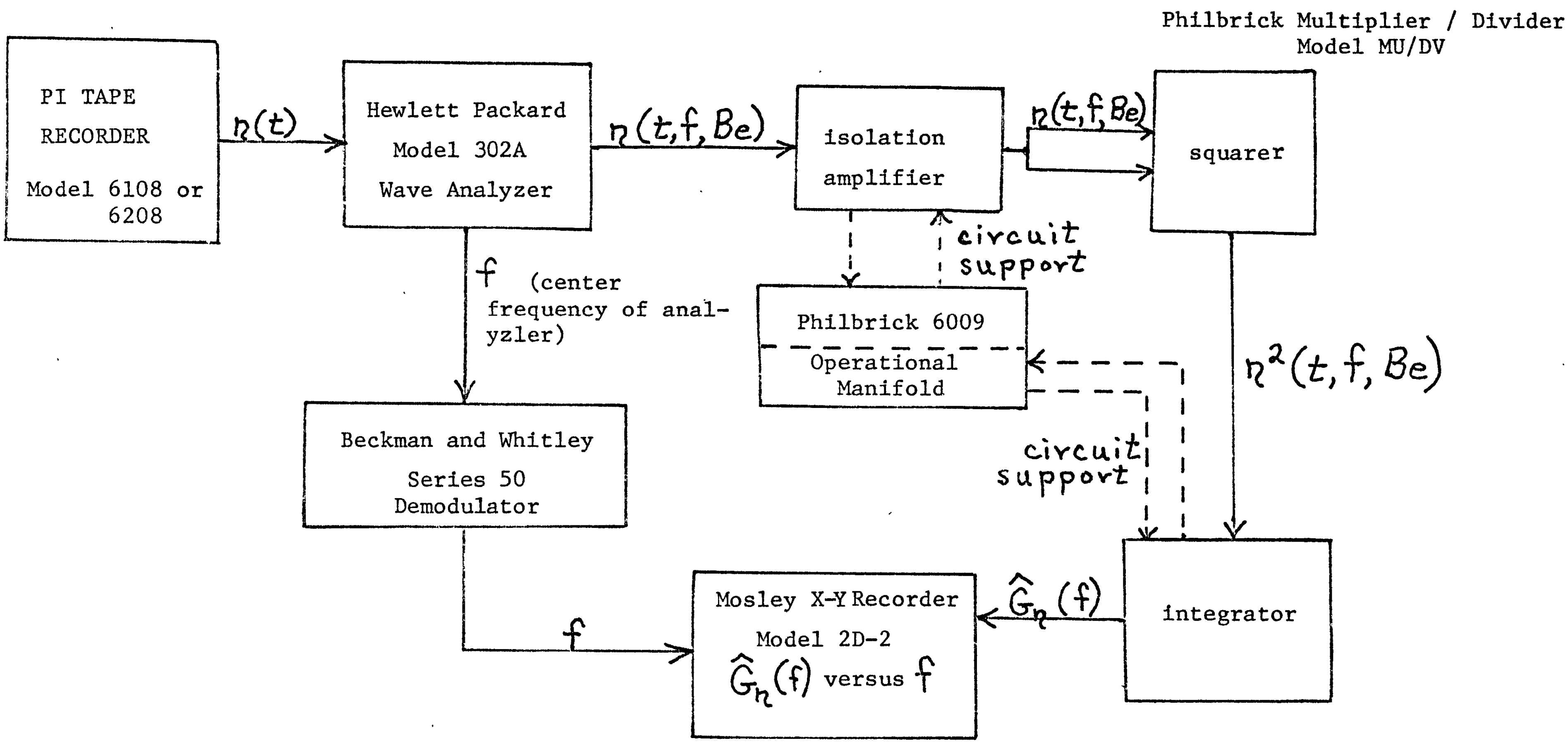

Figure C.2 Block diagram for power spectral density analyzer. This system and one very similar to it were used to produce the power and amplitude frequency spectra.

For power spectral density measurements with the SD equipment, the speeded up data signal was fed to the dynamic analyzer and the filtered signal output was used. This signal was amplified using a model 255 ITHACO low noise amplifier, squared in a Philbrick Q3-MIP multiplier, and integrated by an appropriately modified Philbrick Q3-AIP stabilizer amplifier. The integrator output was plotted against the linear DC output of the sweep oscillator on an x-y plotter. The dynamic analyzer and sweep oscillator appear in figure C.3.

In both systems the multipliers were a source of trouble. The spectrum desired was difficult to produce because of threshold loss or clipping from overdriving.

The accuracy and resolution of analog power spectral density measurements depends upon the analyzer bandwidth, scan-rate, the integration time constant, and the record length. (This discussion is based in part on Bendat and Piersol 1966, Chapter 6.)

If we have a sample voltage time history record $\eta(t)$ (wave height, wind velocity, pressure flucuations) from a stationary or quasi-stationary random signal, we can estimate $G_\eta(f)$, the power spectral density function, from

$$\hat{G}_\eta(f) = \frac{1}{BeT} \int_0^T \eta^2(t,f,Be)dt \tag{C.1}$$

where $\eta(t,f,Be)$ is that part of $\eta(t)$ passed by a narrow band-pass filter with a frequency bandwidth of Be cps and whose center frequency is f cps. T is the sampling time or record length. This was done in our procedures described above.

The normalized mean square error, ε^2, of the estimate of $G_\eta(f)$ is given by

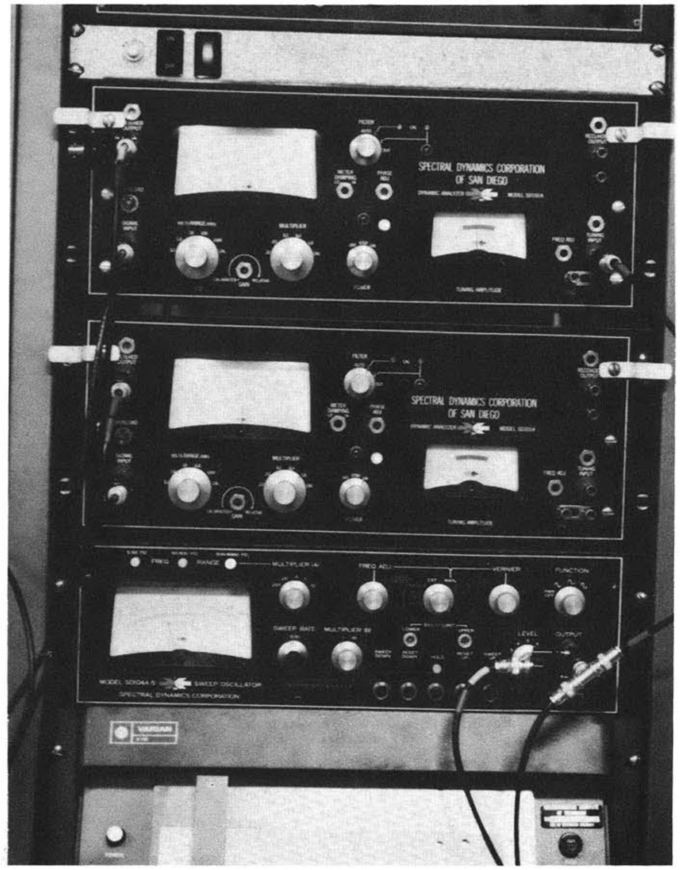

Fig. 3 Ca. A front view of two Spectral Dynamics Corp. Dynamic analyzers model SD101A, with the SD sweep oscillator mounted below them.

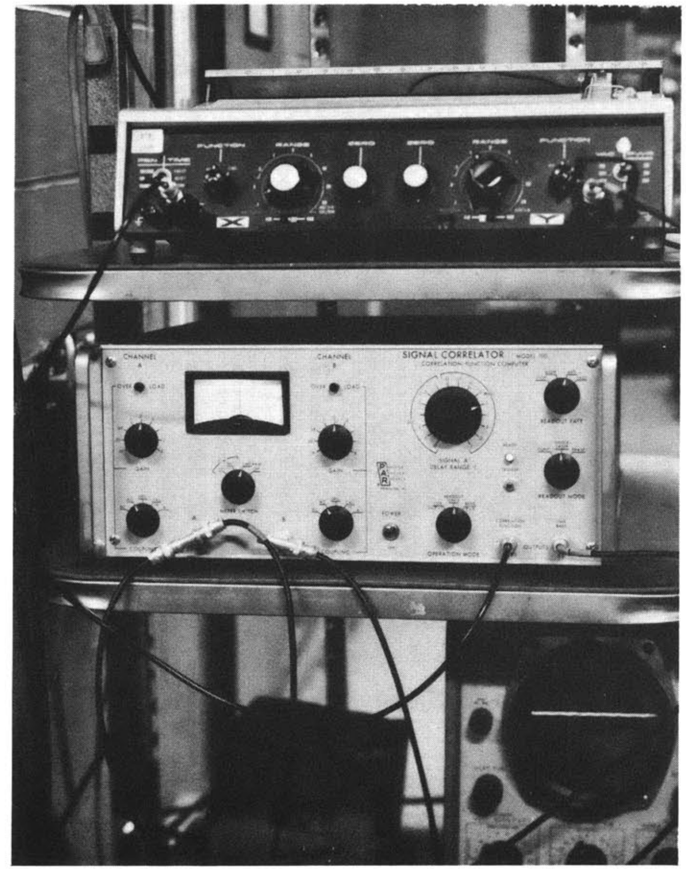

Fig. 3. Cb. The Princeton Applied Research Corp. correlation function computer, model 100, in use in the laboratory.

(C.2) $$\varepsilon^2 = \frac{E[(\hat{G}\eta(f) - G\eta(f))^2]}{G^2_\eta(f)} \approx \frac{1}{BeT} + \frac{Be^4}{576}\left(\frac{G''_\eta(f)}{G_\eta(f)}\right)^2$$

(Bendat and Piersol p199)

where E stands for the expected value and $G''_\eta(f)$ is the second derivative of $G_\eta(f)$ with respect to f. If we define

(C.3) $$\lambda(f) = \left| \frac{G_\eta(f)}{G''_\eta(f)} \right|^{1/2}$$

then

(C.4) $$\varepsilon^2 \approx \frac{1}{BeT} + \frac{1}{576}\left(\frac{Be}{\lambda(f)}\right)^4$$

Here $\lambda(f)$ is the "spectral bandwidth" of the process under investigation and has units of frequency. In (C.4) the first term on the right is called the variance term and the second the bias term.

The normalized standard error is a measure of the confidence to be placed in the estimated value of $G_\eta(f)$. If $\hat{G}_\eta(f_1)$ is the value of the estimate at a frequency f_1, then at the 95% confidence level we can say that

(C.5) $$(1-2\varepsilon)G_\eta(f_1) < \hat{G}_\eta(f_1) < (1+2\varepsilon)G_\eta(f_1)$$

where $G_\eta(f_1)$ is the true value at f_1. So if $\varepsilon = .20$ then with 95% confidence it can be stated that the value of $\hat{G}_\eta(f_1)$ obtained lies within the real value range 0.60 $G_\eta(f_1)$ to 1.40 $G(f_1)$. Often this is stated the other way around and really makes very little difference provided ε is not too large, in fact this is the manner in which it is used herein. That is, we say that at the 95% confidence level the true value of the function at a given frequency lies within $\pm 2\varepsilon\hat{G}_\eta(f)$ of our value $\hat{G}_\eta(f\ )$.

From equation (C.4) we see that the normalized standard error is most dependent upon the filter frequency bandwidth (Be) and record length (T). Therefore we are faced with some difficult choices, for the statistical accuracy can be increased by increasing either Be or T within certain reasonable limits; however, not without cost. If a narrow filter bandwidth is increased ε decreases rapidly at first, but increasing the window width reduces our resolution, that is, the bias error increases. The loss of resolution blurs abrupt changes or sharp peaks in the power spectrum which are likely to be important especially in the case of ocean wave spectra.

A reasonable criterion for acceptable resolution in practice is a bandwidth which is one-fourth the bandwidth of the narrowest peak in the spectrum to be measured (Bendat and Piersol p 261). I am now, however, more uncertain than previously as to how wide the peaks of ocean wave spectra are or how many peaks there are under a given set of conditions.

The statistical accuracy is also increased by lengthening T, the record length. The wave generating process however is nonstationary and by selecting T too long information which is not statistically similar may be included on the same record. When averaging nonstationary data, an error (called the time interval bias error), arising from the smoothing of nonstationary time trends in the data caused by the averaging operation, can become important. The error is a function of T and the nonstationarity of the data. If the data's time trend is small and T relatively short this error is small. In all cases for small T it is necessary that the filter bandwidth be greater than the reciprocal of the averaging time, $Be > \frac{1}{T}$ (Bendat and Piersol p 362). For our wave and wind studies I believe the time

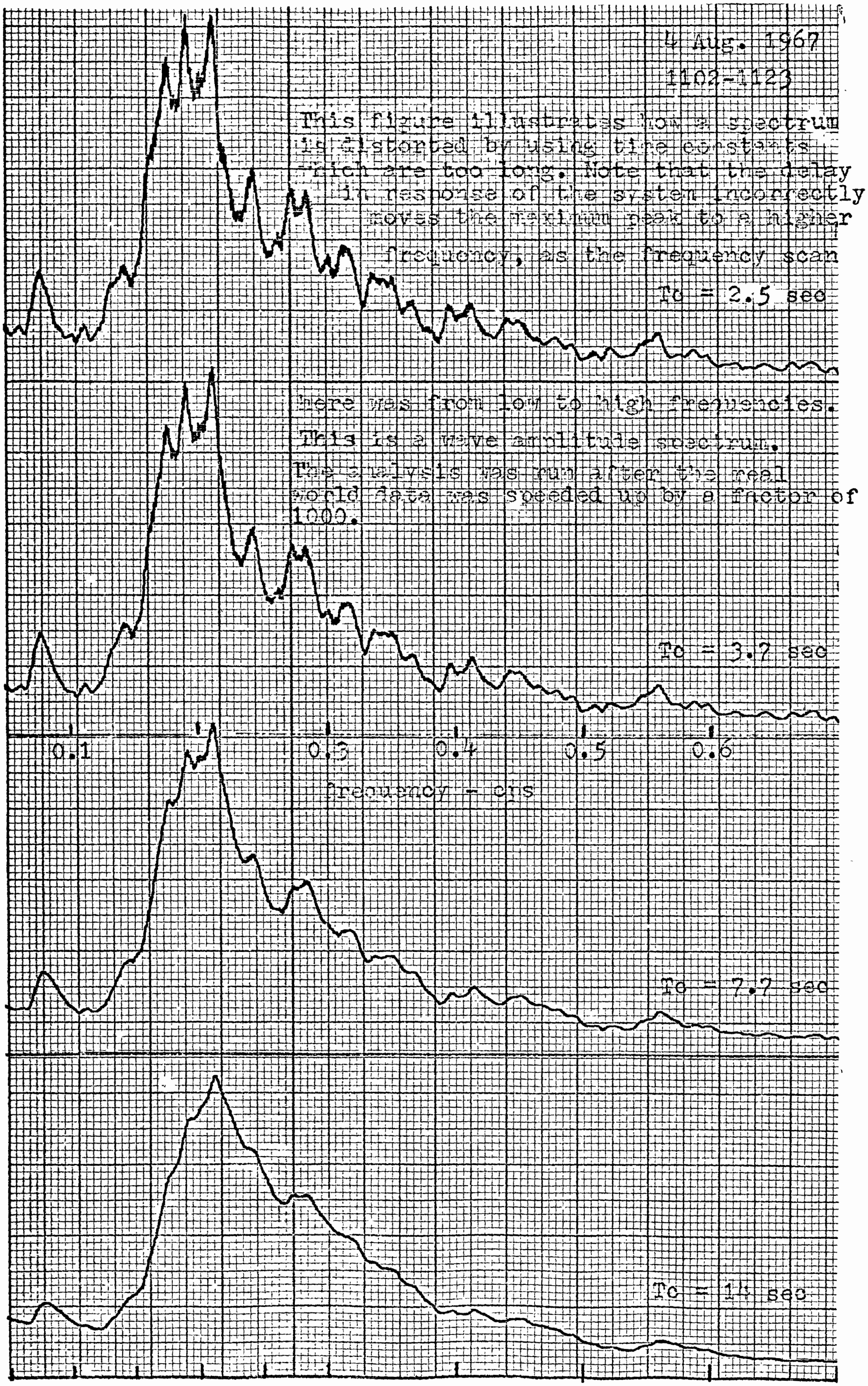

Figure C.4 The effect of time constants on a spectrum.

interval bias error is small for the data is quasi-stationary during the 21 minute periods analyzed and Be $\geq$ 4/T. Nevertheless, one of the important parameters of interest here is how the spectra change with time.

Averaging time of the integrator is important, it must be short enough to properly respond to changes in signal level but not so short that it over reacts to noise. For RC averaging the time constant should be set about equal to the record length. Figure C.4 indicates how a spectrum is distorted by using some time constants which are too long.

The scan rate must be sufficiently slow to permit adequate response of the system to the data. The record length, time constant, and bandwidth must all be considered. The record should be scanned fully about four times while the window passes a frequency, so that the integrator has time to respond to any signal energy at that frequency. Of course the slower the scan rate, the longer the processing time a given record requires. Barber (1961 p 96) discusses the conflict between speed in getting the spectrum and sufficient accuracy and detail. Whether our data is scanned from low to high frequencies or vice versa should make little difference in the spectrum obtained if all parameters are properly chosen. See figure C.5.

Bendat and Piersol (p 267) show that for a power spectral density analyzer with a half-power point bandwidth of Br cps, that $B_s = \pi Br$, where B_s is the equivalent statistical bandwidth. Using B_s = Be and approximating (C.4) with

$$\varepsilon \approx \frac{1}{\sqrt{\pi BrT}} \qquad \text{(C.6)}$$

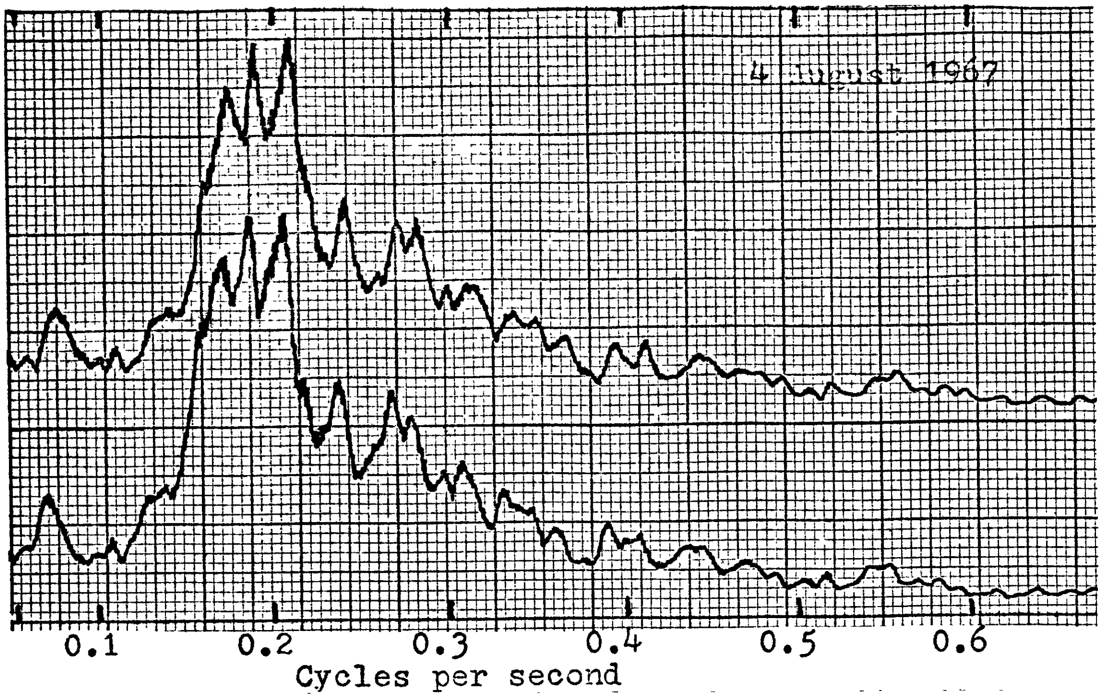

Figure C.5 Two amplitude frequency spectra made from the same wave record. In the upper trace the center frequency of the 7 cps bandwidth wave analyzer was increased at 1.5 cps/sec, while in the lower the center frequency was slowly decreased at the same rate. The integration time constant was 2 seconds. The analysis was run after the data was speeded up by a factor of 1000.

since the bias term is negligble with the narrow bandwidth used, permits us to find the standard normal error.

As the record lengths used in this study were tape loops with 1.26 seconds of data in analysis time, and the usual filter half-power point bandwidth was 5.2 cps, the value of ε is 0.22 for most records. Some longer records were analyzed, three seconds long or 50 minutes of real time data, where $\varepsilon = 0.14$. A spectrum for the longer period was a good average of the spectra covering the same period with shorter records. Compare figure 8 and 13. For Br = 7 cps, $\varepsilon = .19$, while $\varepsilon = .07$ if Br = 50 cps but the resolution for 50 cps is very poor.

The selection of the record length, scan-rate, analyzer bandwidth, and integration time constant was thus a compromise. Acceptable accuracy was sought calling for a large bandwidth and long record, but the need for high resolution to see the time development in the data called for small bandwidth and shorter records. Scan-rate had to be slow enough and integration time fast enough to properly sample and respond to the data, yet time is valuable and slow scan-rates drag out the processing. Too fast a time constant lets undesirable noise appear in the spectra (produces grassy spectra). All of the factors affect one another and a feel for their interactions is only fully appreciated after one has had to juggle them in order to extract the most from some data. The balance achieved here hopefully provides for the most valuable information with a reasonable expenditure of time, effort, and money.

For those not interested in the high degree of resolution shown, the accuracy of the spectra can be improved considerably by simply smoothing the curves by hand with a pencil.

Correlations

The primary purpose of the correlations performed on the data in this study was to determine the time and phase relationships of wave, wind velocity variations, and the atmospheric pressure variations.

About one half of a man-year of work was spent attempting to build a working correlator from a two channel Ampex model 306-2 tape recorder with two separate pairs of record and playback heads. One playback head was mounted on a movable arm so it could physically be moved to induce a delay in the playback of one channel. The outputs of the two channels, one now delayed, were amplified and multiplied. The signal was then integrated and the result plotted against the movable arm's position which was a measure of τ (delay time). Auto- and cross-correlations were obtained in this manner, but they were of only fair quality and could not provide the resolution needed. Numerous problems encountered included tape flutter, small variations in tape recorder speed, non-linear drive for the delay head, and inaccurate positioning of the head. The inaccuracies involved were of order 10^{-3} inches. Discussions with those involved in analog data processing in two other departments at M.I.T indicated similar problems were encountered, and their efforts were only partially successful. This correlator is shown in figure C.1b.

The Department of Marine Engineering and Naval Architecture made available their model 100 PAR correlator (Princeton Applied Research Corp. correlation function computer). The correlator computes a correlation, $C_{12}(\tau)$, at 100 evenly spaced points from $\tau = 0$ to $\tau = T$ where T is a variable, maximum delay time. On the PAR model 100 correlator T is adjustable from 100 μsec to ten seconds in steps of 1, 2, 5, and 10. The unit used had an averaging time of 50 seconds which was long as the units are normally equipped with a 20 second time constant that would have been more suitable for this work. The long time constant about doubled the time necessary to run a given number of correlations; however, the time to compute correlations on the model 100 was still only one half that required to compute a less satisfactory correlation using our own correlator.

The specified computation error of the PAR model 100 correlator is within 1% of the true value of the correlation (as received from the tape loop). The accuracy of the delay range value is ±2% for the ranges used in this work. The unit has a memory which is extremely useful in plotting out correlations. The readout circuitry is also versatile enough to permit viewing the correlation on an oscilliscope.

The PAR correlator has two input channels and computes the cross-correlation,

$$(C.7) \qquad C_{21}(\tau) = \lim_{T\to\infty} \frac{1}{T} \int_{0}^{T} f_2(t)f_1(t+\tau)dt$$

where $f_1(t)$ and $f_2(t)$ are the time function inputs to channels A and B respectively. The actual operation performed is

$$(C.8) \qquad C_{21}(\tau) = \lim_{T\to\infty} \frac{1}{T} \int_{0}^{T} f_1(t)f_2(t-\tau)dt$$

To obtain the cross-correlation over the delay range (from $-T\leq\tau\leq T$), the input of the channels was reversed to obtain $C_{12}(\tau)$. This value was plotted out with the polarity of τ inverted. Since

$$(C.9) \qquad C_{12}(\tau) = C_{21}(-\tau)$$

the plot obtained was $C_{21}(-\tau)$ for the range $-T \leq \tau \leq 0$.

Considerable misunderstanding arose over the sense of τ which was negative as used with both the Ampex and the PAR correlators. Thus, if two related signals, $f_1(t)$ and $f_2(t)$ arising from some physical process at points 1 and 2 respectively, are cross-correlated, where $f_1(t)$ is the delayed signal, and a maximum in the correlation is observed for a value of $\tau = t_2$; then this means, that in the real world an event, $f_1(t_1)$ at time t_1 is generally followed by a similar or related event $f_2(t_1 + t_2)$. The similar event at point 2 occurs a time t_2 after the original event at point 1. That is, a positive value of τ indicates a lag time, representing how much the delay signal had to be delayed in time when compared to the undelayed signal to produce the value of the cross-correlation at that point.

In plotting out both sides of the correlation it was noticed that a small shift in the zero point (voltage) of the τ value occurred from time to time. By plotting out the auto-correlation from $-T \leq \tau \leq T$ of a known sine wave twice a day, this error could be determined and the τ plotting zero point adjusted to eliminate the error. This error was negligble compared to that induced by the slight difference in the spacing of the tape recorder heads; however, in other work it might be significant depending upon the frequencies of interest.

The PAR model 100 correlator is shown in figure C.3b.

Correlations of filtered data were obtained by using a pair of Krohn-Hite Corporation model 330 filters to filter the inputs to the correlator. These filters can handle frequencies in the 0.2 to 20,000 cps range. A minimum bandpass is obtained by setting the individually set high and low cut-off frequencies equal. In this case, the lower and upper down 3db power points are 0.77 and 1.3 times the center frequency respectively. Usually a minimum band-pass was used in filtering the data, although wider limits could be selected. Test runs on the filters indicated that they introduced a small phase shift in the data which was aggravated by not matching the settings of the filters. This problem could be handled but illustrates another disadvantage of analog data processing.

The value sought from the correlations was τm (or τ max), the delay time at which the maximum correlation occurred. The zero crossings were also considered when making this determination. The delay time of the maximum correlation was used to compute the phase relationships between the waves and variations in wind velocity and pressure and also between the wind variations at various heights. The frequencies of interest were determined by reference to the power spectral density plots. The raw data obtained in this way was then corrected for any delay induced by instrumentation to obtain a good measure of the true time relationships.

The magnitude of the correlation at τm is important as a measure of the degree of correlation. Here, however, its importance is relative in nature only, for the slight difference in gain of the various channels of information at each rerecording stage served to reduce the significance of the value of the amplitude of the correlation at τm. This magnitude then was only a rough guide as to the extent of the correlation.

Correlations made with the Ampex and PAR correlators appear in figures C.6 and C.7 respectively.

Recommendations for electrical analog data processing.

1. Before attempting to gather any data, the analysis should be completely planned and tested if possible. Every effort should be made to keep the data handling to a minimum. If the original record can be used directly much time and effort will be saved.

2. In power spectral density measurements a filter or wave analyzer with a continuously variable bandwidth whose center frequency

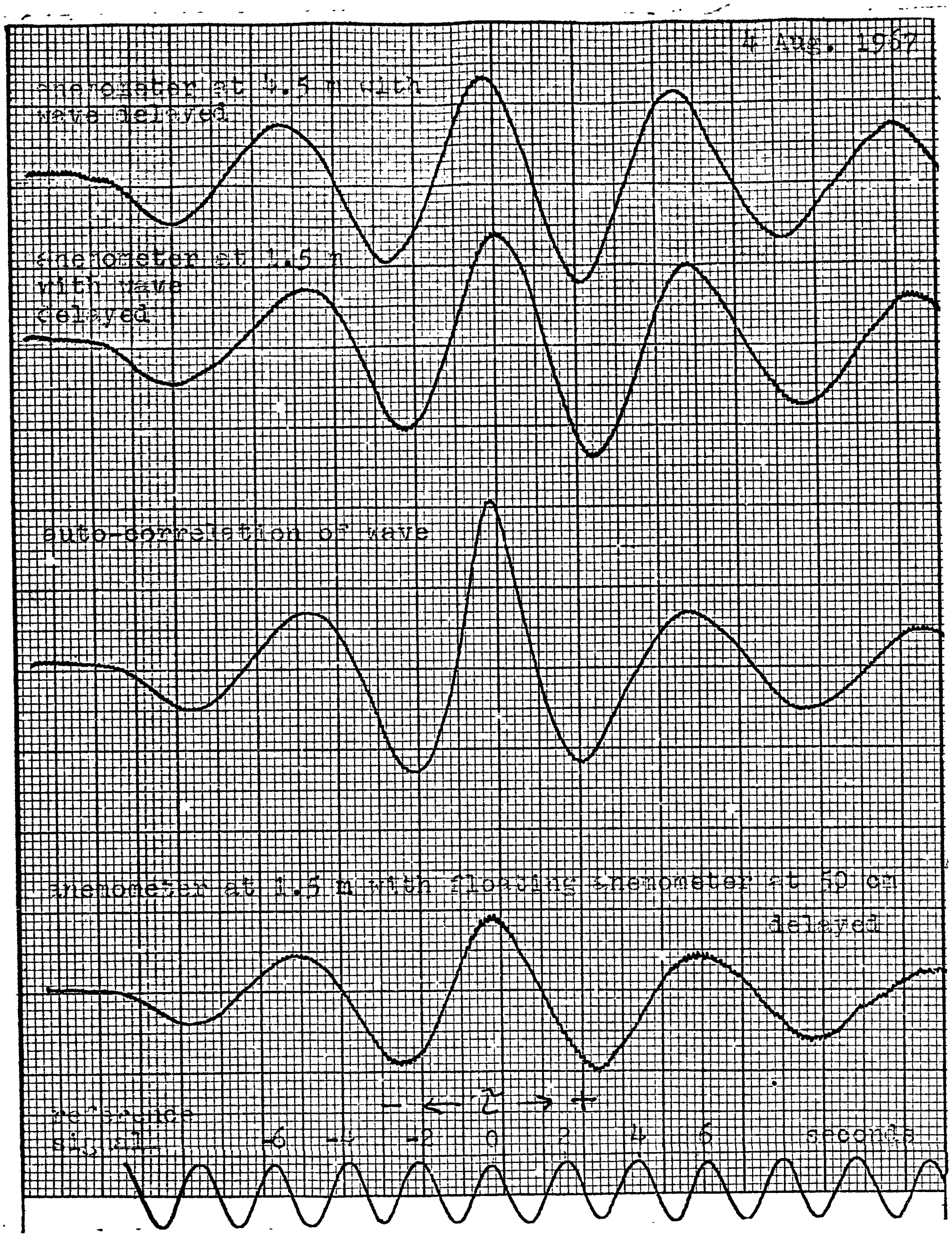

Figure C.6. Correlations made using the modified Ampex model 306-2 tape recorder. For the demodulated wave gauge signal a decrease in voltage represents an increase in water height, while an increase in wind velocity increases its signal voltage. Therefore, a maximum in cross-correlation between wind and wave near zero time delay indicates a maximum wind velocity occurring above the trough. Here the wind input has been filtered of frequency components below 0.1 cps. Note that there is no zero amplitude reference.

can be linearly swept either electrically or mechanically is extremely desirable. Unfortuantely such devices are very expensive, but a good compromise is a filter or wave analyzer whose bandwidth can be changed in moderate discrete steps by replacing a crystal and whose center frequency can be swept.

3. For filtering prior to correlating, a pair of matched narrow bandwidth filters is useful. Filtering the same signal by each unit simultaneously and cross-correlating the output will determine any difference in phase shift introduced by the units.

4. If the tape recorder used has two or more record or two or more playback heads the spacings between heads require careful checking. Heads need also be tested for skewness.

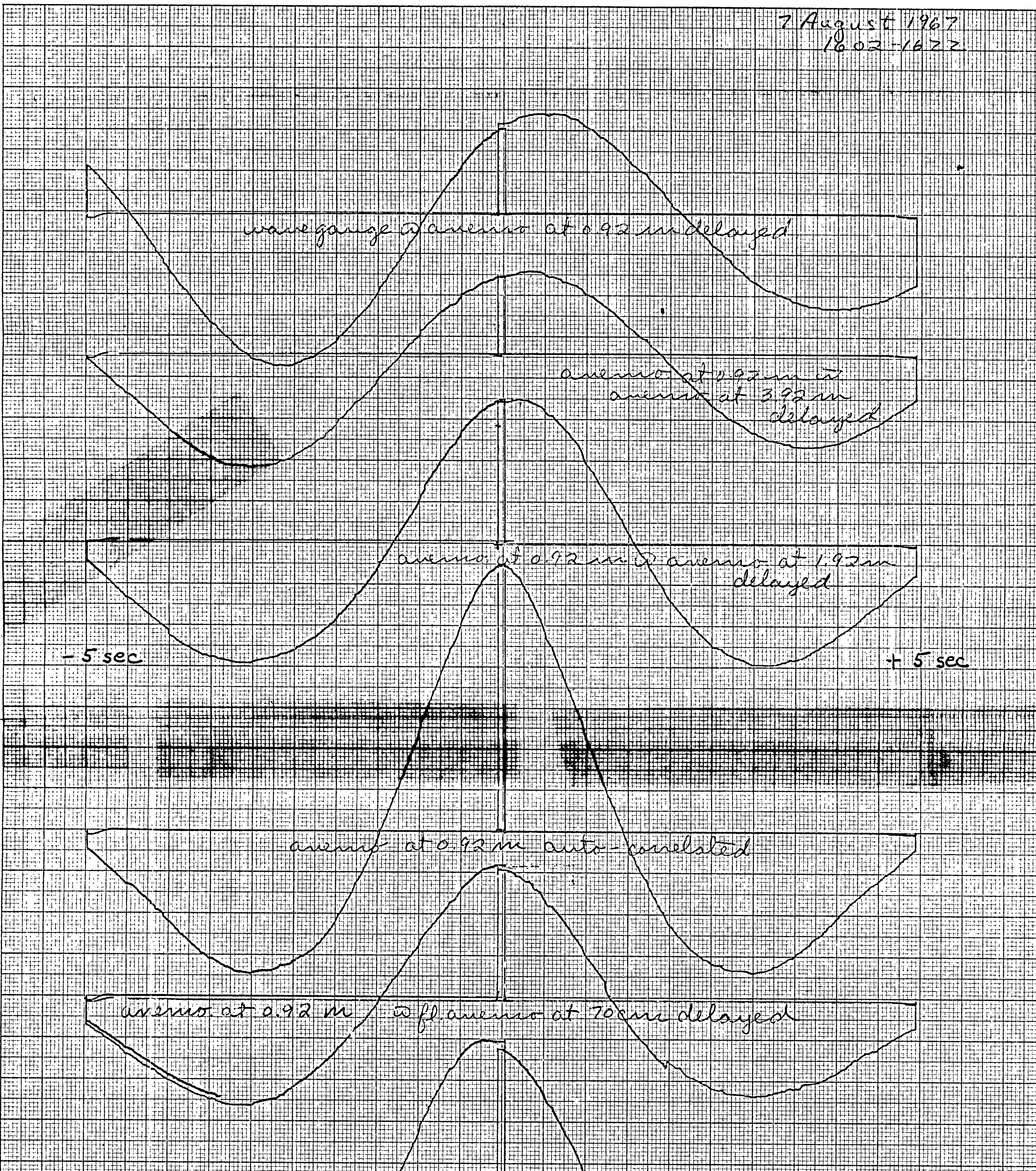

Figure C.7. Correlations performed on the Princeton Applied Research Corporation (PAR) correlator. The positive and negative sides of the correlations were computed and plotted out separately. For the demodulated wave signal increasing water level decreased the voltage, while for the wind velocity signal increasing velocity increased the voltage. Therefore, a maximum peak in the cross-correlation near $\tau = 0$, means the maximum wind velocity occurred above the trough. (The wind input here was filtered of frequency components below 0.1 cps before correlating.)

Appendix D

Supplementary Information

This appendix contains some information in more detail than was necessary for the primary investigation but which may be useful to those interested in various aspects of air-sea interactions. Data of interest to many meteorologists and oceanographers, but not directly related to the problem is also presented, as is certain amplifying information.

The appendix can be divided into the following major sections:

1. Wind velocity data. This section includes figures D.1 through D.3 which are vertical profiles of wind velocity. Table D.1 gives specific information on wind velocities and some temperatures. RMS values of wind velocity variations are in table D.2.

2. Drag coefficients and friction velocities. Table D.3 presents friction velocities and drag coefficients computed from the profiles. The dependence of friction velocity on the wind velocity at two meters is plotted in figure D.4.

3. Wave, wind, and pressure spectra. Figures D.5 through D.12 supplement the spectra in the main text. Two amplitude spectra, Fig. D.5 and D.6, are shown. Below figure D.8 is an explanation of how to use the spectra to obtain the energy in a particular frequency band. A comment on energy distribution in wave spectra appears below figure D.12a.

4. Critical height and the computation of $\overline{W}^2$. Figure D.13 illu-

strates a change in critical height resulting from changes in wind velocity and the dominant wave velocity. A plot of curves used in finding approximations for $\overline{W}^2$ appears in figure D.14.

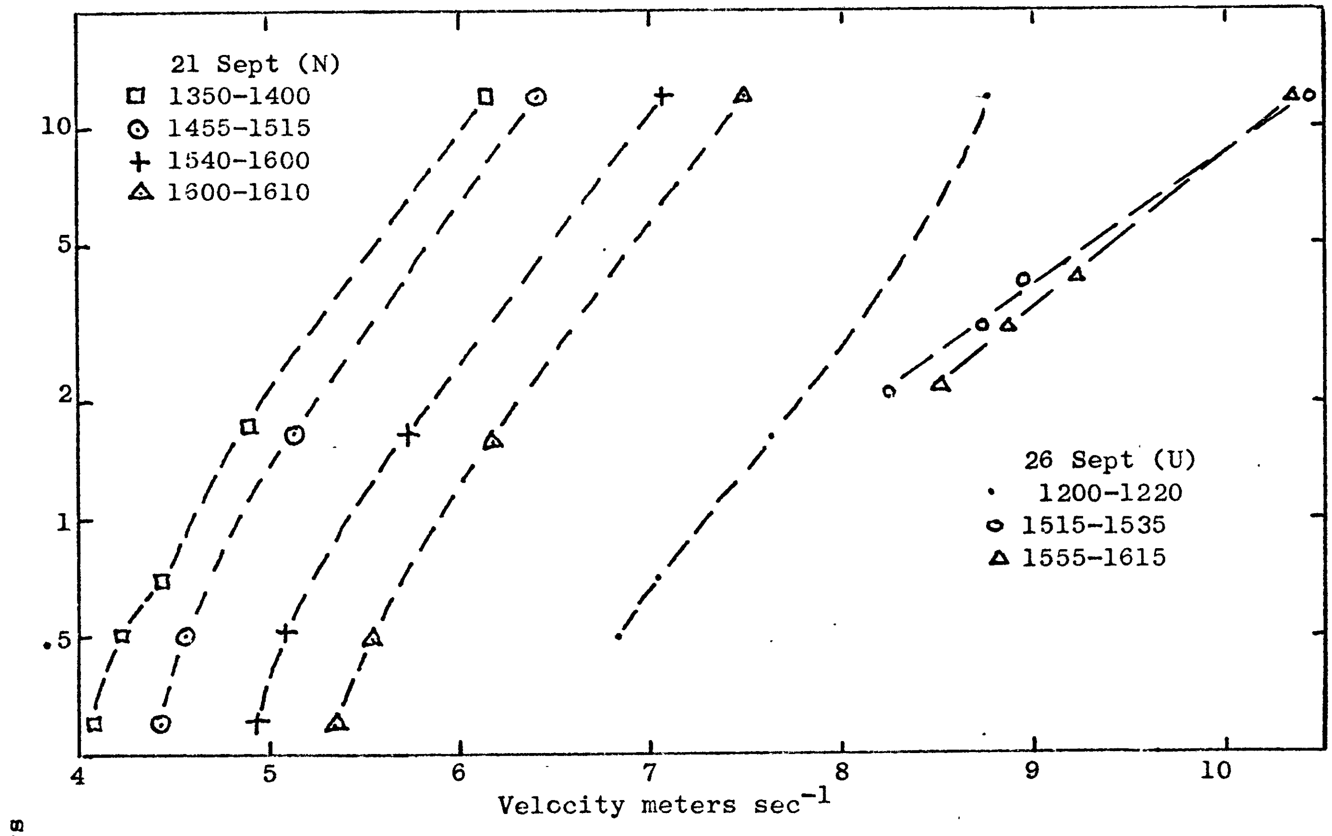

Figure D.1 Vertical wind velocity profiles from Buzzards Bay 1967

Stratification:
- (N) Neutral or near neutral
- (S) Stable
- (U) Unstable

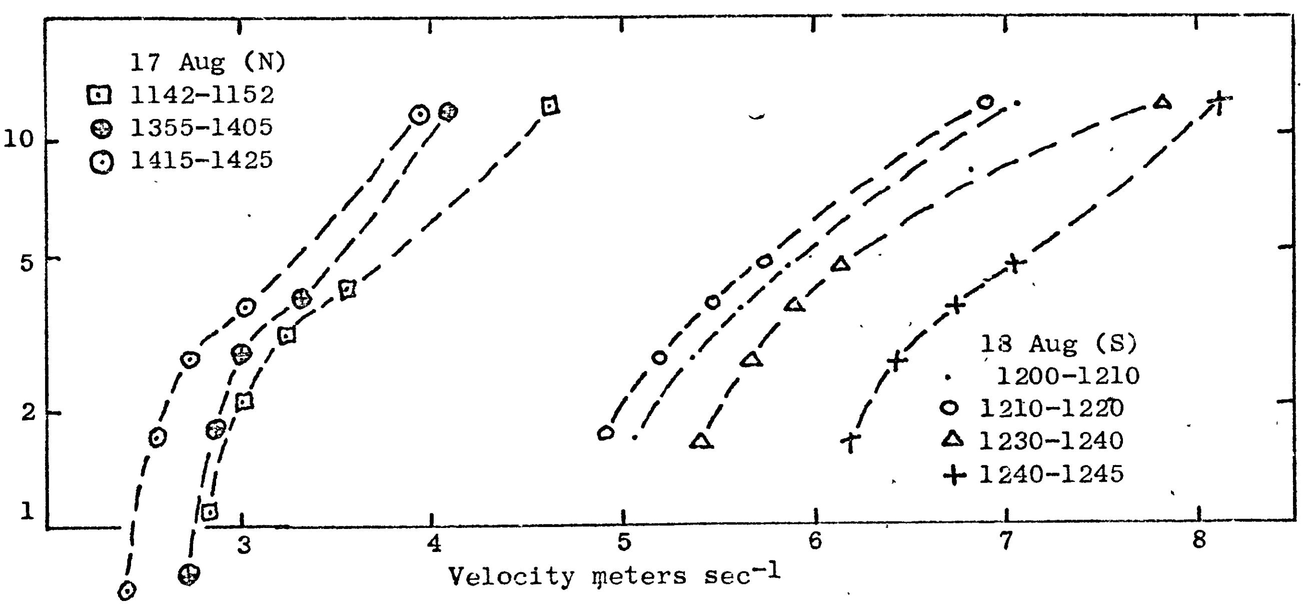

Figure D.2 Vertical wind velocity profiles from Buzzards Bay 1967.

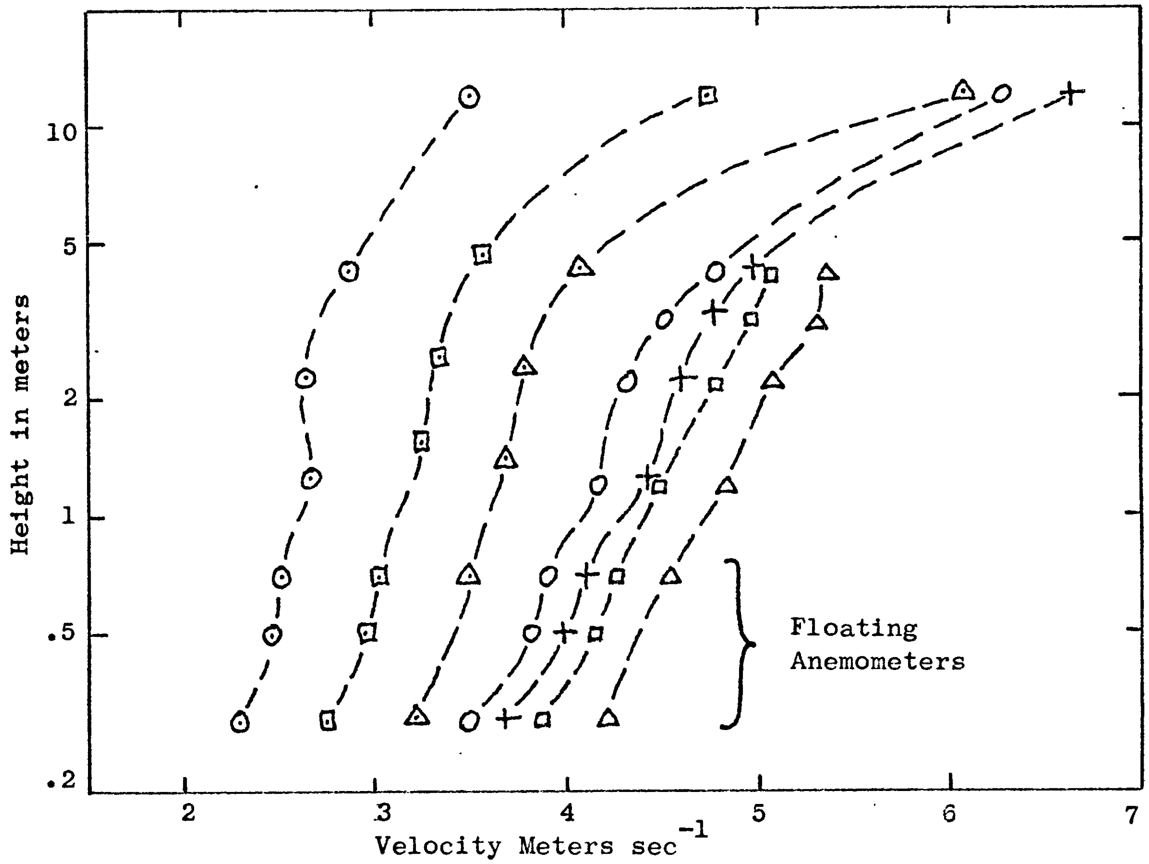

Figure D.3 Vertical velocity profiles from Buzzards Bay, 1967.

2 August (N)	9 August (N)	15 August (S)
△ 1630-1640	+ 1605-1615	⊙ 1225-1235
◻ 1701-1705	o 1642-1652	⊡ 1430-1440
		⚠ 1505-1515

Stratification:
- (N) Neutral or near neutral
- (S) Stable

TABLE D.1

Vertical Profiles of Wind Velocity from Buzzards Bay

2 August 1967 (N) T air= 19.6°C. T sea = 19°C Clear

Time	1630-1640	1640-1650	1701-1705	
Ht. #1	121	117	119	
Anemo.				
30 cm	421	414	387	Wind from 150°T
50 cm			415	
70 cm	455	446	427	
1	484	478	449	
2	508	500	479	
3	531	519	497	
4	537	534	506	
12				

3 August 1967 (N) T air = 20.0°C. T sea ≑ 19°C. Fog

Time	1159-1209	1209-1219	1218-1228	1236-1246	1246-1256	
Ht. #1	127	121	120	113	106	Wind from 165°T
Anemo.						
30 cm	248	305	341	335	333	
50 cm	265	327	366	363	360	
70 cm	269	330	367	368	364	
1	282	345	381	381	383	
2	307	377	416	412	408	
3	315	391	432	426	424	
4	344	413	455	450	445	
12	428	458	525	538	541	

Stability: (N) Neutral or near neutral.
(S) Stable.
(U) Unstable.

Velocities are in cm sec^{-1}.

Ht. #1 gives the height in centimeters of anemometer 1 above MSL. This was the lowest "fixed" anemometer.

Anemometers at 30, 50, and 70 cm floated at that height above the surface.

Anemometers 2,3, and 4 were 1, 2, and 3 meters above anemometer 1 respectively.

Anemometer 12 was at the masthead, 12 meters above MSL.

TABLE D.1 (continued)

Vertical Profiles of Wind Velocity from Buzzards Bay

4 August 1967 (N) T air = 21.5°C. Wind from 225°T Overcast

Time	1100-1110	1110-1120	1118-1128	1135-1145	1145-1155	1155-1205
Ht. #1	156	151	164	172	158	153
Anemo.						
30 cm	571	616	642	668	672	635
50 cm	621	670	693	724	724	682
70 cm	637	690	711	741	746	705
1	706	757	781	824	838	776
2	744	797	822	869	870	817
3	766	822	850	895	900	845
4	788	846	873	921	923	871
12	880	1005	940	980	1030	940

7 August 1967 (N) T air = 19.5°C. Wind from 255°T changing slowly to 225°T Haze

Time	1440-1450	1450-1500	1510-1520	1520-1530	1530-1540	1545-1555
Ht. #1	119	117	114	113	110	108
Anemo.						
30 cm	316	309	323	355	373	409
50 cm	345	336	359	383	399	440
70 cm	352	346	368	389	405	448
1	378	368	395	413	428	474
2	339	378	407	430	447	499
3	406	390	421	445	467	517
4	431	411	441	463	489	540
12	470	482	530	500	572	642

Time	1555-1605	1605-1615	1620-1630	1630-1640	1635-1645
Ht. #1	103	91	87	80	78
Anemo.					
30 cm	391	403	394	375	
50 cm	447	432	423	405	410
70 cm	456	446	434	416	418
1	484	477	451	430	432
2	505	502	477	456	461
3	523	523	496	475	479
4	543	543	518	496	506
12	605	585	575	563	600

TABLE D.1 (continued)

Vertical Profiles of Wind Velocity from Buzzards Bay

9 August 1967 (N) T air = 19.0°C. T sea = 19.5°C. Clear
Wind from 210°T

Time	1555-1605	1605-1615	1615-1625	1632-1642	1642-1652	1650-1700
Ht. #1 Anemo.	120	125	122	117	119	119
30 cm	379	367	369	368	349	366
50 cm	411	398	399	397	380	399
70 cm	424	409	413	409	388	410
1	454	441	446	440	415	439
2	478	460	467	458	430	460
3	494	476	482	475	450	479
4	517	495	502	494	475	
12	635	661	658	655	624	654

15 August 1967 (S) Wind from 225°T changing slowly to 205°T, at 1310, then to 190°T at 1340.

Time	1225-1235	T°C. sea 18.3	1235-1245	1340-1350	1350-1400	Haze
Ht #1	124		121	137	138	
Anemo.		T°C.				T°C.
30 cm	228	[illegible]	217	257	282	
50 cm	244		232	276	302	
70 cm	250	19.2	238	283	312	19.1
1	263		249	305	337	
2	261	20.0	243	318	354	19.3
4	287	20.3	271	350	385	19.5
6		21.2				19.6
12	350		335	405	470	

Wind from 190°T changing to 220°T at 1530. Conditions of stability changed to more nearly neutral in these runs.

Time	1400-1405	T°C. sea 17.8	1430-1440	1455-1505	1505-1515	T°C. sea 19.0
Ht. #1	138		152	155	140	
Anemo.		T°C.				T°C.
30 cm	290		272	293	320	
50 cm	315		292	313	[illegible]	
70 cm	326	19.1	300	319	348	19.5
1	359		322	336	366	
2	373	19.3	330	344	378	19.6
4	400	19.5	354	366	497	19.8
6		19.7				20.0
12	485		473	430	509	

TABLE D.1 (continued)

Vertical Profiles of Wind Velocity from Buzzards Bay

16 August 1967 (N) T air = 20.7°C. Wind from 215°T Haze

Time	1345-1355	1355-1405	1405-1415	1420-1425	1425-1435
Ht. #1	108	108	100	97	95
Anemo.					
1	341	345	338	342	360
2	358	364	357	361	381
3	368	375	372	372	393
4	385	394	389	387	410
12	450	480	475	520	510

Time	1435-1445	1455-1505	1505-1515	1520-1530	1530-1540
Ht. #1	90	150	150	147	143
Anemo.					
1	353	384	390	364	382
2	373	398	407	376	394
3	388	407	412	384	401
4	404	420	427	399	416
12	516	555	555	520	500

Time	1540-1545	1550-1600	1600-1610	1610-1620	1620-1625
Ht. #1	138	131	126	121	120
Anemo.					
1	410	413	396	405	414
2	427	429	408	421	430
3	439	436	417	429	443
4	453	450	432	445	458
12	505	550	540	540	570

17 August 1967 (N) T air = 20°C. Wind from 220°T Haze

Time	1142-1152	1152-1202	1200-1210	1215-1225	1225-1235	1235-1245
Ht. #1	110	105	105	104	102	102
Anemo.						
1	283	260	263	250	250	288
2	301	280	284	271	267	304
3	324	304	308	296	293	328
4	354	329	336	326	321	355
12	462	462	480			

TABLE D.1 (continued)

Vertical Profiles of Wind Velocity from Buzzards Bay

17 August 1967 (N) T air = 20°C. Wind from 215°T Haze

Time	1245-1255	1255-1305	1305-1315	T°C.	1315-1325	1325-1335
Ht. #1 Anemo.	105	97	95		94	90
1	272	243	255	17.93	239	262
2	288	256	267		250	275
3	310	276	283		265	290
4	338	302	305	17.96	289	313
7				17.96		
12	446	401	403	17.98	383	402

Time	1335-1345	1345-1355	1355-1405	1405-1415	1415-1425	1420-1430
Ht. #1 Anemo.	88	85	78	77	70	72
1	261	287	272	257	241	263
2	274	302	289	271	258	283
3	288	315	303	286	273	300
4	310	338	328	308	300	327
12	396	425	410		396	425

18 August 1967 (S) The stability here was almost classified neutral for Ri ≈ .04. Wind from 245°T. Haze

Time	1155-1205	T°C.	1205-1215	T°C.	1230-1240	1240-1245
Ht. #1 Anemo.	165		166		165	162
70 cm		18.2		18.22		
1	545		499		538	619
2	576	18.3	531		565	642
3	602		557		590	672
4	623	18.45	581		612	702
5		18.55		18.52		
10		18.75		18.7		
12	748		696		780	810

TABLE D.1 (continued)

Vertical Profiles of Wind Velocity from Buzzards Bay

21 September 1967 (N) T air = 18.4°C. T sea=18.5°C.
The weather was clear at 1200 with T = 18.4°C. The temperature dropped steadily to 17.2°C. at 1600 when the sky was overcast. A light drizzle began about 1620. Wind from 150°to 200°T.

Time	1310-1320	1320-1330	1330-1340	1340-1350	1350-1400	1400-1410	1450-1500
Ht. #1	168	170	170	172	173	176	164
Anemo.							
30 cm	363	378	428	412	405	424	459
50 cm	372	393	443	429	421	441	473
70 cm	392	412	464	451	444	461	
1	424	449	508	494	489	511	527
12	554	575	628		612	642	669

Time	1500-1510	1508-1518	1540-1550	1550-1600	1600-1610	1610-1620	1455-1515
Ht. #1	164	166	164	161	159	156	164
Anemo.							
30 cm	440	459	477	504	530	514	442
50 cm	458	480	495	522	552	536	457
1	513	516	559	588	618	601	512
12	635	619	684	725	748	736	640

26 September 1967 (U) T air = 15.7°C. T sea = 17.9°C.
Wind from 225°T. Clear

Time	1200-1210	1210-1220	1220-1230	1230-1240	1240-1250	1250-1300	1300-1310
Ht. #1	163	161	159	159	157	157	157
Anemo.							
50 cm	669	693	680	679	692	689	680
70 cm	690	717	704	702	713	714	706
1	746	775	756	756	769	769	757
12	861	885	855	865	894	858	858

Time	1309-1319	1515-1525	1525-1535	1535-1545	1545-1555	1555-1605	1604-1614
Ht. #1	157	210	212	215	216	218	217
Anemo.							
30 cm	664						
50 cm	687						
70 cm	712						
1	770	841	816	822	834	862	838
2		887	860	860	873	907	875
3		904	880	874	888	927	893
12	870	1045	1038	983	970	1052	1023

TABLE D. 1 (continued)

Vertical Profiles of Wind Velocity from Buzzards Bay

26 September 1967 (U) For convenience these profiles cover the period of the spectra in figures 11 and 12.

Time	1200-1221	1225-1246	1258-1319	1515-1536	1538-1559	1554-1615
Ht. #1	162	159	157	211	216	217
Anemo.						
50 cm	682	688	680			
70 cm	704	711	706			
1	761	766	760	828	841	849
2	[illegible]			873	884	887
3				892	899	920
12	873	872	865	1042	982	1038

Stability: (N) Neutral or near neutral.
(S) Stable.
(U) Unstable.

Velocities are in cm sec^{-1}.

Ht. #1 is the height in cm of anemometer 1 above MSL.

Anemometers at 30, 50, and 70 cm floated at that height above the surface.

Anemometers 2, 3, and4 were 1, 2, and 3 meters above anemometer 1 respectively.

Anemometer 12 was at the masthead,12 meters above MSL.

TABLE D.2

RMS Values of Horizontal Wind Velocity Variations during Generating Periods

Date	4 Aug.	4 Aug.	18 Aug.	21 Sept.	21 Sept.
Time	1100-1130	1130-1200	1200-1240	1310-1340	1340-1410
Anemo.					
30 cm	115	126			
50 cm	115	126		57	66
70 cm	103	117		57	66
1	103	120	66	57	66
2	97	120	60		
3	103	126	60		
4	103	120	60		

Date	21 Sept.	21 Sept	26 Sept.	26 Sept.
Time	1450-1515	1540-1620	1200-1315	1515-1615
Anemo.				
30 cm				
50 cm	71	77	100	
70 cm			97	
1	66	74	100	120
2				111
3				109

Values are in cm sec^{-1}.

The values in the table are correct to about ± 5 percent.

Friction Velocities and Drag Coefficients

The formula for the logarithmic profile under adiabatic conditions is

(D.1) $$u(z) = \frac{u_*}{K} \ln z/z_o$$

where, $u(z)$ = the horizontal wind velocity at height z,

u_* = the friction velocity,

K = the von Karman constant = 0.4

z_o = the roughness length.

It is possible to solve D.1 for the friction velocity if the wind at two height is known,

(D.2) $$u_* = \frac{K[u(z_1) - u(z_2)]}{\ln z_1/z_2}$$

The expressions for turbulent shear stress and surface drag are

(D.3) $$\tau = \rho u_*^2$$ and

(D.4) $$\tau_o = \rho C_z U_z^2,$$

where ρ = density of air,

τ = turbulent shear stress,

τ_o = surface drag of wind at the sea surface.

C_z is a dimensionless constant called the resistance or drag coefficient for the height Z. Solving for the drag coefficient yields,

(D.5) $$C_z = \left(\frac{u_*}{u_z}\right)^2.$$

The friction velocity and drag coefficient at two meters were calculated for various periods on each day for which observations were made using velocities from the lowest (1 meter) and highest (4 meters) fixed Thornthwaite anemometers. The values of C_2 fell primarily in the range from 0.78 x 10^{-3} to 3.60 x 10^{-3}. This is in agreement with the findings of most observers. For two generating days values of u_* and C_{10} were also calculated using velocities from the anemometer at 4 meters and the masthead anemometer. The computed surface drag for one run on 18 August using the different results varied by 500 percent. The difference was usually much less.

Friction velocities and drag coefficients for numerous time periods are listed in table D.3. Note how the drag coefficient changed between the early and late runs on 26 September.

Zubkovski and Timanovski (1965) in observations made over the Black Sea noted a linear dependence of ${U_*}^2$ on $(U_2)^2$ for profile observations with low velocities under neutral conditions of stability. Figure D.4 is a plot of points showing this dependence for the Buzzards Bay data. For low velocities a weak linear orientation of the points is observable. The mean slope of the data, however, is steeper than Zubkovski and Timanovski had observed.

TABLE D.3

Friction Velocities and Drag Coefficients

Time	u_{10}	u_{*10}	$C_{10} \times 10^3$	u_2	u_{*2}	$C_2 \times 10^3$
4 August 1967 (N)						
1100-1110	860	38.1	1.97	725	30.6	1.78
1110-1120	968	64	4.36	780	33.1	2.18
1145-1155	1010	43.1	1.82	855	31.8	1.39
1155-1205	915	37.6	1.69	800	34.6	1.87
18 August 1967 (S)						
1155-1205	722	50.2	4.84	556	29.8	2.86
1205-1215	677	46.5	4.7	512	30.9	3.64
1230-1240	738	63.6	7.44	550	27.9	2.58
1240-1245	790	43.6	3.06	628	31.4	2.50

Time	u_2	u_{*2}	$C_2 \times 10^3$
21 September 1967 (N)			
1310-1330	447	24.3	2.95
1350-1400	497	24.3	2.40
1455-1515	523	24.9	2.26
1540-1600	585	26.4	2.02
1600-1610	631	29.4	2.16
26 September 1967 (U)			
1200-1210	757	22.6	0.89
1210-1220	787	22.0	0.78
1230-1250	774	22.8	0.87
1515-1535	812	37.7	2.16
1538-1558	829	36.0	1.89
1555-1615	841	43.4	2.65
2 August 1967 (N)			
1630-1640	502	16.96	1.14
1640-1650	495	17.63	1.27
1701-1705	474	18.15	1.46
3 August 1967 (N)			
1159-1209	301	18.5	3.78
1209-1219	373	21.8	3.60
1218-1228	411	23.7	3.32
1236-1246	408	21.3	2.52
1246-1256	406	18.5	2.08

u_n = horizontal wind velocity at a height of n meters.

u_{*n} = friction velocity for a height of n meters

C_n = drag coefficient, computed for the height n meters.

Velocities are in cm sec^{-1}.

TABLE D.3 (continued)

Friction Velocities and Drag Coefficients

Time	u_2	u_{*2}	$C_2 \times 10^3$
7 August 1967 (N)			
1440-1450	387	16.9	1.89
1510-1520	406	14.3	1.25
1530-1540	444	18.6	1.77
1545-1555	497	19.8	1.58
1605-1615	504	18.21	1.31
1630-1640	461	17.94	1.51
9 August 1967 (N)			
1555-1605	463	19.5	1.78
1605-1615	455	17.7	1.52
1615-1625	463	18.4	1.58
1632-1642	454	17.0	1.40
1642-1652	427	19.0	1.97
1650-1700	455	16.3	1.28
15 August 1967 (S)			
1225-1235	261	7.8	0.90
1340-1350	314	15.9	2.57
1400-1405	366	14.1	1.48
1430-1440	327	11.7	1.28
1505-1515	375	10.8	0.84
16 August 1967 (N)			
1355-1405	362	15.3	1.79
1435-1445	375	14.4	1.48
1520-1530	370	13.4	1.31
1550-1600	424	13.1	0.96
1610-1620	418	13.4	1.04
17 August 1967 (N)			
1142-1152	300	22.7	5.72
1215-1225	270	24.1	7.40
1305-1315	269	15.5	3.32
1355-1405	292	15.2	2.71
1415-1425	261	15.7	3.65

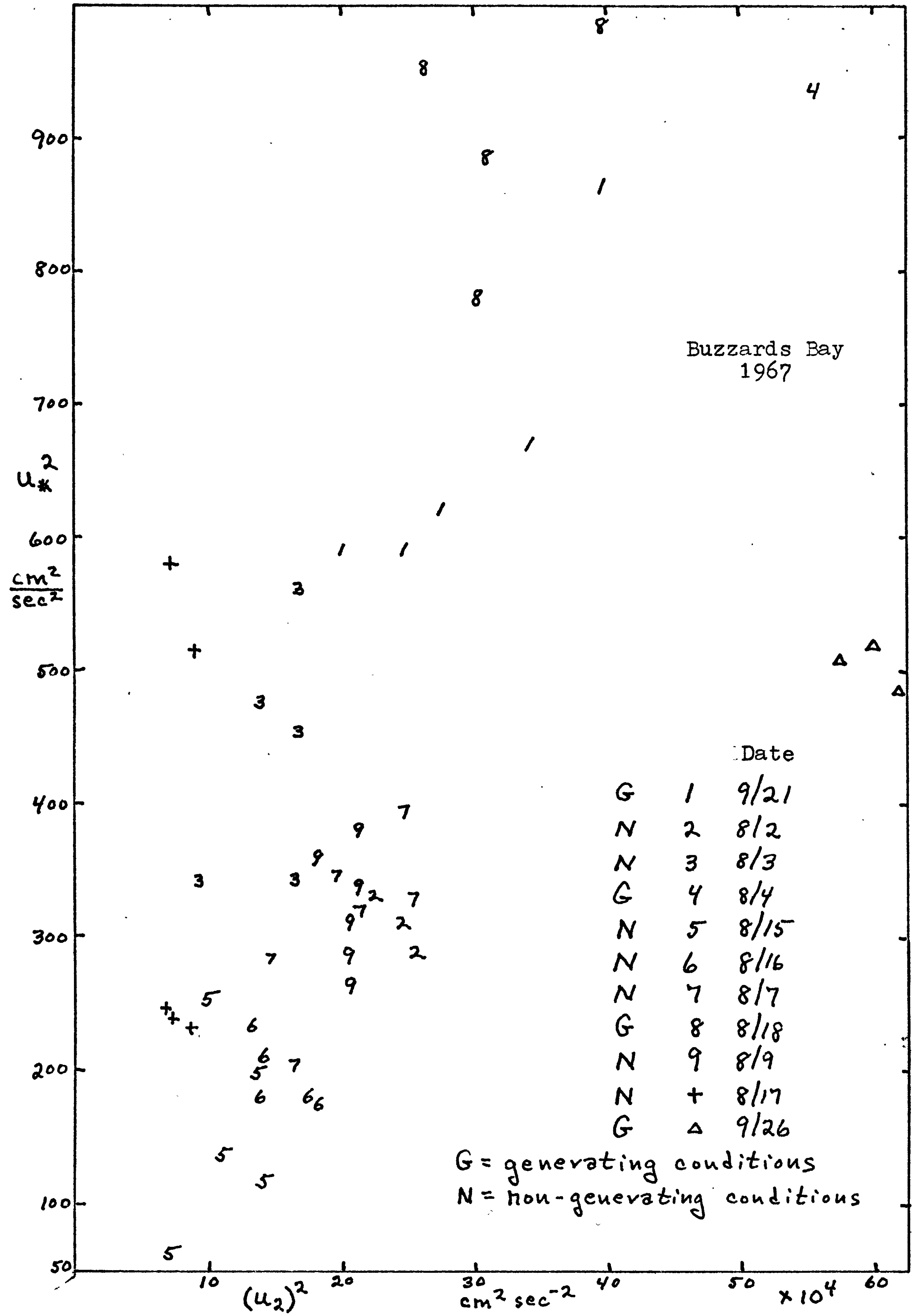

Fig. D.4. Dependence of friction velocity, u*, on wind velocity at two meters, u_2.

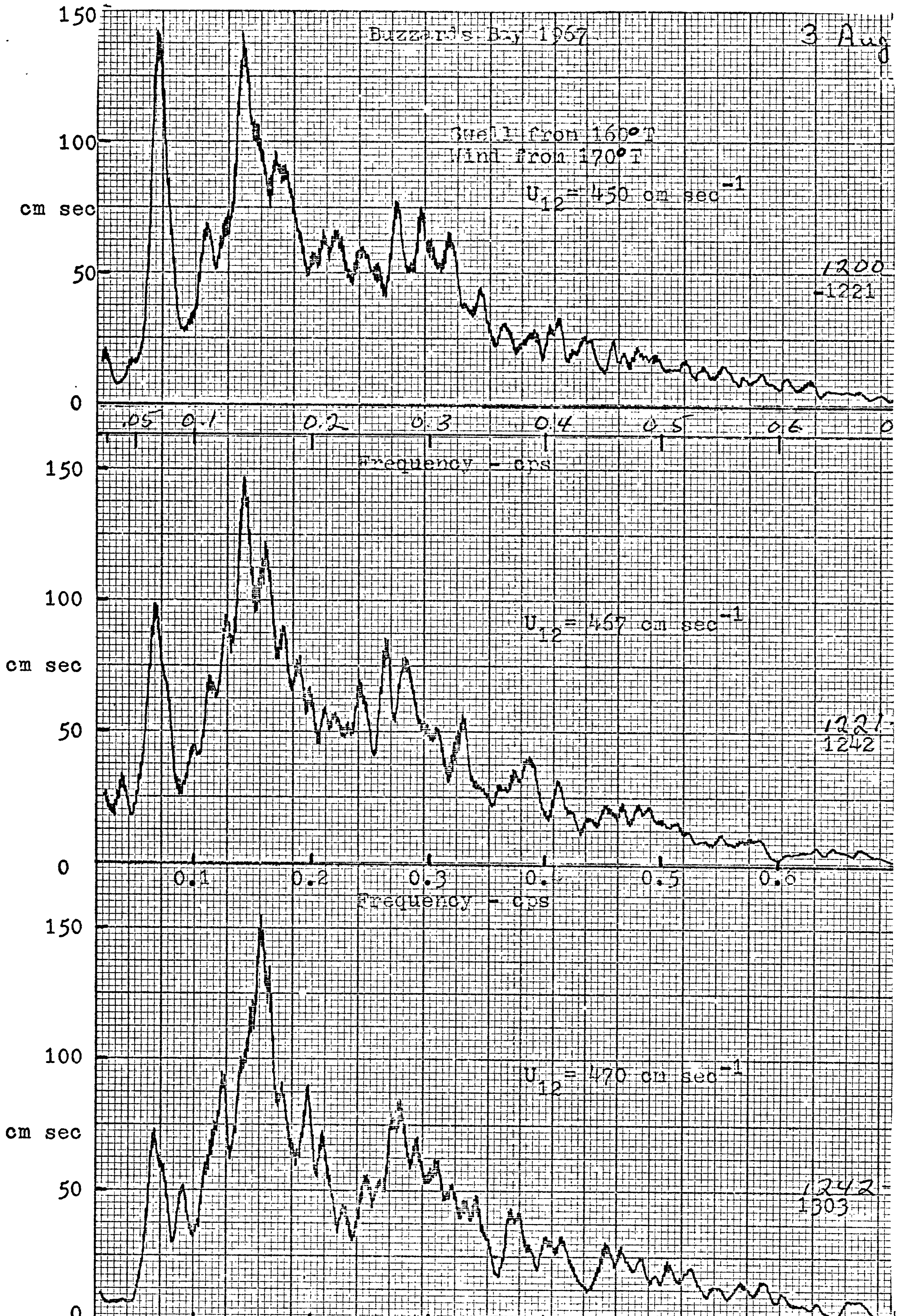

Figure D.5. Wave amplitude spectra.

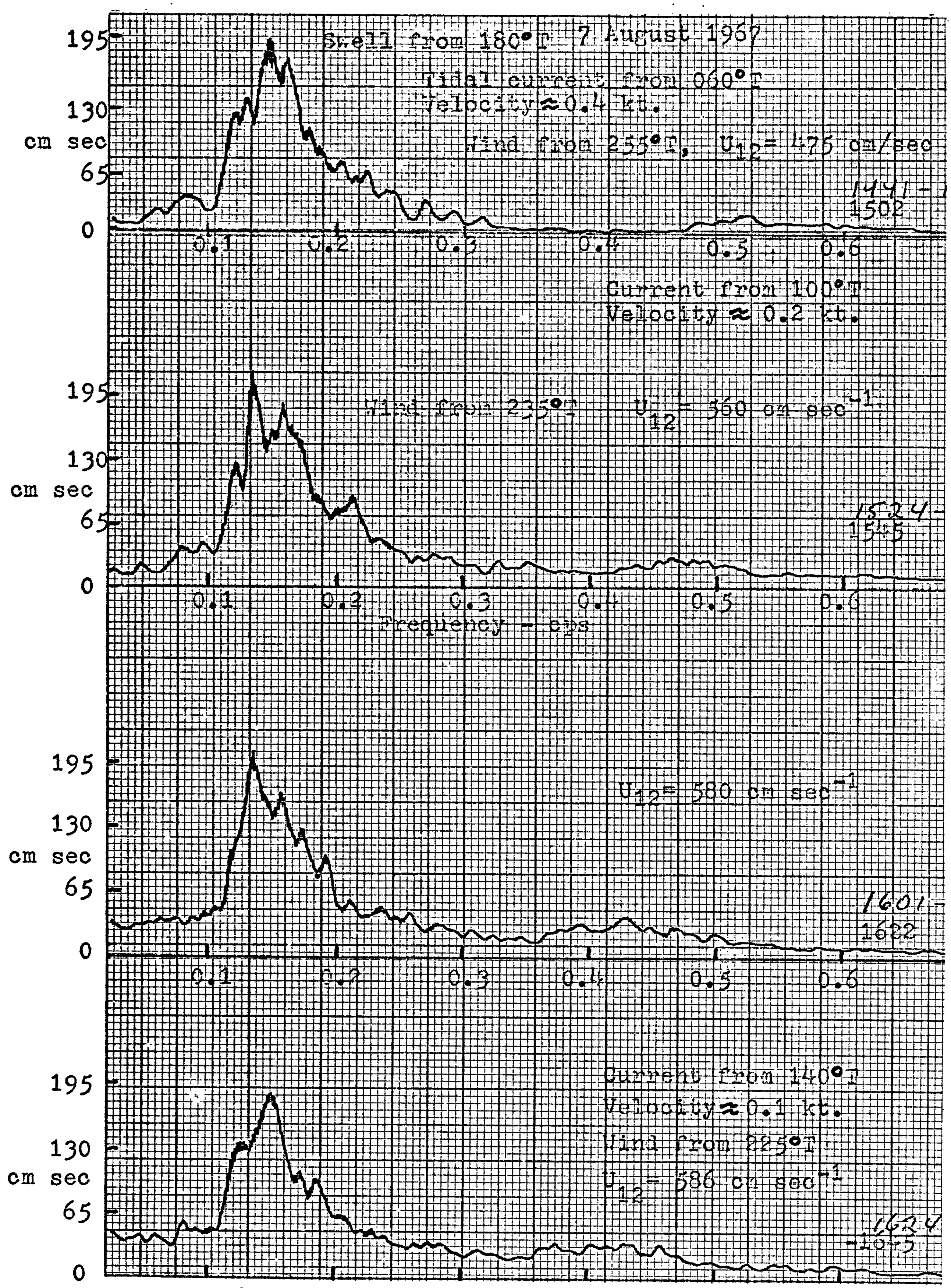

Figure D.6. Wave amplitude spectra.

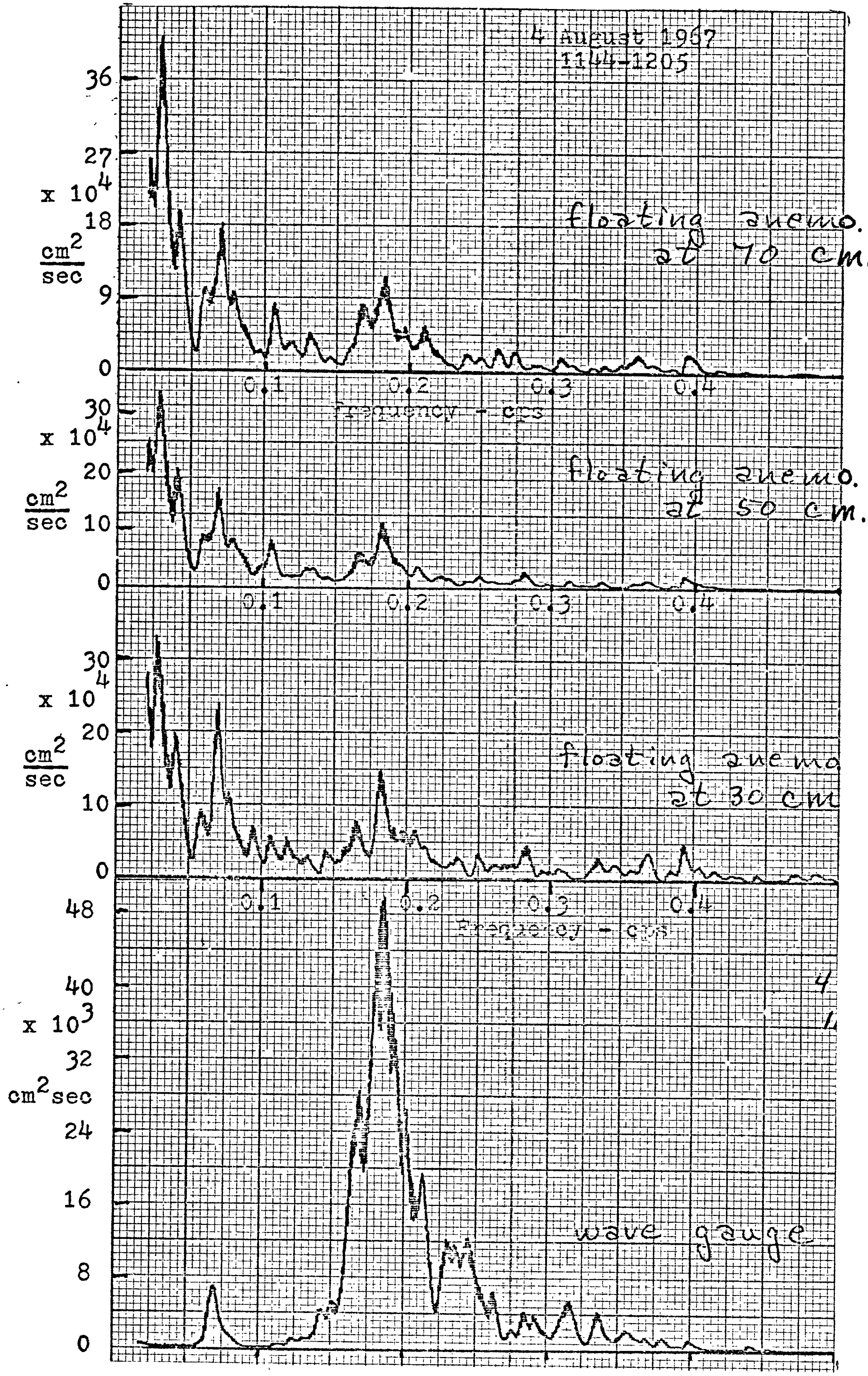

Fig. D.7a. Wind and wave energy spectra. The anemometers floated a fixed distance above the surface.

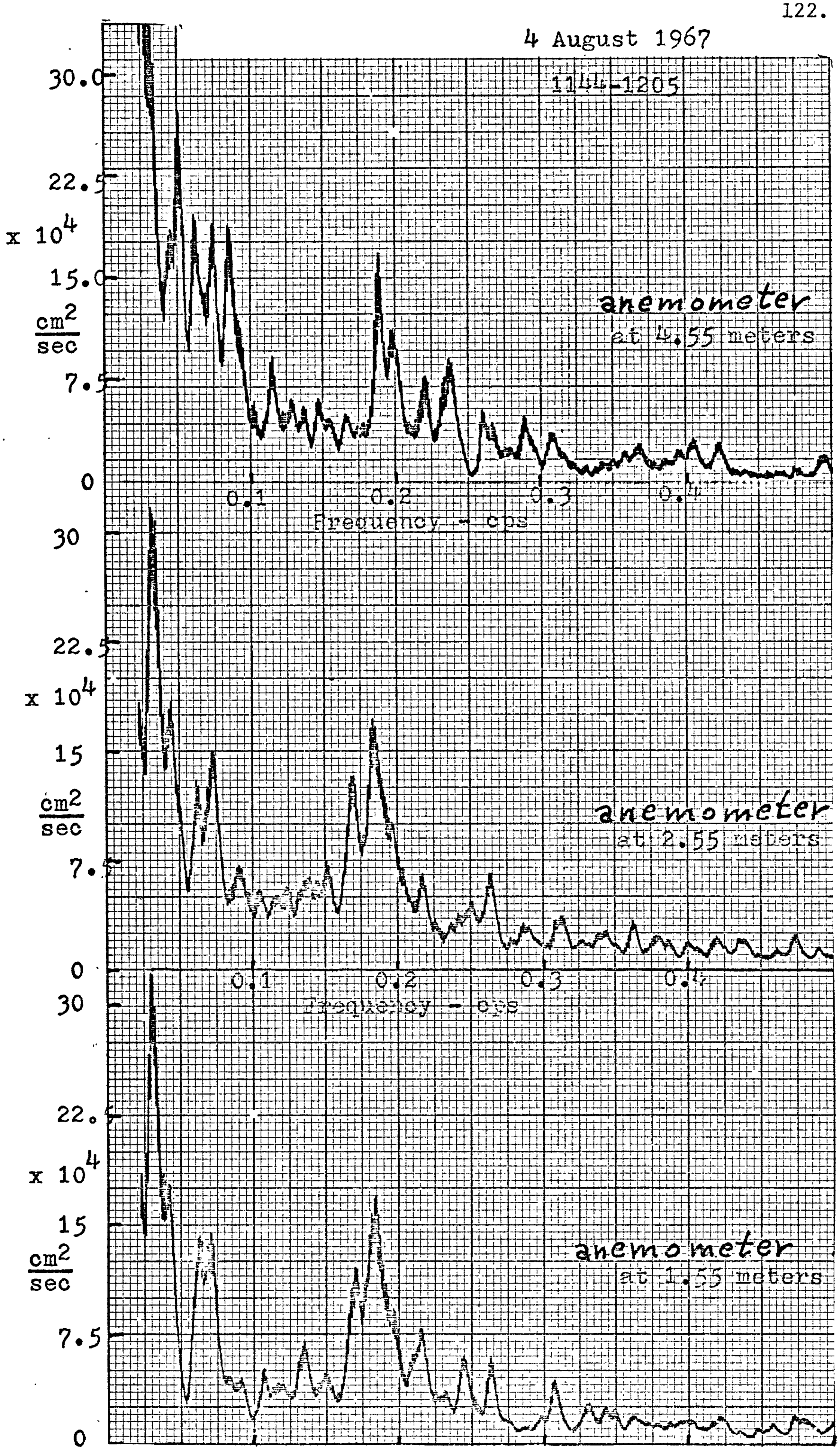

Fig.D.7b. Wind spectra associated with wave spectra in figure D.7a.

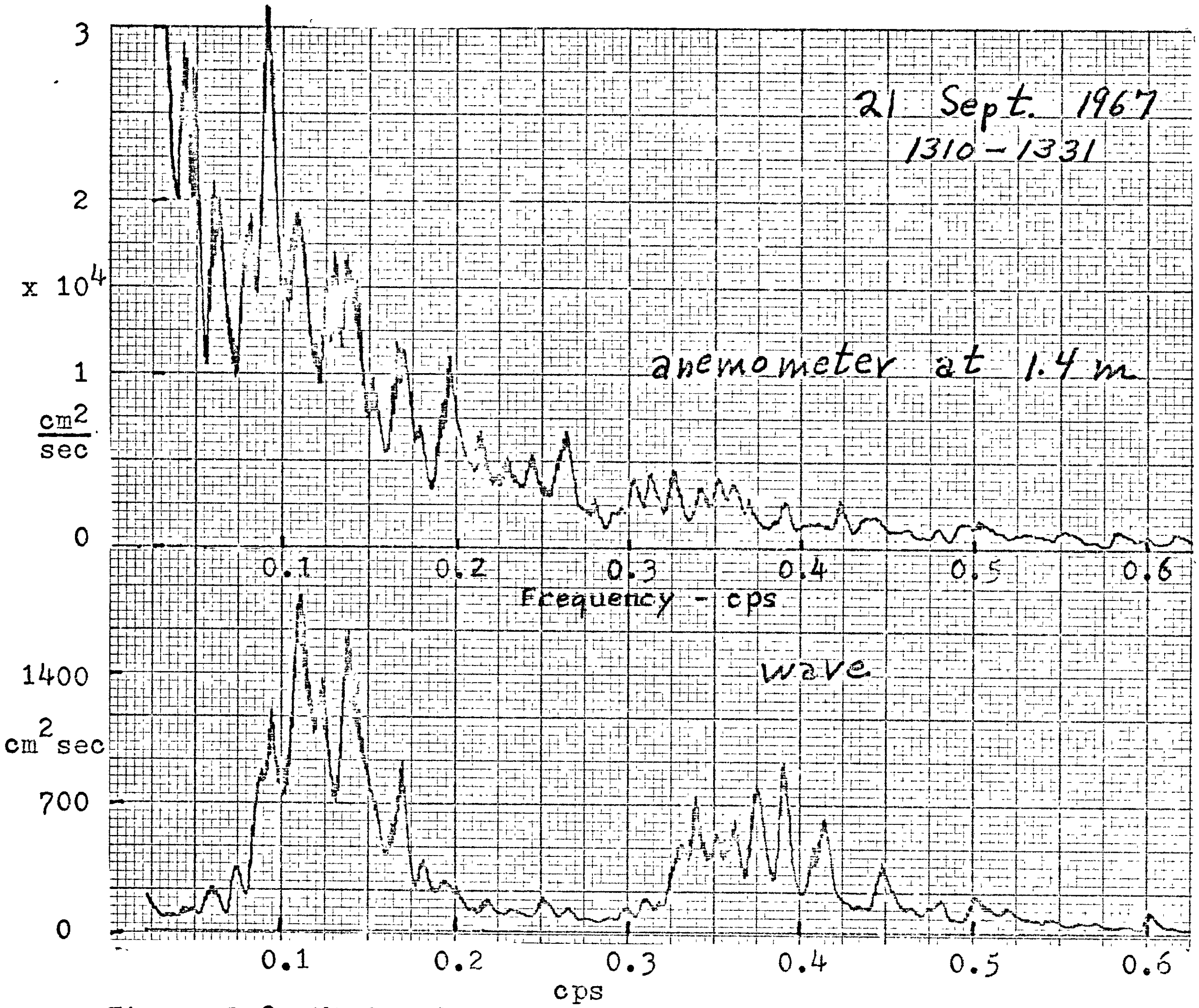

Figure D.8. Wind and wave energy spectra.

It is possible to obtain the energy within a frequency band from the spectra. For example, in figure D.8 if one wants the component of the wave energy within the frequency band from 0.325 to 0.425 cps, he first finds the average height of the spectrum between the two frequencies. A good value for this is 500 cm^2 sec. As the band width is 0.1 cps, the wave energy in the band is 50 cm^2 of sea water. This is equivalent to the energy a simple wave with a height of about 20 cm possesses (rms amplitude = 7 cm).

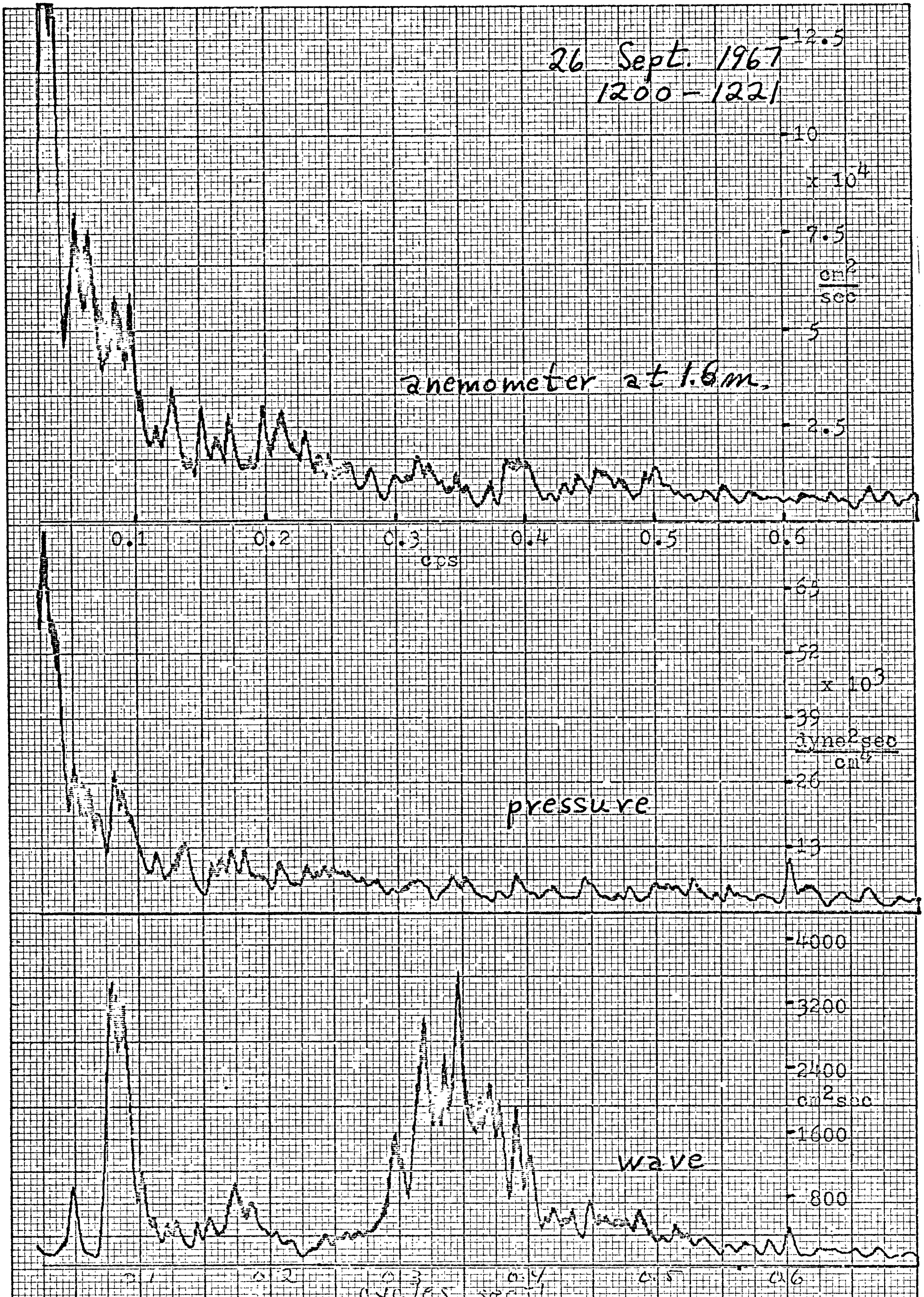

Fig. D.9. Wind, pressure, and wave energy spectra.

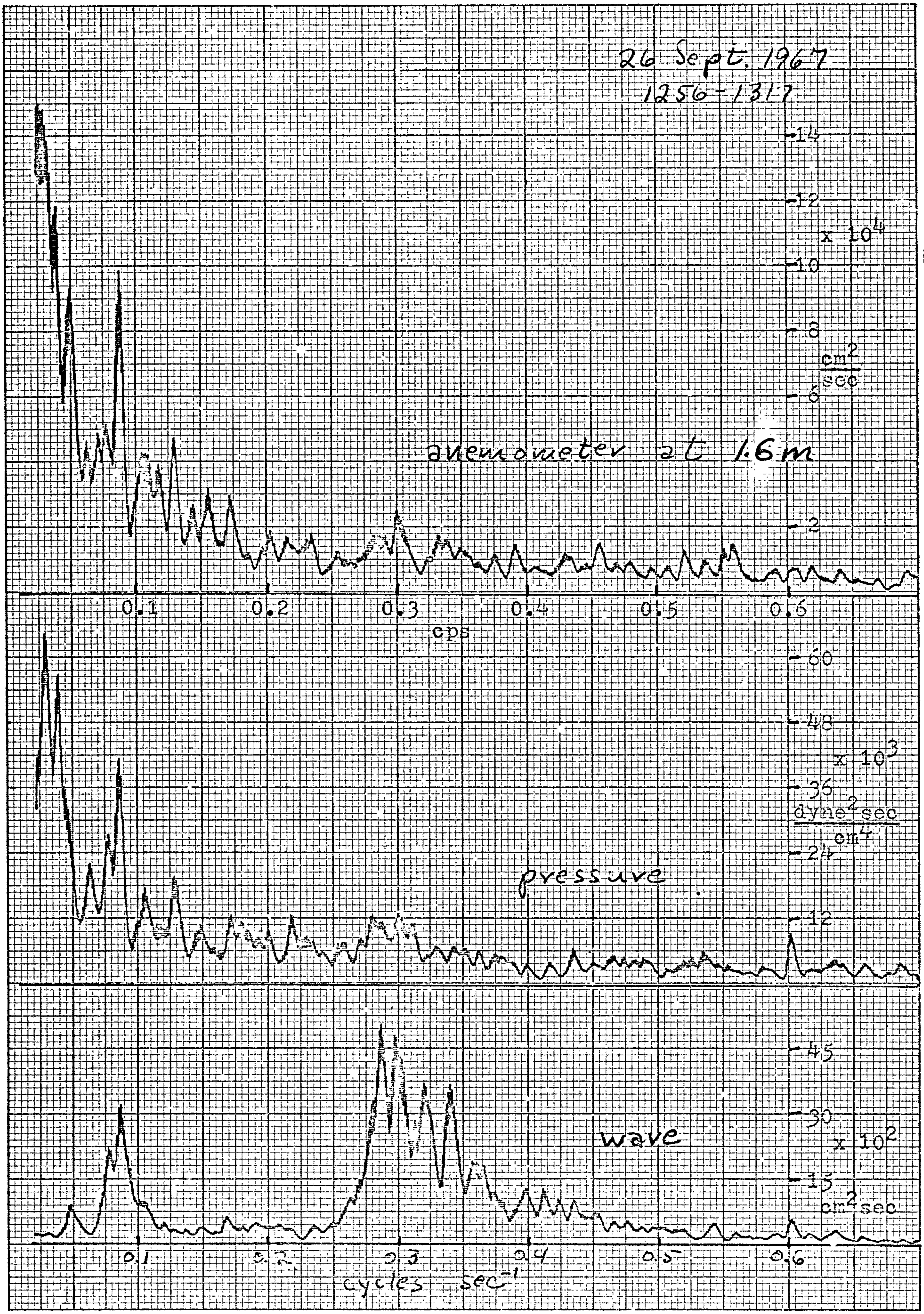

Fig. D.10a. Wind, pressure, and wave energy spectra.

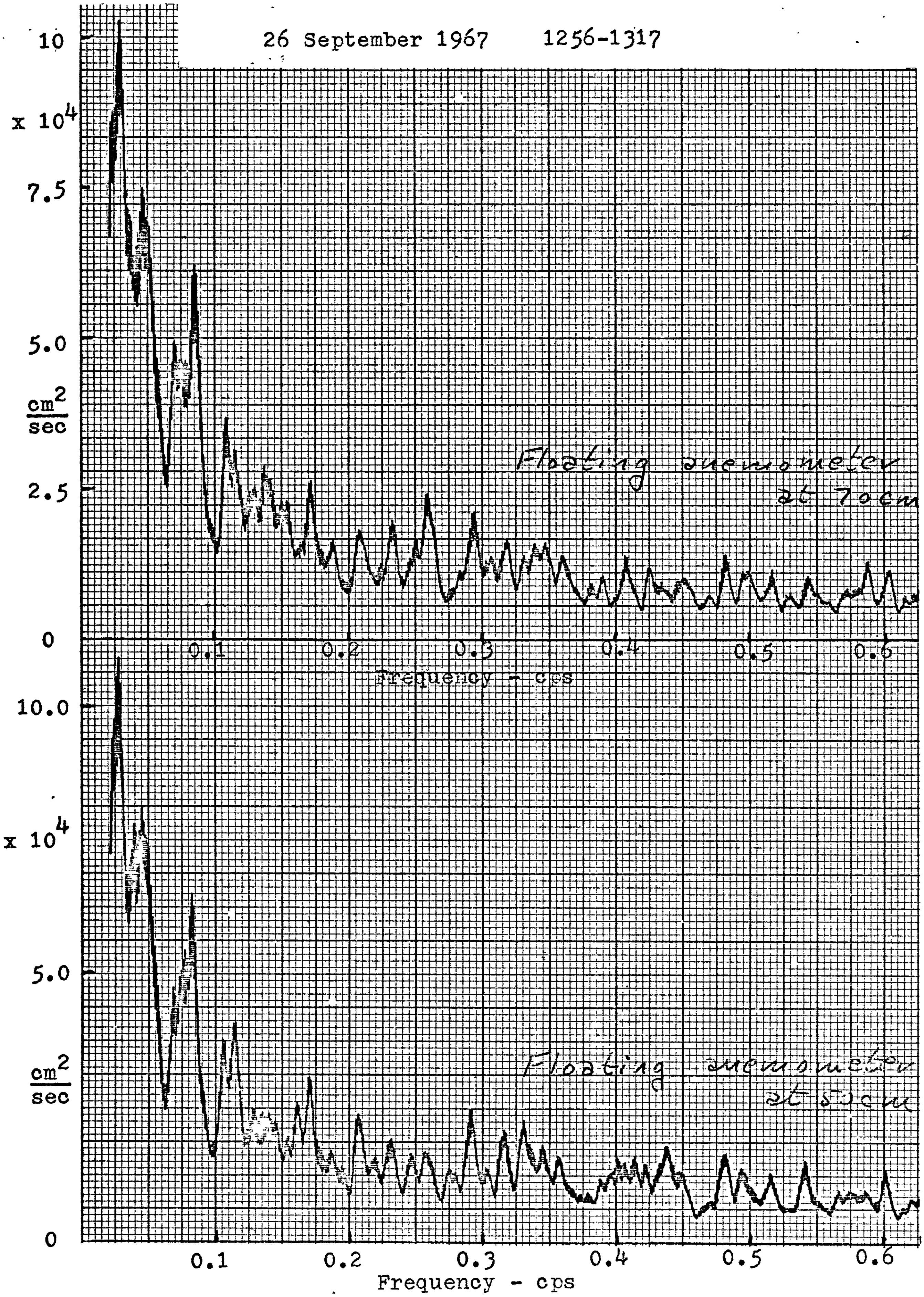

Fig. D.10b. Wind spectra associated with wave spectra in Fig. D.10a.

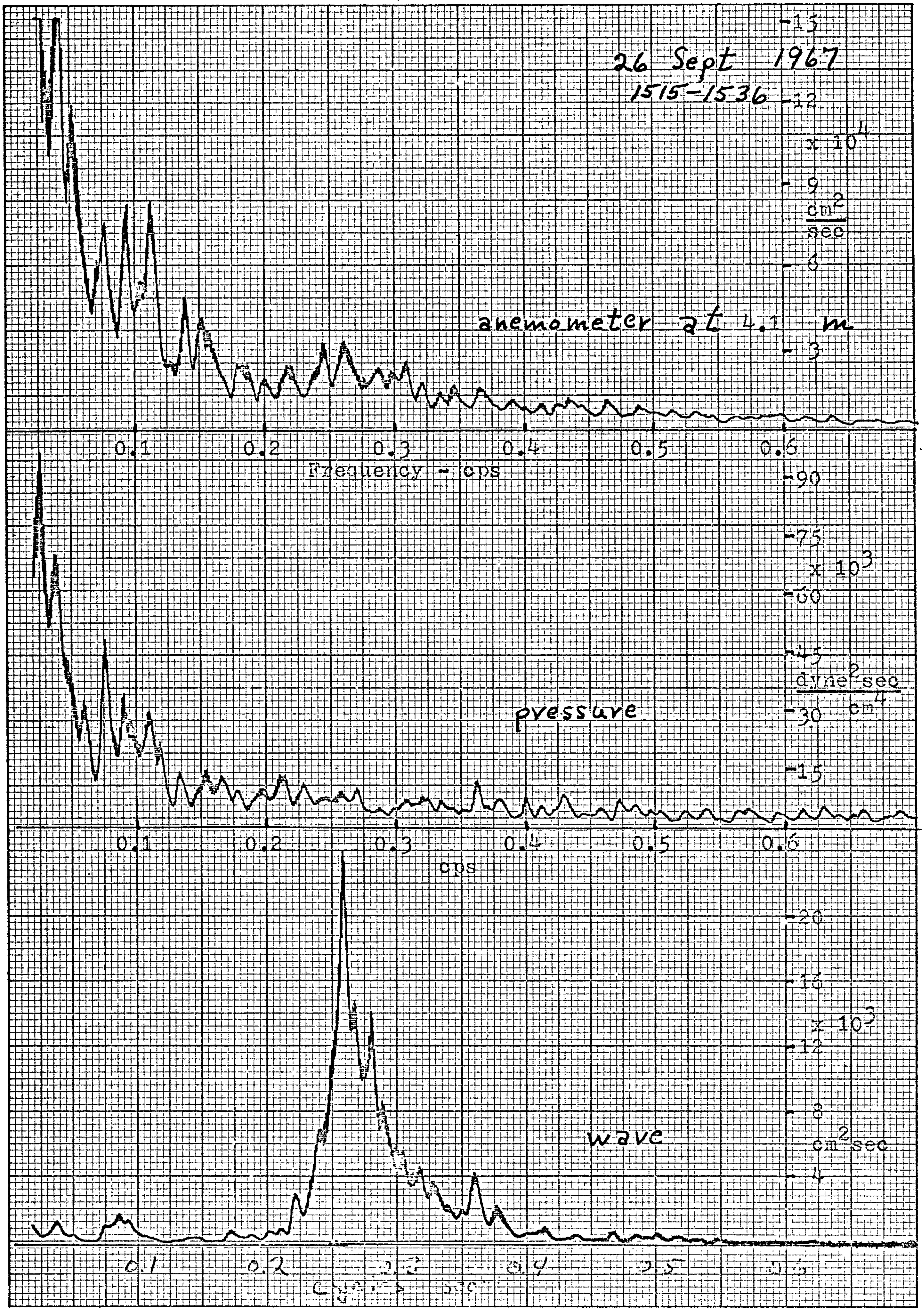

Fig. D.11. Wind, pressure and wave spectra.

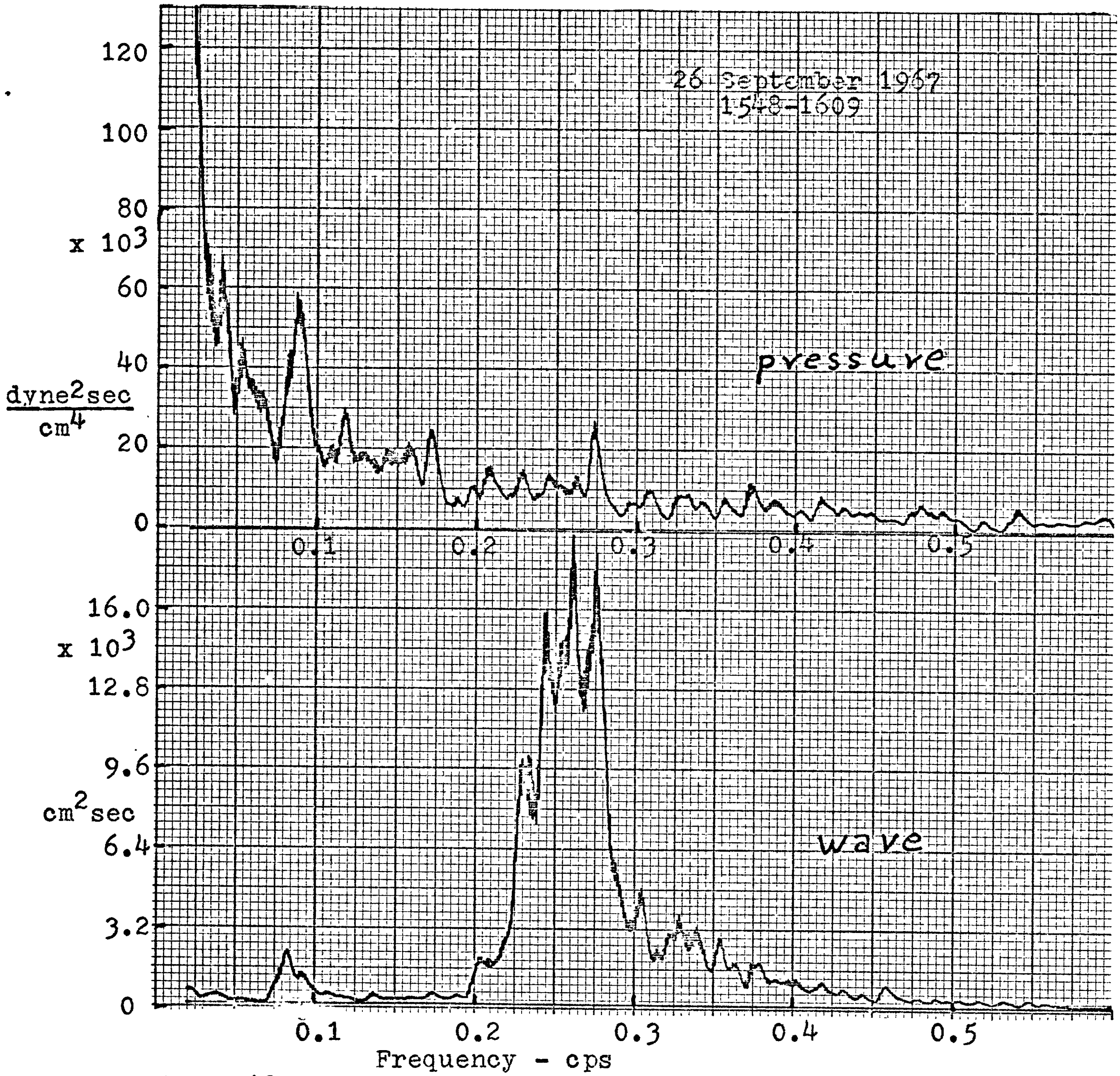

Fig.D.12a. Pressure and wave spectra. See fig.D.12b for wind spectra during this period.

The energies at various frequencies higher than the frequency of the energy peak in a wind driven wave spectrum were compared against one another. This was done for many spectra. The results indicate that energy in this part of the spectrum decreases about as f^{-5}. This is in agreement with the findings of most observers.

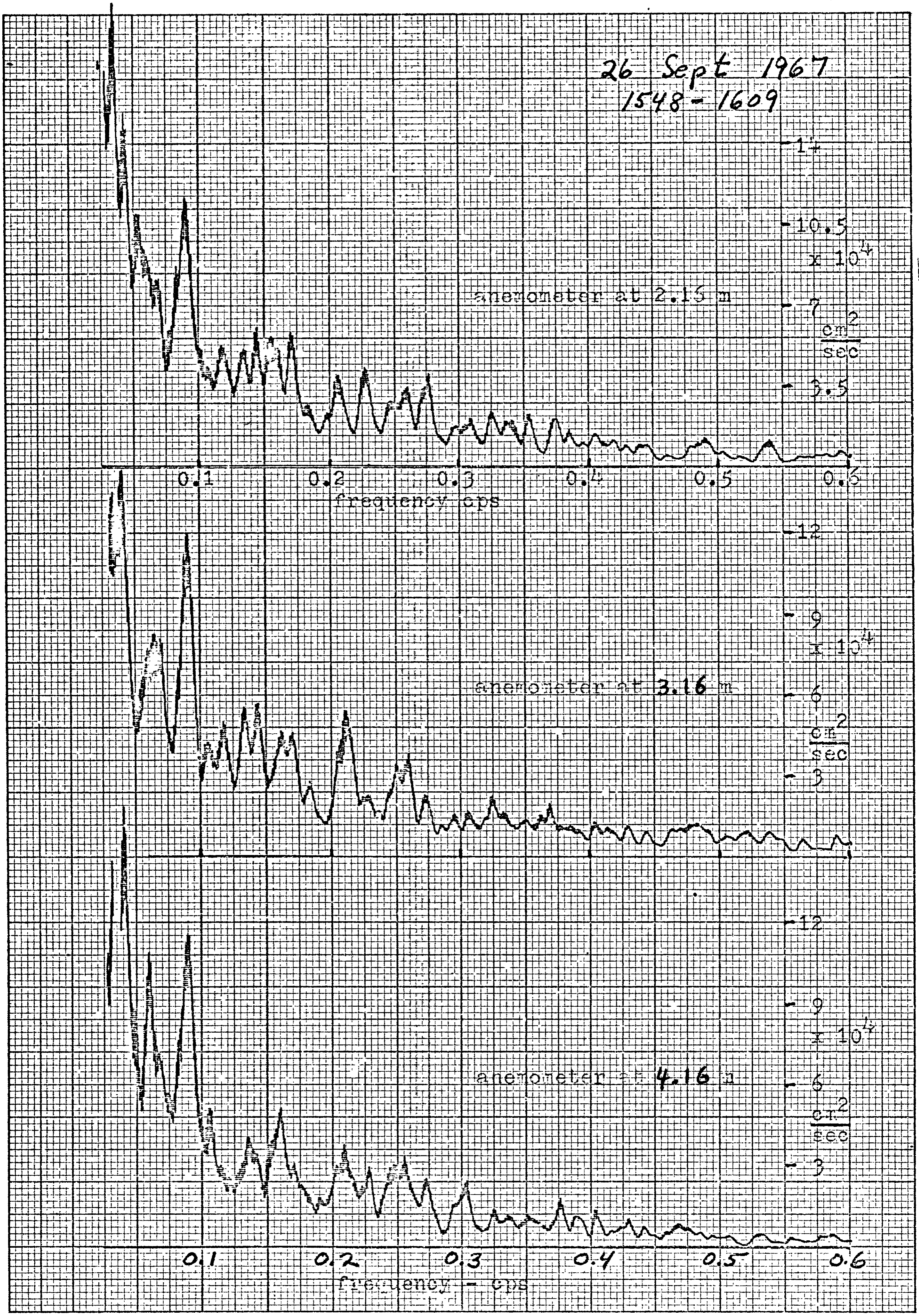

Fig. D.12b. Wind energy spectra associated with wave spectra in fig.D.12a

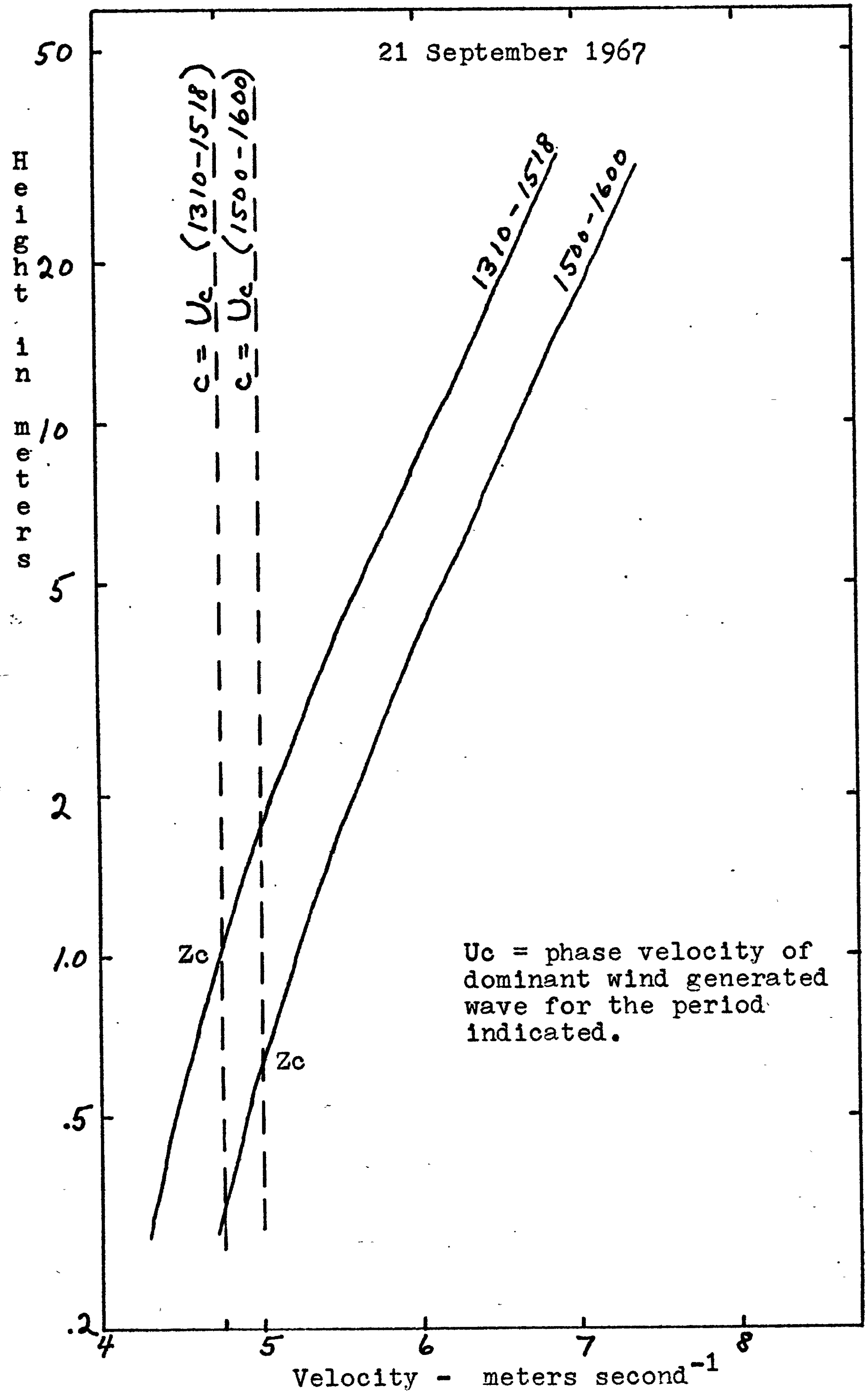

Figure D.13. Vertical profiles of wind velocity indicating how the critical height, Zc, changed on 21 September 1967. Taking an average of the two periods, instead of the periods separately, would have changed Zc, U"(Zc), and U'(Zc) substantially.

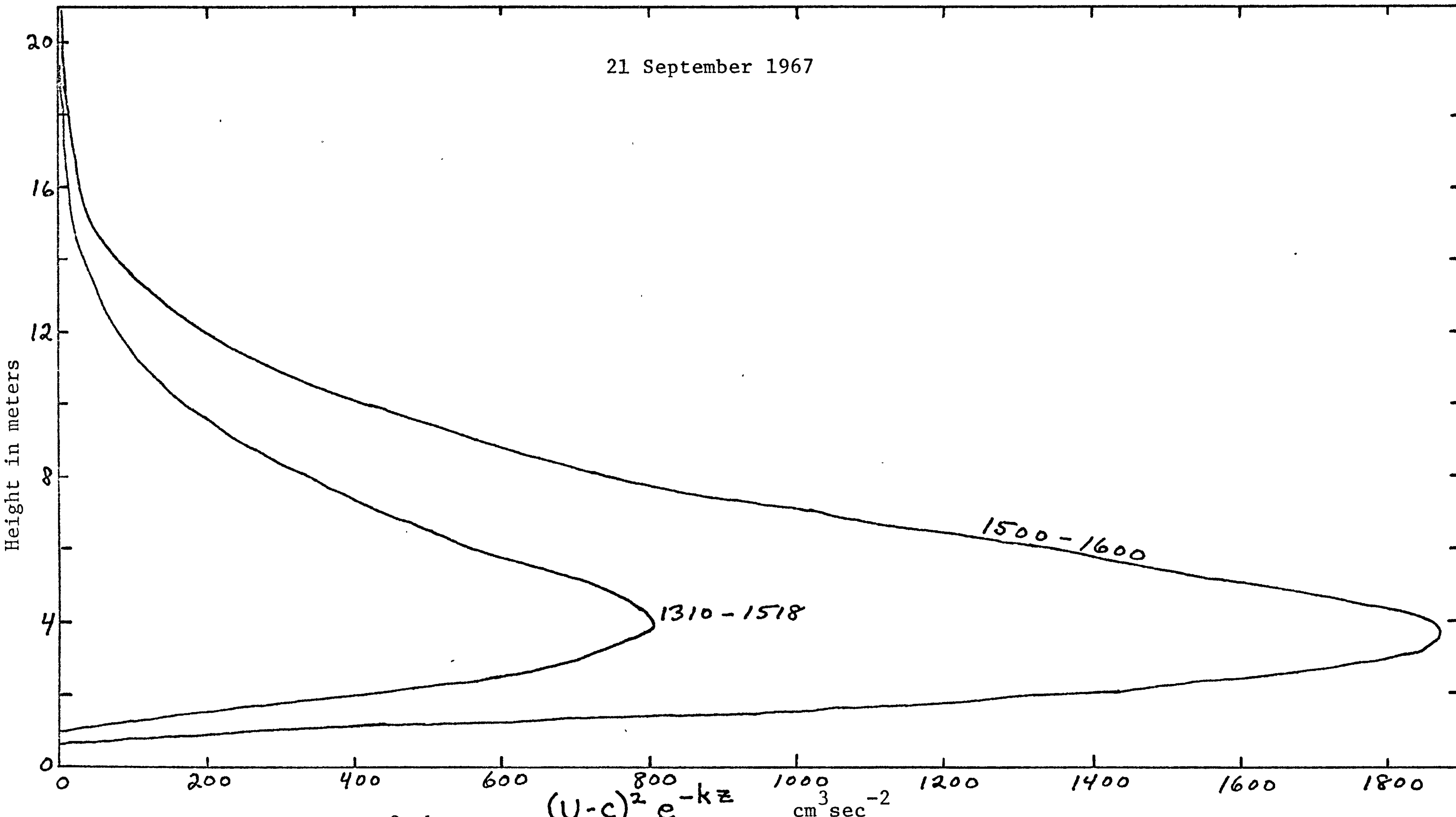

Figure D.14. A plot of $(U-c)^2 e^{-kz}$ versus z illustrating the change in the integral between the two cases shown in figure D.13. The integral is the area under the curve and is used to calculate the effective vertical velocity, $|\overline{W}|$, which is important in Miles' theory. Table 4 contains values for the integral under several different conditions.

Appendix E

Field Support

Cuttyhunk Island is the nearest land to BBELS and partly because of this was selected for the field support site. The island has a good harbor and a sheltered anchorage which can take vessels with a draft of nine feet. Fuel and commercial lodging are available on the island. In summer a passenger ferry serves the island daily from New Bedford. There is also seaplane taxi service to the mainland available. The proximity of Cuttyhunk to the site somewhat offset the rather inaccessible nature of Cuttyhunk itself.

Usually daily trips to the site were made using a local lobsterman hired for that purpose. The lobsterman, Alan Wilder, knew the local waters well and was an excellent small boatsman. His help and interest in rigging and unrigging at the buoy ~~was~~ were extremely valuable. For three weeks in August when the M.I.T. Research Vessel R.R. Shrock was at Cuttyhunk, it was used for transportation and support.

A Zodiac rubber liferaft was towed or carried to BBELS each trip and was most useful in transferring equipment and personnel between the support craft, BBELS, and the buoy. The Zodiac made going alongside the buoy relatively easy on many days when it would not have been safe to approach the buoy in a larger craft with solid sides.

An electronic van was moved to the Cuttyhunk waterfront and connected to the island power supply. This van contained complete lighting, heaters, and a work bench. It was extremely useful for working on equipment which had failed during the day or required checkout prior to use the next day. The van also provided convenient storage for the equipment, spare parts, and numerous items not currently in use at the buoy. As no electronic, hardware, or other supplies were available commercially on Cuttyhunk, the van was well equipped by the summer's end.

Appendix F

Some Preliminary Preparations and Failures

A study of wind and wave interaction was at one time planned using a very small boat (14" x 10" x 3") equipped with battery powered anemometers and surface slope sensing devices. The boat steadied by a sea anchor contained a radio used to telemeter information from the sensors. Although the concept works well in principle and tests of the system were barely satisfactory, numerous problems arose. These included poor drift characteristics of the boat, interference on telemetering frequencies, difficulties in anemometer operation and in referencing the system because of the roll, pitch, and yaw of the boat, interference of the boat with the wind, no accessto equipment once set adrift, and the information gathered from this method is difficult to interpret as it contains much noise. Because of these difficulties an alternate type of platform was desired.

When plans for using a buoy were proposed it was hoped we would measure wind within 15 cm of the instantaneous water surface. As any anemometers that close to the surface under conditions of a fresh breeze would probably be dunked rather often, development of a suitable dunkable cup type anemometer was attempted. The best solution seemed to be an upside down anemometer whose cups and shaft could withstand brief dunkings. A suitably rugged anemometer was built using plastic cups and teflon bearings; however, the anemometer when tested had the rather large distance constant of 2.3 meters.

Some brief consideration was given to using hot wire anemometers but the proximity to salt water would almost surely have precluded successful operation.

A DISA hot film probe was obtained in late June 1967 and should prove satisfactory for use as an anemometer. It was however received too late in the 1967 season to provide for the proper use of a set of these during that summer's work. This type probe will be used by those continuing the investigation.

The above experiences absorbed much effort and time. As it was desired to go into the field with proven equipment, the commercially available Thornthwaite anemometers were selected. These were available too as they had been used in earlier work from BBELS. It was not possible to get closer than 30 cm to the water surface with the Thornthwaites.

Bibliography

Barber, N. F. 1961 Experimental Correlograms and Fourier Transforms. New York: Pergamon Press.

Bendat, J. S. and A. G. Piersol, 1966 Measurement and Analysis of Random Data. New York: John Wiley and Sons, Inc.

Bernstein, A. B. 1967 A note on the use of cup anemometers in wind profile experiments. J. Applied Meteor. 6 280-286.

Brooke Benjamin, T. 1959 Shearing Flow over a Wavy Wall. J Fluid Mech. 6 161-205.

Etkin, B., 1959 Dynamics of Flight, New York: John Wiley & Sons, Inc.

Favre, A. J., J. J. Gaviglio and R. J. Dumas, 1958 Further Space-Time correlation of velocity in a turbulent boundary layer, J. Fluid Mech., 3 344-356.

Gill, G. C., L. E. Olsson and M. Suda, 1966 Errors in measurements of wind speed and direction made with tower-or stack-mounted instruments. Univ. of Michigan, ORA Project 06973 report for U. S. Public Health Service.

Hidy, G. M. and E. J. Plate, 1966 Wind action on water standing in a laboratory channel, J. Fluid Mech., 26 651-688.

Jeffreys, H., 1924 On the formation of waves by wind, Proc. Royal Soc. A 107 189-206.

Kinsler, L. E. and A. R. Frey, 1950 Fundamentals of Acoustics, New York: John Wiley & Sons, Inc.

Kinsman, B. 1965 Wind Waves, Their Generation and Propagation on the Ocean Surface, Englewood Cliffs, New Jersey: Prentice-Hall, Inc.

Kraus, E. B., J. Ching and R. Elsberry, 1966 Aruba Expedition, 1965-Observations and Analysis, Woods Hole Ocean. Inst. Ref. No. 66-70, Woods Hole, Mass. Unpublished manuscript.

Lighthill, M. J. 1962 Physical interpretation of the mathematical theory of wave generation by wind, J. Fluid Mech. 14 385-398.

Longquet-Higgins, M.S., D.E. Cartwright and N. D. Smith 1963 Observations of the directional spectrum of sea waves using the motions of a floating buoy. Ocean Waves Spectra, pp. 111-132. Englewood Cliffs, New Jersey: Prentice-Hall, Inc. (Paper presented in 1961).

MacCready, P.B. Jr., and H. R. Jex, 1964, Response characteristics and meteorological utilization of propellor and vane wind sensors, J. Applied Meteor. 3 182-225.

MacCready, P.B. Jr., 1966, Mean wind speed measurements in turbulence, J. Applied Meteor. 5 219-225.

Miles, J. W. 1957, On the generation of surface waves by shear flows, J. Fluid Mech., 3 185-204.

Miles, J. W. 1959, On the generation of surface waves by shear flows, Part 2, J. Fluid Mech., 6 568-582.

Miles, J. W. 1960, On the generation of surface waves by turbulent shear flows, J. Fluid Mech. 7 469-478.

Miles, J. W. 1962, On the generation of surface waves by shear flows, Part 4, J. Fluid Mech. 13 433-448.

Miles, J. W. 1965, A note on the interaction between surface waves and wind profiles, J. Fluid Mech. 22 823-827.

Miles, J. W. 1967 On the generation of surface waves by shear flows, Part 5, J. Fluid Mech. 30 163-175.

Mollo-Christensen, E. and J. R. Seesholtz, 1967, Wind tunnel measurements of the wind disturbance field of a model of the Buzzards Bay Entrance Light Tower, J. Geophys. Res. 72 3549-3556.

Motzfeld, H. 1937 Die turbulente Strömung an welligen Wänden, Z. Angew. Math. Mech. 17 193-212.

Phillips, O.M. 1957, On the generation of waves by turbulent wind, J. Fluid Mech. 2 417-445.

Phillips, O,M. 1966, The Dynamics of the Upper Ocean, Cambridge University Press.

Project Windy Acres, Wind and Temperature Profiles from 1967 AFCRL-67-0339, Special reports, No. 65, Meteor. lab. project 7655, L. G. Hanscom Field, Bedford, Mass. Unpublished manuscript.

Roll, H. U. 1965 Physics of the Marine Atmosphere, London: Academic Press, Inc.

Shemdin, O. H. and E. Y. Hsu, 1966 The dynamics of wind in the viscinity of progressive water waves, Proc. 10th Conf. Coastal Eng. Tokyo.

Shonting, D. H. 1966, Observations of particle motions in ocean waves. Sc. D. thesis, Dept. of Meteor., M.I.T., Cambridge, Mass.

Snyder, R. L. and C. S. Cox, 1966, A field study of the wind generation of ocean waves, J. Mar. Res. 24, 141-178.

Stewart, R. W. 1961, The wave drag of wind over water, J. Fluid Mech. 10, 189-194.

Stewart, R. W. 1967, Mechanics of the air-sea interface. Physics of Fluids Supplement 10, S47-S55.

Super, A. B. 1964, Preliminary Results of an Air Mass Modification Study over Lake Mendota, Annual Rpt., Dept. of Meteor. U. of Wisconsin, 1-21.

Sverdrup, H. U. and W. Munk, 1947, Wind, sea and swell, U.S.N. Hydrog. Off. Pub. No. 601, Wash., D.C.

Taylor, R. J. 1958, Thermal structures in the lowest layers of the atmosphere. Australian J. of Physics 11, 168-176.

Wiegel, R. L. and R.H. Cross, 1966, Generation of wind waves, J. of the Waterways and Harbors Div., ASCE 92, No. WW2, Proc. Paper 4816, 1-26.

Zubkovski, S. L. and D. F. Timanovski, 1965, An experimental study of the turbulent regime in the near-water air layer, Izv. Atmospheric and Oceanic Physics, Series 1, 1005-1013.

Biographical Sketch

The author was born in Ashland, Pennsylvania on 30 March 1933 to Mr. John F. and Mrs. G. Elizabeth Seesholtz. They provided him with the inspiration to attempt many things he may not have otherwise tried. He spent his childhood in Reading, Pennsylvania and worked as a truck driver and produce salesman while in high school and during the year 1951-1952, while enrolled as a pre-medical student at Albright College, Reading, Pennsylvania.

In 1952 he entered the U.S. Naval Academy and upon graduation with distinction in June 1956 was commissioned as Ensign in the U.S. Navy. Mr. Seesholtz participated in Operation Deepfreeze in the Antarctic during 1956-1958 while serving in the USS ARNEB (AKA-56). A one year tour on the staff of the Commander Amphibious Training Command, U.S. Atlantic Fleet followed. From there he went to Submarine School and then served in the USS CHARR (SS-328) for fourteen months and the USS THOMAS A. EDISON (SSBN-610) for three years. In July 1964 he entered the U.S. Naval Postgraduate School, Monterey, California to study oceanography and transferred from there to M.I.T. in September 1965.

An article by Professor E. Mollo-Christensen and the author, entitled "Wind Tunnel Measurements of the Wind Disturbance Field of a Model of the Buzzards Bay Entrance Light Tower", was published in the Journal of Geophysical Research, Volume 72, in July 1967.

The author is a member of the U.S. Naval Institute, Society of the Sigma Xi, the American Geophysical Union, and the Marine Technological Society.

Lieutenant Commander Seesholtz is happily married to the former Marylee Gehris of Leesport, Pennsylvania. They were blessed with twins eight years ago, a boy, Daniel, and a girl, Amy.

Upon graduation the author will report to the USS TIGRONE (AGSS-419) for duty as Executive Officer.